
[All ETDs from UAB](#)

[UAB Theses & Dissertations](#)

2011

Behavior Of Midbrain Vergence Cells During Stepwise Transfers Of Gaze And Oblique Tracking In Depth

Leah Corthell
University of Alabama at Birmingham

Follow this and additional works at: <https://digitalcommons.library.uab.edu/etd-collection>

Recommended Citation

Corthell, Leah, "Behavior Of Midbrain Vergence Cells During Stepwise Transfers Of Gaze And Oblique Tracking In Depth" (2011). *All ETDs from UAB*. 1422.
<https://digitalcommons.library.uab.edu/etd-collection/1422>

This content has been accepted for inclusion by an authorized administrator of the UAB Digital Commons, and is provided as a free open access item. All inquiries regarding this item or the UAB Digital Commons should be directed to the [UAB Libraries Office of Scholarly Communication](#).

BEHAVIOR OF MIDBRAIN VERGENCE CELLS DURING STEPWISE TRANSFERS OF
GAZE AND OBLIQUE TRACKING IN DEPTH

by

LEAH C. CORTHELL

CLAUDIO BUSETTINI, COMMITTEE CHAIR
RODERICK J. FULLARD
PAUL D. GAMLIN
TIMOTHY J. GAWNE
KRISTINA M. VISSCHER

A DISSERTATION

Submitted to the graduate faculty of The University of Alabama at Birmingham,
in partial fulfillment of the requirements for the degree of
Doctor of Philosophy

BIRMINGHAM, ALABAMA

2011

Copyright by
Leah Christina Corthell
2011

BEHAVIOR OF MIDBRAIN VERGENCE CELLS DURING STEPWISE TRANSFERS OF GAZE AND OBLIQUE TRACKING IN DEPTH

Leah C. Corthell

Vision Sciences

A long standing debate regarding the neural organization of oculomotor control began in the late 1800's with Hering and von Helmholtz proposing two opposing ideologies. Von Helmholtz proposed a monocular structure of the oculomotor circuitry in which each eye receives separate motor commands. Hering offered his law of equal innervation, which states that all eye movements are the sum of binocular vergence and conjugate commands. As a test of Hering's binocular proposal, this project compared the behavior of midbrain vergence cells during: 1) saccade-free stepwise transfers of gaze in depth; 2) combined saccade-vergence eye movements; 3) pure vergence tracking, and 4) smooth tracking in depth along oblique directions in space. Hering's law of equal innervation requires that vergence cell firing would remain consistent whether the movement is a pure vergence movement or a combination of vergence and conjugate commands. For this project, the perturbing conjugate commands of the first experiment were saccades, and smooth pursuit was introduced in the second experiment. Evidence for the majority of midbrain vergence cells to encode only part of the vergence response during these interactions directly challenges Hering's law of equal innervation.

Keywords: saccade, vergence, smooth pursuit, oculomotor, eye movements, Hering, von Helmholtz, primate, macaque, haplorhini, strabismus, binocular, monocular, disparity, eye alignment, midbrain, Matlab, Simulink

TABLE OF CONTENTS

	<i>Page</i>
ABSTRACT	iii
DEDICATION	vi
ACKNOWLEDGEMENTS	vii
LIST OF TABLES	viii
LIST OF FIGURES	ix
INTRODUCTION	1
BACKGROUND AND SIGNIFICANCE	17
Current knowledge of the vergence circuitry	17
Midbrain Vergence Cells.....	22
Vergence Accommodation Cross-talk and the Near Triad	28
Vergence Models.....	31
Vergence-saccadic Interactions	35
Vergence Smooth Tracking.....	43
METHODS	47
Visual Stimuli.....	47
Data Acquisition and Calibration Procedures	53
Eye Movements and Accommodation Calibration	54
Recordings and Stimulations.....	55
Data Analysis	57
Animal Protocol and Veterinary Care	59
Animal Training and Surgical Procedures	60
Fluid Intake Management.....	64
Euthanasia	65
EXPERIMENTS	66
Experiment 1: The quantification of midbrain vergence cell behavior	

during discrete transfers of gaze through single unit electrophysiological recordings	68
Rationale.....	68
Experimental Procedures.....	71
Data Analysis	72
Cell Types.....	72
Modeling of Saccade-Free Vergence Responses to Target Steps in Depth	91
Vergence enhancement encoded by midbrain vergence cells	103
Experiment 2: The quantification of midbrain vergence cell behavior during oblique tracking in depth through single unit electrophysiological recordings	105
Rationale.....	105
Experimental Procedures.....	109
Data Analysis	111
Results	111
CONCLUSIONS.....	120
Coding of vergence eye movements by the midbrain vergence cell during saccade-free step transfers of gaze.....	120
Coding of vergence eye movements by the midbrain vergence cells during saccade-vergence combined trials.....	121
Coding of vergence eye movements by the midbrain vergence cells during oblique tracking in depth	124
REFERENCES	126
APPENDIX.....	135
A Parsing by the MatLab Simulink Model	135
B IACUC Approval Form.....	140

DEDICATION

To my kind and generous husband, John T. Corthell, for his constant love, support, and encouragement, and to my mother, her persistence has been an inspiration. For my wonderful siblings: Brian, Traci, and Elijah. To my dear friend and pastor, E.L. Peck, for encouraging me to attend graduate school. To Dr. Michael Shadlen, thank you for your continuing tutelage and mentorship. Finally, to Dr. Claudio Busetini as an expression of my gratitude.

ACKNOWLEDGEMENTS

I would like to thank Dr. David Swofford for shaping my academic direction during the last year of my undergraduate studies. Thank you, Dr. Claudio Busetini, for painstakingly and repeatedly editing my writing and being patient through life's many twists and turns. I also certainly have to thank Dr. Kevin Schultz for his assistance with MatLab modeling, his training, and his invaluable friendship.

The funding sources of this project were: NEI/NIH (1 R01 EY017283 and ARRA Administrative Supplement) "Neural Organization of Eye Movements in Depth", awarded to Dr. Claudio Busetini, and NEI/NIH (P30 EY03039) "Core Grant for Vision Research", awarded to Dr. Kent Keyser.

LIST OF TABLES

<i>Table</i>	<i>Page</i>
1 Statistics for saccade-free model estimations using all parameters.	102

LIST OF FIGURES

<i>Figure</i>	<i>Page</i>
1 Monocular field of vision.....	1
2 Binocular field of vision	2
3 Cyclopean perspective	3
4 The neuroanatomy of the horizontal subcortical oculomotor pathways.....	7
5 A schematic representation of the connections of the primate vergence system.....	18
6 Sensitivity profiles of disparity detecting neurons.....	20
7 Midbrain vergence cell locations	23
8 Convergence burst cell behavior.....	25
9 Tonic cell firing.....	25
10 Burst-tonic cell firing.....	26
11 Schematic of the Dual Model of Interaction between vergence and accommodation	30
12 Rashbass continuous feedback model.....	32
13 Dual Mode Model of vergence	34
14 The Robinson Local Feedback Model of the saccadic system	38
15 OPN Multiply Model	38
16 Monocularly induced vergence.....	46
17 Optical schema of the haploscope system	47
18 Examples of stimuli used in the first set of experiments	51
19 Examples of stimuli used in the second set of experiments.....	52

20 Illustration of the PEEK strips and of the head post.....	62
21 Oculomotor contributions encoded by the saccadic and vergence burst cells during saccade-vergence interaction	70
22 Primarily tonic cell with gradual buildup and no vergence enhancement	74
23 Pure tonic cell with abrupt onset and evident vergence enhancement.....	76
24 Convergence burst cell with no vergence enhancement	79
25 Convergence burst cell with vergence enhancement	80
26 Example of a convergence burst cell with early cessation of firing	82
27 Example of a convergence burst cell with a firing covering the entirety of the vergence response	83
28 Example of a divergence burst cell.....	84
29 Example of a divergence burst-tonic cell.....	85
30 Convergence burst cell with directionally-dependent vergence enhancement	87
31 Same convergence burst cell found in Fig. 30: directional dependence of enhancement amplitude	88
32 Same cell as Fig. 30: conjugate firing.....	89
33 Convergence tonic cell with a pause for saccades	90
34 Position and velocity vergence models.....	93
35 Pulse-step variation.....	95
36 Pulse-step parsing	97
37 Typical results of position and velocity models	103
38 Vergence cells which do not encode saccadic enhancement	106
39 Saccade at the onset of vergence	106
40 Example of an enhanced burst cell and the effect of this enhancement on the velocity model.....	107

40 Symmetric convergence movements in response to steps vs. ramps	114
42 Symmetric divergence movements in response steps vs. ramps.....	116
43 Results of position model for a convergence burst-tonic cell while executing oblique vergence movements	118
44 Results of the velocity model for a divergence burst cell while executing oblique vergence movements	118

INTRODUCTION

The position of the eyes in the head plays a key role in how an animal perceives the visual world and how the movements of its eyes are controlled. For animals with lateral eyes, like the frog, each eye has a wide field of view, but there is no overlap between the two fields, as depicted in Fig. 1. The purpose of this arrangement is to have the largest coverage of the visual world: panoramic vision. With each eye exploring separate views, it is not surprising that within these animals the movements of the two eyes are also independently controlled through a monocular organization of the oculomotor systems. The objects of interest seen by one eye are not seen by the other eye, and the animal scans the visual scene with separate right-eye and left-eye oculomotor commands.

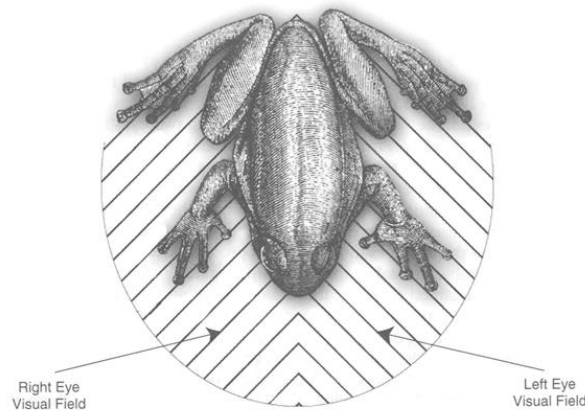


Figure 1: Monocular field of vision. In the frog, an animal with lateral eyes, there is no overlap between the visual fields of the two eyes. Each eye scans the visual world independently, with separate controls of the movements of the two eyes. Adapted from Steinman et al 2000.

Animals with lateral-facing eyes possess an area of heightened resolution, the area centralis, into which objects of interest are preferentially driven by movements of the eyes and the head. These animals do not have an actual fovea.

Animals with frontal eyes, such as the primate, have a smaller overall field of view, due to the loss of posterior vision, and a large frontal overlap of the right-eye and left-eye fields, as is illustrated in Fig. 2. Primates have binocular vision, a unified perception built from the visual inputs from the two eyes, which are not necessarily identical due to the fact that the two eyes have differing locations in the head. Despite having these two eyes to collect visual information, we experience our world with cyclopean perception, as though viewing with a single eye located at the center of

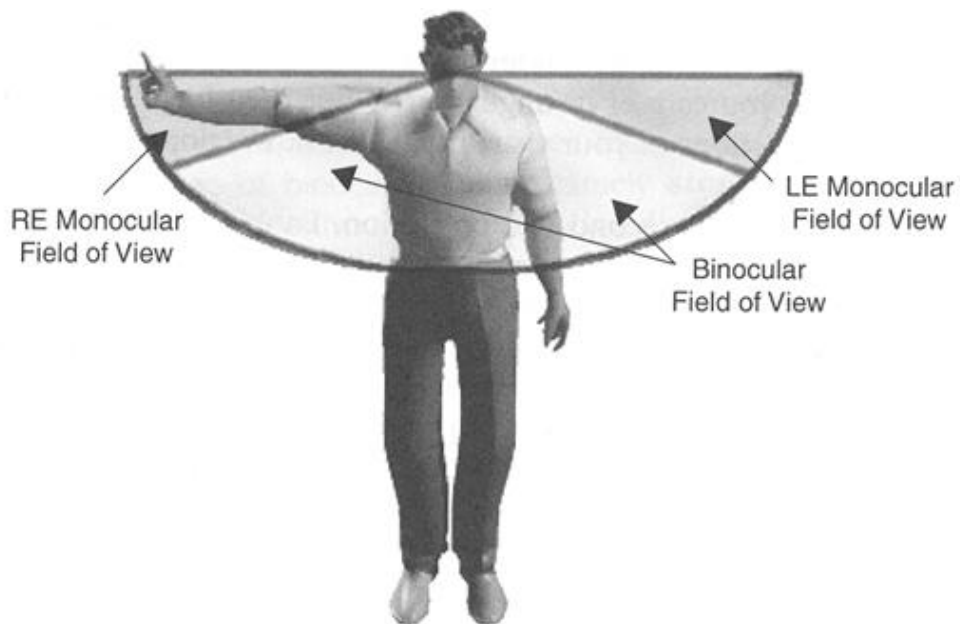


Figure 2: Binocular field of vision. The lighter area in this man's central vision represents the wide range of binocular overlap in the viewing field of animals with forward-facing eyes. Adapted from Steinman et al 2000.

the forehead (Fig. 3). This cyclopean “average” of the images being seen by the two eyes is only part of our binocular vision. Due to the interocular distance, the distance between the visual axes of the two eyes, the images projected onto the retina of each eye are slightly displaced from one another. These displacements, called disparity, are directly correlated to the distance between the observer and the objects in the visual scene. Our visual system detects the relative disparities between the objects in the scene, and translates them into a percept of relative depth: stereopsis. Precise alignment of the slightly differing views of the two eyes is critical for cyclopean perception, stereopsis, and avoidance of diplopia, or double vision, of the object we are looking at.

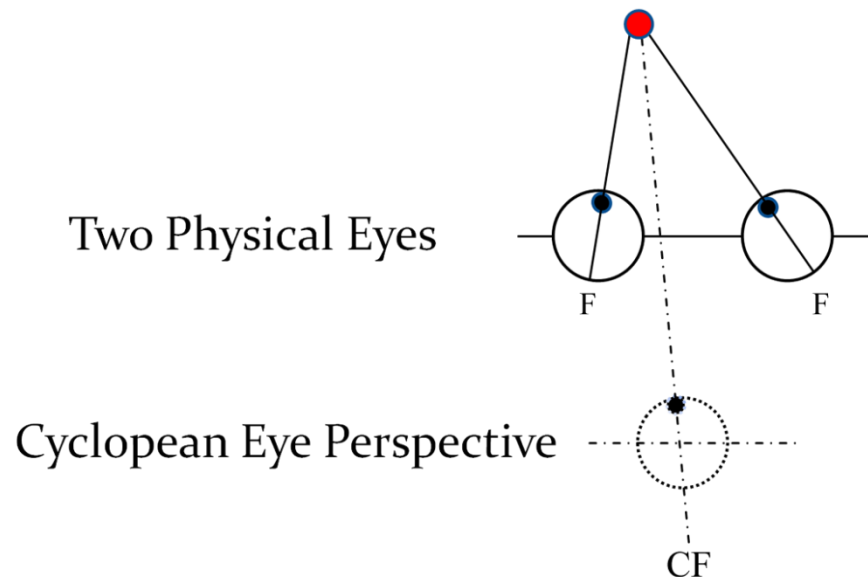


Figure 3: Cyclopean perspective. The two eyes are focused on the visual image of the red dot (top). Perceptually these two views are merged into a single image, as though the target were being viewed by a cyclopean eye located centrally between the two eyes (bottom). F: right-eye and left-eye foveae. CF: cyclopean fovea.

Binocular vision has a major advantage with respect to panoramic vision: a vastly improved three-dimensional percept of the surroundings, but it is also very demanding with regard to the precision of the movements of the two eyes. Between 2 and 4% of the US population has an impairment of their binocular alignment (Hillis et al 1983, Preslan and Novak 1996) that directly impacts their stereopsis, or perception of relative depth, which is often permanently lost or never developed (stereoblindness). How then do the visual and oculomotor systems produce this precise relative alignment? A monocular solution, in which each eye is managed independently, is not the most neurally or computationally efficient. Each eye can rotate by a magnitude of 60° or more, while disparity-related alignments often require adjustments of only fractions of degrees. A monocular organization would require circuitry with very high signal-to-noise ratio and very high positional resolution. Furthermore, since only monocular error information would be available, a monocular solution would pose quite a challenge to determining whether or not a precise binocular alignment had been achieved. Any slight gain change in either of the monocular systems (left eye or right eye) would be very disruptive. Instead, the primate binocular visual system uses an independent oculomotor system that can directly convert disparity information into vergence eye movements, changes in the angle between the two eyes, to control binocular alignment. As will be described in greater detail later, the primate has two vergence sub-systems – a coarse vergence system and a locking vergence system. The coarse vergence system has a wide functional disparity range, allowing for the adjustment of large disparity misalignments. The locking vergence system rectifies smaller disparities and precisely superimposes, or “locks”, the images of the right and left eyes together with the precision needed to activate

stereoscopic vision. The rotations of the cyclopean perspective (Fig. 3) are left to be accomplished by other systems through conjugate eye movements.

The existence in humans of separate vergence and conjugate systems was postulated by Hering in 1868 with his law of equal innervation, which states that all eye movement commands are the sum of paired conjugate and vergence commands. The conjugate commands rotate both eyes by the same amount in the same direction, and therefore control the orientation of the cyclopean eye. The vergence commands rotate both eyes by the same amount in opposite directions, and therefore control the angle between the right and left eyes. Internuclear ophthalmoplegia (Cogan 1970, Gamlin et al 1989), a phenomenon in which the subject is unable to rotate the eye toward the nose during conjugate eye movements but retains a full range of convergence, was later seen as strong clinical evidence for a separation between conjugate and vergence pathways to the oculomotor motoneurons that drive the medial rectus muscles. It is worth noting that Chen et al (2011) recently challenged this view with the observation that monocular saccadic signals better fit their data. Several behavioral observations also alluded to the possibility of separate systems. To name a few:

- Monocular saccades lack the gain precision required for monocular-based binocular alignment.
- Vergence eye movements have much slower dynamics than saccadic eye movements, which are conjugate rapid transfers of gaze.
- The direct functional link between vergence, accommodation, and pupillary responses suggests a specialized triad for viewing in depth.

- Monocular adaptation studies of the saccadic system in which one eye is adapted while the other eye is patched, show that the patched eye responds to the adaptation just as the visually adapted eye, implying the saccadic system is conjugate in nature.

The first explicit neural evidence for a distinct vergence system in primates was not published until 1984 (Mays). This finding was subsequently expanded upon by a string of other publications that followed during the mid 1980's and early 1990's (Cumming and Judge 1986; Judge and Cumming 1986; Mays et al 1986; Mays et al 1991; Zhang et al 1991; Zhang et al 1992). Thus, beginning with the 1984 publication by Mays, many points of evidence have emerged to support the view that the primate oculomotor system is comprised of independent conjugate and vergence systems, as stated by Hering's law of equal innervation. The notion that all eye movement commands in the primate are the sum of conjugate and vergence commands became widely accepted in the oculomotor field. Under this paradigm, conjugate commands control the orientation of the cyclopean eye, while vergence commands control alignment in depth.

The neuroanatomy of the subcortical oculomotor pathways fully supports Hering's proposal of a conjugate/vergence schema. Note the separation of the vergence pathways from the conjugate saccadic, vestibular, optokinetic, and smooth pursuit pathways in Fig. 4. For example, the medial vestibular nucleus (MVN) is activated during vestibular, optokinetic, and smooth pursuit movements. In addition to sending inhibitory input to the ipsilateral abducens nucleus (CNVI), the MVN also sends excitatory input to both the contralateral abducens nucleus (CNVI) and to the ipsilateral oculomotor nucleus (CNIII)

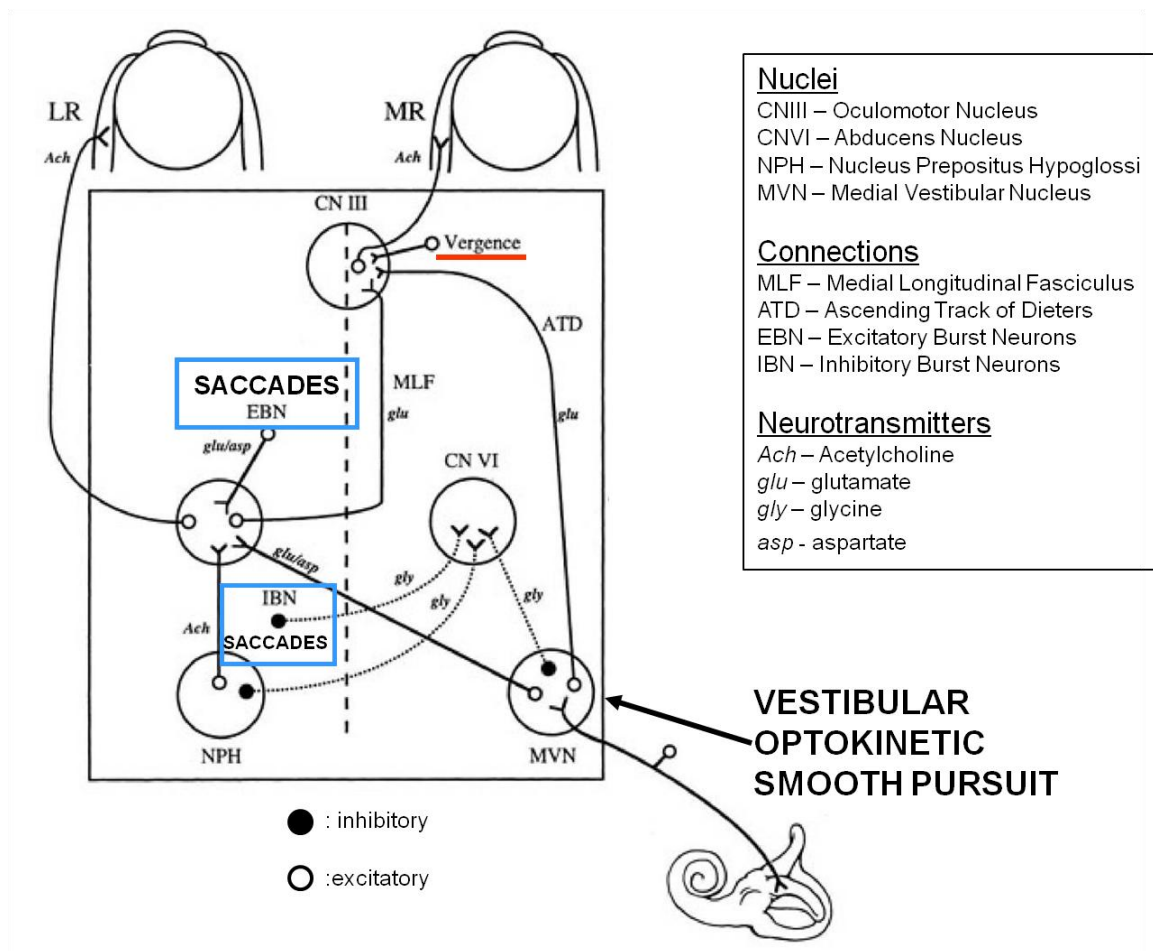


Figure 4: The neuroanatomy of the horizontal subcortical oculomotor pathways. Each connection and nucleus has a contralateral counterpart, which is not shown, with the exclusion of the abducens nucleus (CN VI), where both nuclei are shown. Adapted from Leigh and Zee 2006.

through the ascending tract of Dieters (ATD), the function of which is poorly understood. However, Chen-Huang and McCrea (1998) reported that the modulation of neurons in this pathway is correlated with viewing distance, and it has been shown that two types of vestibular signals – linear vestibulo-oculomotor response and short-latency ocular following responses – are inversely correlated with viewing distance (Schwarz et al 1989). During horizontal saccades, excitatory burst neurons (EBNs) send commands to the ipsilateral abducens while the inhibitory burst neurons send input to the *contralateral*

abducens in accordance with Sherrington's law of reciprocal inhibition (Sherrington 1894). The medial longitudinal fasciculus (MLF) pathways then carry copies of the activity of each abducens nucleus to the correspondent contralateral oculomotor nucleus, thus satisfying Hering's law of equal innervation. Notice that the vergence system gives excitatory input directly into the horizontal area of the oculomotor nuclei, which control the medial rectus muscles, independently of these other pathways. This schema well explains internuclear ophthalmoplegia as a specific damage to one or both of the MLF pathways. There is a loss of crossed signaling from one or both abducens nuclei to the associated contralateral oculomotor nucleus, but this alters only the conjugate responses. Vergence remains unaffected. It is also important to point out that the abducens nuclei, which control the lateral rectus muscles, do receive input from the vergence system (Mays 1984), as would be required by Sherrington's law of reciprocal inhibition. However, it is not known from where within the vergence circuitry.

Of course, even under this model of strict segregation of vergence and conjugate oculomotor commands, both signal streams must reach the same final destination: the oculomotor muscles. This reality requires the eventual merger of these two signals, which does occur within the oculomotor and abducens nuclei at the level of the motoneurons and interneurons, which in turn deliver the signal to the oculomotor muscles (Mays and Porter 1984; Gamlin and Mays 1992). However, several types of muscle fibers exist within the extraocular muscles (Wasicky et al 2000). Some of these fibers are more optimized for slower movements, such as: vergence eye movements, smooth pursuit, vestibular and optokinetic responses, and tonic contractions, while others are more suited to saccadic ultra-fast contractions. These muscles are also segregated into orbital and

global layers. The global layers are the acting movers of the globe of the eye, while the orbital layers control the lines of actions of the muscles through muscle pulleys (Miller 1989; Miller 2007). Together, these features suggest that there may be some level of specialization regarding the distribution of oculomotor commands at the level of the muscle fibers, but the oculomotor field has only recently begun to address this matter.

Less is known about possible additional upstream locations where these signals may interact. Since the majority of eye movements made in the natural environment are neither strictly conjugate nor strictly vergence, there will necessarily be co-activations of conjugate and vergence systems. These co-activations produce responses which possess very different properties and dynamics than would be expected by a simple linear summation (Busettini and Mays 2005a; Zee et al 1992; Collewyn et al 1995), making it quite difficult at times to distinguish between these two combined signals. To further complicate the matter, some of these interactions may be interpreted as deviations from Hering's law of equal innervation, and the manifestation of some forms of monocular encoding. Binocular versus monocular encoding will be the focus of this dissertation.

Three paradigms are often used to generate what appear to be deviations from Hering's law. The first is transfer of gaze between stationary objects located at different cyclopean angles and depths, which is achieved by a combination of vergence and saccadic responses. During the saccade there is an acceleration of the vergence response (Busettini and Mays 2005a; Zee et al 1992; Collewyn et al 1995). There is an intense debate about whether this acceleration is an actual acceleration of the vergence system related to the ongoing saccade, or the result of disconjugate (monocular) saccadic commands to the two eyes. (For an in-depth review, see King 2011 and Cullen and Van

Horn 2011). The latter would imply that the saccadic system is not a conjugate system in a strict sense. The evidence regarding a monocular organization of the saccadic system, which supports the view that the intrasaccadic acceleration in the vergence response is the result of monocular asymmetric commands to the two eyes, is briefly reviewed here.

In the key study by Van Horn et al (2008), the authors compared the firing characteristics of saccadic long-lead and short-lead burst neurons during conjugate saccades and during combined saccadic-vergence eye movements. These cells carry the saccadic velocity burst to the oculomotor plant and most likely encode the entirety of the saccadic command. Stimulation of the omnipause neurons, which cause inhibition of these cells, stops a saccade from occurring and interrupts an ongoing saccade in midflight (Gandhi and Keller 1999). Thus, the analysis of the activity of the premotor excitatory and inhibitory saccadic burst neurons is critical for understanding the behavior of the saccadic system. For the vergence system, the cells of crucial importance are the midbrain vergence cells. Consistent with the findings of Zhou and King (1998), Van Horn et al (2008) found that a slight majority of the burst cells better correlated with the behavior of the ipsilateral eye rather than the version component of the movement. Hering's law of equal innervation requires the (conjugate) saccadic system exclusively encode the version component of the movement.

Several issues remain unresolved. A 5 ms Gaussian kernel was used to compute the spike density function. This approach has a strong filtering effect, and it is unclear how this might have affected the dynamic analysis. Modeling the dynamic transformation of firing behavior into the oculomotor response with separate dynamic blocks, as in our study, would have yielded results based on a more punctilious

representation of the original data. Additionally, the combined movements of this study were limited to those during which both eyes moved in the same direction. According to current saccadic models, saccadic-driven eye movements in which the two eyes move in opposite directions are necessarily accompanied by an ongoing vergence response. At this time, there is neither behavioral nor neuronal evidence that the superior colliculus is capable of generating opposite-direction saccades, or even disconjugate for that matter. Various types of stimulations, single-site single side (Schiller and Stryker 1972), dual-site single-side, or even simultaneous both-side stimulations, result in conjugate vector-average saccades, unless there is an ongoing vergence response (Chaturvedi and Van Gisbergen 1999, 2000). The co-occurrence of a vergence response is necessary to generate intrasaccadic asymmetries.

Although previously published results showed the degree of intrasaccadic vergence enhancement to be directly related to saccadic dynamics (Busettini and Mays 2005b), the Van Horn (2008) work did not attempt to address any relationship of the firing behavior to vergence dynamics. Perhaps, their characterization of cells according to monocular, binocular, and conjugate groups (Table 1 in Van Horn et al 2008) could have been better accomplished by describing them according to their vergence-related sensitivity. For example, conjugate cells, which would code version during both purely conjugate movements and combined movements, would show no sensitivity to changes in the vergence aspect of the movement. This approach would not forcibly assume a monocular interpretation of the data. Also, the previously reported fact that an ongoing vergence movement can affect the version dynamics of a saccade (Collewijn et al 1995) was not addressed. Walton and Mays (2003) reported an unspecific suppression of the

saccadic burst cells during both convergence and divergence and no shifts in the motor fields of the cells consistent with a monocular encoding. These observations, when added to the vector-averaging results of microstimulation, strongly imply a lack of monocularity in the superior colliculus cells, which are the main inputs to the long-lead and short-lead burst tonic cells (Scudder et al 1996).

In a later paper (van Horn and Cullen 2008), a dissociation of version and (horizontal) vergence components using combined vergence and vertical saccades was attempted. As was illustrated by Busetini and Mays (2005b), vertical saccades elicit an enhancement in the vergence dynamics very similar to that caused by horizontal saccades. The majority of horizontal burst neurons are not responsive during pure vertical saccades, and Hering's law would predict them to also be unresponsive during combined movements vergence and vertical saccades, which show no change in horizontal version. The data reported by Van Horn and Cullen (2008) indicated this was not the case; the cell fired in relation to the horizontal vergence transient. In the monocular case, the vergence enhancement caused by the vertical saccade would be saccadic, and therefore encoded by the horizontal burst cells. It is important to note that when a purely vertical saccade is introduced during an ongoing vergence movement, the rotation of the two eyes is equal in magnitude but opposite in direction, and these directions switch for convergence relative to divergence. This scenario, a true test of this experimental design, was not addressed in the publication. To date, there is no known mechanism within the saccadic system that allows for oppositely directed bursts in the two eyes. No data exists describing the behavior of the superior colliculus during this situation. The expected results of a study of this nature of the superior colliculus range from a monocular co-activation of both sides

to complete silence. The former would have the superior colliculus breaking the vector averaging rule, while the latter would indicate an alternative extra-collicular saccadic pathway, likely from cortex or the cerebellum.

The second paradigm often used to generate what appear to be deviations from Hering's law is related to the first. The smooth vergence following the saccade is sometimes not symmetric. Even more specifically, Enright (1996) reported slow-velocity asymmetrical vergence responses in the absence of saccades. While this can be interpreted as a co-activation of the conjugate smooth pursuit system, it can also be seen as unequal vergence commands being sent to the two oculomotor nuclei. This time the vergence system is breaking Hering's law. The third case is asymmetric smooth tracking, for example, one target moves away from the subject while maintaining alignment with one eye. In this task, called the Müller paradigm, often only one eye moves. It was proposed that asymmetric smooth vergence tracking is actually a special case of monocular smooth pursuit (King and Zhou 1995). This assumes the smooth pursuit system is not a conjugate system as would be expected by Hering's law.

Given these apparent contradictions, it is not surprising that some researchers doubt the strict segregation between the conjugate and vergence systems, suggesting that these systems may instead be carrying monocular signals. In the extreme interpretation of this view, the conjugate responses are simply special cases of monocular signaling in which the two monocular signals are identical and of the same sign, and symmetric vergence responses are special cases in which the monocular signals happen to be equal and of the opposite sign. Another more commonly held belief is that the conjugate systems are normally conjugate but can break conjugacy under certain conditions, and

similarly, the vergence system is usually symmetric but can also become temporarily asymmetric. For example, the vergence system might send an asymmetric command if the fovea of one eye is already on target and a symmetric command would drive that eye away from the target. As another example, the saccadic system could become momentarily disconjugate during saccade-vergence interactions by sending asymmetric commands to the two eyes.

One group of researchers studied the motoneurons of the oculomotor nucleus, the neurons of the central mesencephalic reticular formation (cMRF), and the burst-tonic neurons of the nucleus prepositus hypoglossi (NPH in Fig. 4), which is considered the site of the horizontal conjugate neural integrator of the excitatory and inhibitory burst commands being sent to the abducens nuclei, and declared that the majority of cells in these areas preferentially encode the velocity and position of a single eye (Sylvestre and Cullen 2002; Sylvestre et al 2003; van Horn and Cullen 2009). A detailed review of the work of this group can be found in Cullen and van Horn (2011). Similar observations were made by Zhou and King (1998). Based on behavioral data, King and Zhou (1995) suggested that smooth pursuit is a response to monocular retinal slip. Interestingly, the superior colliculus, the most appropriate center for the coding of asymmetric saccades during these types of movements, did not show any clear evidence of 3-dimensional organization (Walton and Mays 2003; Chaturvedi and van Gisbergen 1999; van Opstal et al 1991; van Gisbergen et al 1987).

This dissertation aims to address two specific issues of this rather spirited debate:

1) The behavior of midbrain vergence responses to stepwise changes in depth. The evidence that the saccadic-vergence interaction is a saccade-related vergence enhancement and not the result of monocular saccadic commands resides in the observation that some midbrain vergence cells have an increase in firing during the intrasaccadic period of combined vergence-saccadic responses. (Mays and Gamlin 1995; Mays and Gamlin 2000). This preliminary evidence has never been fully analyzed. We will use an unconventional approach to address this issue. In a first step, we will estimate a dynamical model of the cell using only smooth vergence trials with no saccadic responses. This model will attempt to predict the smooth vergence response from the cell firing. We will then input the firing of the cell during combined saccadic-vergence responses into the same model to see how well it predicts the intrasaccadic vergence acceleration. Smooth-only cells will ignore the enhancement and simply follow a smooth-only profile. Busetini and Mays (2005b) demonstrated that the post-saccadic smooth vergence accounts for the preceding enhancement, whatever its source, with a very short non-visual latency correction, indicating the existence of an internal non-visual vergence feedback loop. We will try to determine from the firing of smooth-only cells the actual latency of this correction. During very strong asymmetric post-saccadic responses we will also be able to determine if the vergence cells continue to encode the symmetric vergence or become monocular.

2) Smooth oblique tracking of a target in depth. This aim will analyze the behavior of midbrain vergence cells during oblique tracking in depth. This will directly test the hypothesis that visual tracking in depth may be under monocular control rather than binocular (Zhou and King 1995). Recordings in frontal eye fields of the cortex have found cortical cells that code these movements in three dimensional space (Fukushima et al 2002), which would be consistent with a monocular mechanism. Two years earlier, Gamlin and Yoon (2000) reported the discovery of a vergence area located elsewhere in the frontal eye fields. It has also been reported (Judge and Cumming 1986) that midbrain vergence cells do not fire or change their activity during fronto-parallel (i.e., conjugate) tracking. They clearly fire for pure tracking in depth by definition, but there are no data regarding their behavior during oblique tracking, where, according to the binocular hypothesis, a co-activation of vergence and smooth pursuit tracking is expected. Is the vergence cell firing consistent with a simple vector decomposition of the movement in fronto-parallel and in-depth components?

BACKGROUND & SIGNIFICANCE

The introduction presented the basic concepts pertaining to binocular vision and conjugate and vergence systems. Since the focus of this dissertation is on the vergence system, specifically the behavior of midbrain vergence responses to stepwise changes in depth and smooth tracking of a target moving along an oblique trajectory in depth, this section will concentrate on the vergence system, its organization, and how this dissertation will contribute to the knowledge of its neural circuitry and function.

Current knowledge of the vergence circuitry

Fig. 5 shows that our knowledge of the vergence system is still quite fragmentary, particularly in regard to the interconnections between the areas showing vergence-related activity. For example, the schematic in Fig. 5 shows five inputs to the supraoculomotor area (SOA), four of them being represented by question marks to denote that the current understanding of these connections is incomplete.

The cerebellum plays an important role in vergence and accommodation (Gamlin et al 1996), as is evident in patients with cerebellar lesions (Sander et al 2009). May et al (1992) have reported that the fastigial (F) and interpositus nuclei (IP) of the cerebellum have reciprocal connections with the supraoculomotor area (SOA), which is one of the targets of our single unit recordings. Little is known about the function of the fastigial nucleus in vergence or accommodation, although Gamlin and Zhang (1996) showed that

lesions in the fastigial oculomotor region cause vergence anomalies. The posterior interposed nucleus has a burst-tonic firing pattern related to divergence and far accommodation (Zhang and Gamlin 1998). The nucleus reticularis tegmenti ponti (NRTP) has a preferential burst-tonic activity related to convergence and far accommodation (Gamlin and Clarke 1995). The Edinger-Westphal (EW) nucleus drives accommodation (Gamlin et al 1994).

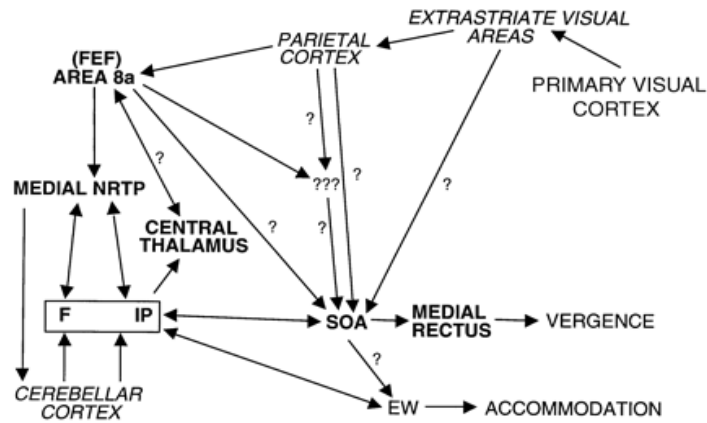


Figure 5: A schematic representation of the connections of the primate vergence system. The question marks denote areas lacking complete information.

As we illustrated in the introduction, the main drive of vergence eye movements is disparity. One aspect regarding the sensory processing of the vergence system that remains unclear concerns the difference in disparity detection associated with the coarse system versus the locking system. The disparity detectors in the visual areas V1, V2, MT, and MST (Barlow et al 1967; DeAngelis 1998; DeAngelis and Newsome 1999; Hubel and Wiesel 1970; Hubel and Livingstone 1987; Maunsell and Van Essen 1983; Poggio

and Fischer 1977; Poggio and Talbot 1981; Poggio et al 1985; Poggio et al 1988, Roy et al 1992; Takemura et al 2001; Eifuku and Wurtz 1999) have a very restricted functional range of one to three degrees (Fig. 6). If those signals are driving vergence responses, they are active only during the locking mechanism. These short range movements occur within a very limited time scale, earning them the label of short latency or ultra short latency. These ultra short latency vergence responses have been shown to be mediated by the medial superior temporal area (MST) and also to be true symmetric vergence responses, exhibiting the coordinated movement of both eyes even during looming and monocular stimulation (Busetini et al 1996; Busettini et al 1997; Busettini et al 2001). When shifts in depth of 1 to 2 degrees are applied to anti-correlated random dot patterns, these responses invert their sign and occur without the subject even perceiving the depth change, implicating a short-range, early stage disparity computation as the impetus for these motor adjustments (Masson et al 1997, Cumming and Parker 1997). MST neurons show significant sensitivity to vergence (Inoue et al 1997), and MST has been implicated as a driving force of the short latency vergence response through deficit studies involving ibotenic acid injections and bilateral MST lesions (Takemura et al 2001; Takemura et al 2007).

None of these short latency cells can detect disparities above one to two degrees. The coarse system can measure disparities as large as 30 degrees or more. The current hypothesis is that, in this case, the brain is looking for plausible disparity rectifications on a much wider range using some kind of long-range feature-matching algorithm between similar elements in the images from the two eyes. The vergence area in the frontal eye

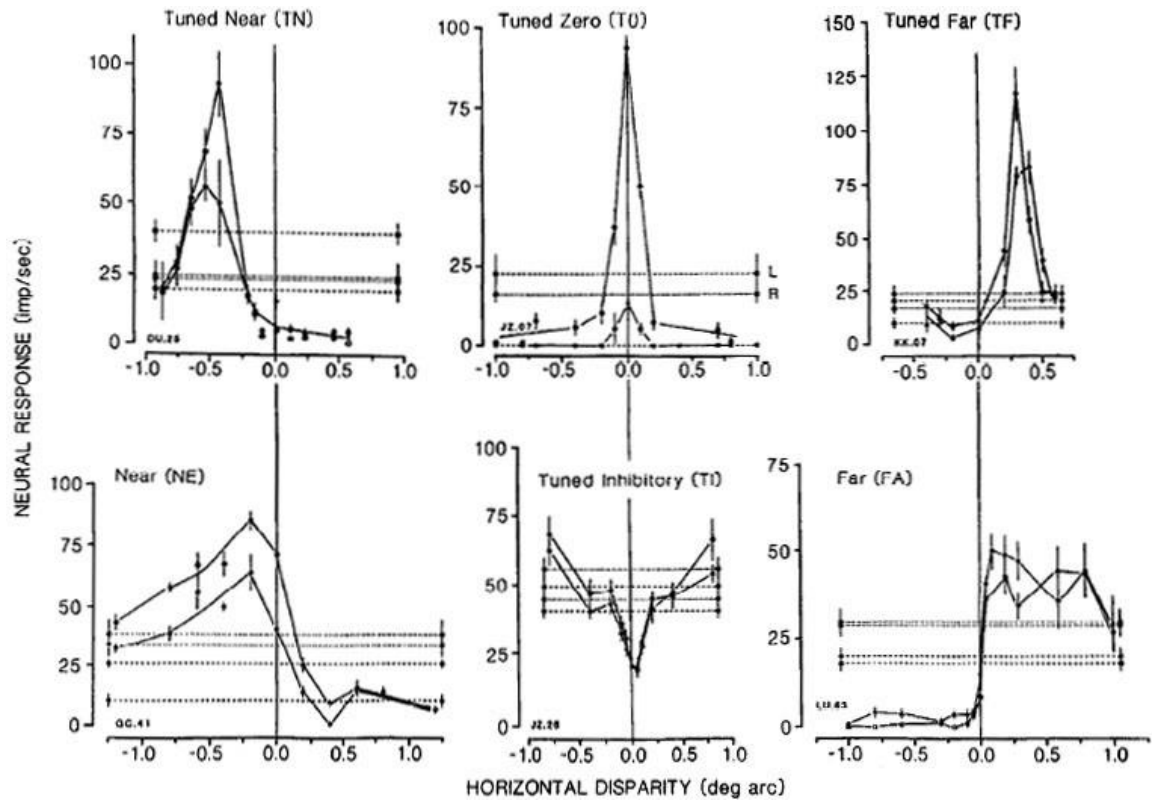


Figure 6: Sensitivity profiles of disparity detecting neurons. These disparity detecting neurons found in areas V1, V2, and V3-V3A of monkey visual cortex, all having a range of 1° or less. Adapted from Poggio et al 1988.

field (FEF) has cells that clearly encode vergence eye movements driven by long-range disparities (Gamlin and Yoon 2000). At this time, there is no indication that they do not also encode short-range locking vergence responses, although the ultra short latency vergence responses described earlier are likely routed downstream before reaching FEF. These reflexive responses are driven by MST, which can directly transmit oculomotor commands downstream through the dorsolateral pontine nuclei (Kawano et al 1992) to the ventral paraflocculus (Shidara and Kawano 1993) without involving FEF, a control center for voluntary eye movements. These two works are focused on the ultra-short latency ocular following, which is a short latency conjugate response comparable to the

short latency vergence response. A specific study of the behavior of FEF, dorsolateral pontine nuclei, and ventral paraflocculus during ultra-short latency vergence responses is not available, and we cannot totally exclude that the vergence responses actually use other cortical and subcortical pathways. Do these vergence-related FEF cells simply encode a visual disparity error (i.e., do they contribute to the driving of the vergence visual feedback loop?), or do they also receive a copy of the downstream vergence motor command and adjust their behavior in real time using both sensory and motor information, making them part of the internal feedback loop? Furthermore, how do these signals reach the subcortical vergence areas? There is still much to be learned regarding these vergence-related FEF cells.

Something more, but not much, is known about the subcortical circuitry. For example we have evidence of cells (vergence burst cells) that code the dynamics (velocity) of the vergence command and cells (vergence tonic cells) whose firing is directly correlated to vergence angle (Mays 1984; Mays et al 1986; Judge and Cumming 1986). The tonic signal is updated during every vergence movement by adding the integration of the vergence burst command, which has been integrated by the vergence neural integrator, to the pre-existent tonic activity of the tonic cell. Where and how this integration is achieved is not known. In 2005, Busetini and Mays (2005b) showed that the vergence system has a local feedback system similar to the one suggested for the saccadic system. Although it likely involves the cerebellum, we have no information as to where it might be located. There is also strong evidence for interactions between the vergence and the saccadic systems, but we do not know where they occur or if they are even inside the vergence system, which is one of the key questions this dissertation will

try to address. The neuroanatomical location of the portion of the vergence system providing the most well defined, well characterized neural correlation to vergence behavior is found in the midbrain. These midbrain vergence cells were the targets of our single unit recordings. They are the ideal targets to precisely quantify the behavior of the vergence system during stepwise transfers of gaze in three dimensions and smooth tracking along oblique trajectories in depth and to identify possible monocular contributions from the other oculomotor systems.

Midbrain Vergence Cells

Two groups of vergence cells have been described previously in the monkey midbrain (Fig. 7). One group of these midbrain vergence-related cells is localized in the mesencephalic reticular formation (MRF) just above the oculomotor nucleus (Mays et al 1986; Bruce and Cumming 1986; Zhang et al 1991, 1992), and is so named the supraoculomotor area (SOA). The second group is located just slightly more superficially (Mays et al 1986), in front of the superior colliculus. This is often termed the dorsal area. Unpublished preliminary data shows evidence of at least two other locations, one near the abducens nucleus and one near the saccadic omnipause neurons. Unfortunately, nothing is known about their functions or connections. However, the cells near the abducens nucleus likely influence the firing rate of the abducens motoneurons during vergence, increasing during divergence and decreasing during convergence. A direct influence from the SOA or the dorsal areas is also possible. Since the number of cells recorded in these areas during this study is insufficient for a proper characterization of these regions, the present examination will be limited to the dorsal and SOA

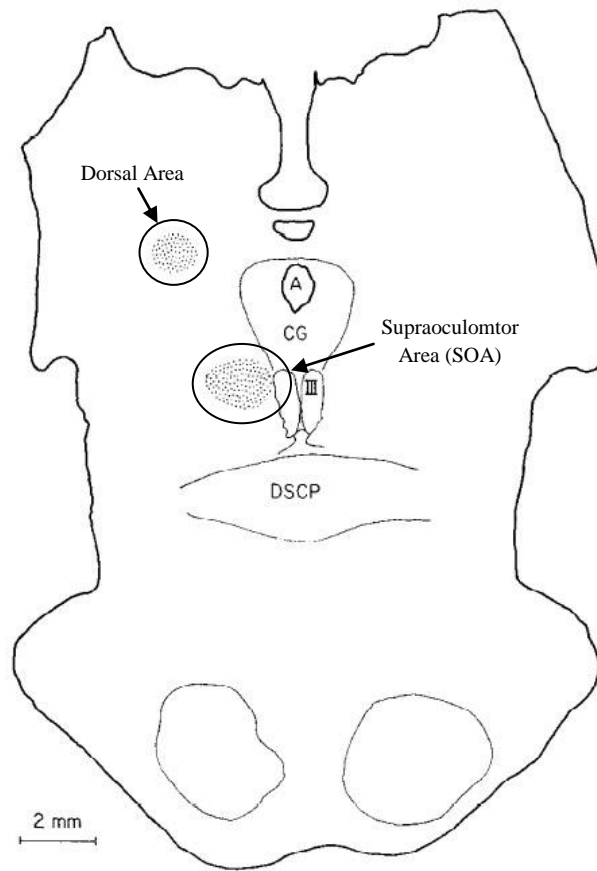


Figure 7: Midbrain vergence cell locations. Midbrain vergence cells appear clustered in two distinct regions, the dorsal area and the supraoculomotor area (SOA). A: aqueduct, CG: central gray matter, III: Oculomotor nucleus, and DSCP: decussation of superior cerebral peduncle. Adapted from Mays 1986.

areas. There is no known difference in behavior when comparing SOA and dorsal groups, although their target neurons and source of inputs are likely different. However, it should be noted that no detailed dynamic analysis has ever been performed. The three identified patterns of vergence cell firings are common to both areas. Vergence burst cells (Fig. 8) dynamically encode changes in vergence position, i.e., velocity, and only fire during the

course of the vergence eye movement. Tonic vergence cells have a firing frequency linearly related to the vergence angle (Fig. 9). Burst-tonic cells have both a dynamic and a tonic component. Most of these cells show no bursts of activity in association with conjugate saccadic eye movements, as in the example in Fig. 8. The tonic firing of the tonic and burst-tonic cells is also invariant with the conjugate position of the eyes exclusively encoding the vergence angle, i.e. the angle between the two eyes. The fact that both areas present cells with tonic firing related to the vergence angle (tonic and burst-tonic cells) is a remarkable difference from the conjugate systems, where the tonic component from the conjugate neural integrators is added to the burst signals at the level of the motoneurons. In the vergence system the tonic component is added within the vergence systems.

Initially, divergence was assumed to be a simple relaxation of convergence, supported by the fact that divergence eye movements are slower than convergence eye movements (Hung et al 1986). However, in the two aforementioned vergence areas of the midbrain, there are both convergence and divergence cells, both of which burst and/or increase their tonic firing during their respective type of movement, indicating that divergence is an active process (Mays 1984 and Mays et al 1986). Convergence burst-tonic cells often cease firing during the dynamic part of a divergence eye movement, and their tonic firing subsequently resumes at a lower level, in accordance with a reduction in the convergence angle. Similarly, divergence burst cells often stop firing during the dynamic phase of a convergence movement and also decrease tonic firing following the movement, in accordance with a reduction in the divergence angle. Interestingly, no

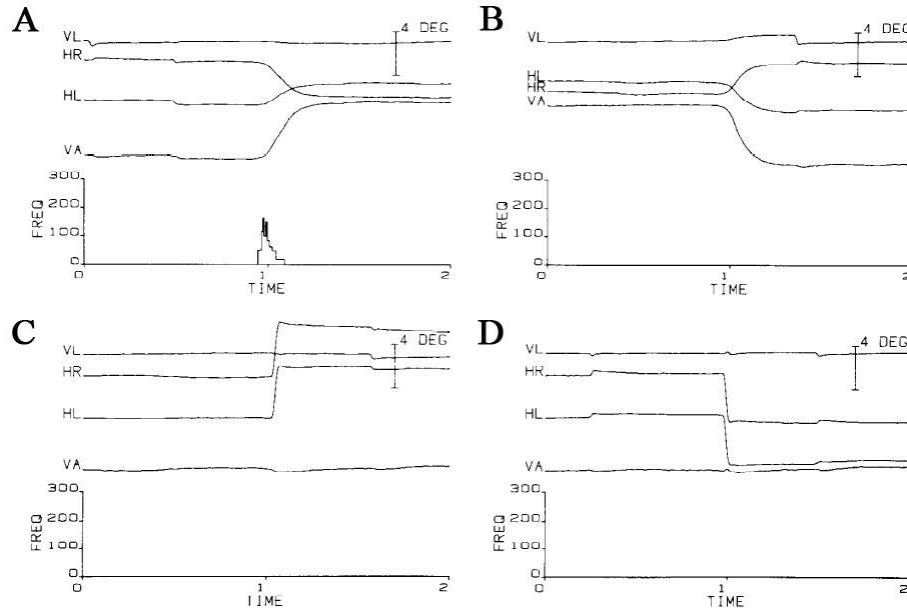


Figure 8: Convergence burst cell behavior. A) a convergence eye movement, B) a divergence eye movement, C) a rightward horizontal saccade, and D) a leftward horizontal saccade. Time is plotted in seconds and spike frequency (FREQ) is shown in spikes per second. Notice that this cell does not fire during divergence movements or conjugate horizontal saccades. Adapted from Mays et al 1986.

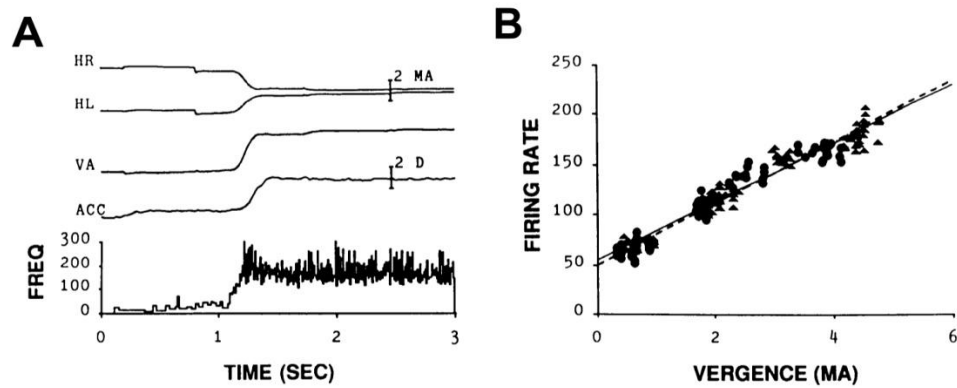


Figure 9: Tonic cell firing. The tonic firing in the tonic and the burst-tonic cells is linearly related with the vergence angle. Time scale is plotted in seconds and spike frequency is plotted in spikes per second. ACC is the accommodation of the animal in diopters (D). The vergence angle is given in meter angles (MA). Adapted from Zhang et al 1992.

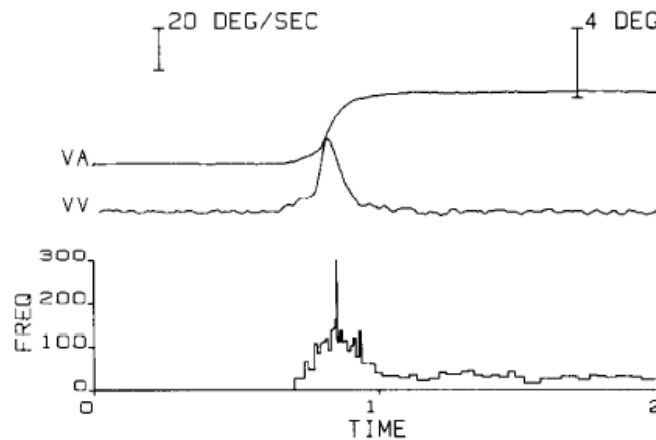


Figure 10: Burst-tonic cell firing. Activity of a convergence burst-tonic cell during a convergence eye movement. Time scale is plotted in seconds and spike frequency (FREQ) is plotted in spikes per second. Adapted from Mays 1986.

evident segregation between near (convergence) and far (divergence) cells has been reported within the two groups. The functional role of the divergence cells is likely associated with the observation that while medial rectus muscles must actively relax during divergence and actively contract during convergence, lateral rectus muscles must do the opposite and actively relax during convergence and actively contract during divergence, as is required by Sherrington's second law of reciprocal inhibition (Sherrington 1894). It is possible that these cells participate in modulating this relationship between convergence and divergence. For example, it could be that during convergence eye movements, as convergence cells have an excitatory effect on the motoneurons of medial rectus muscles, these same convergence cells could also in turn have an inhibitory effect on the lateral rectus muscles through inhibitory interneurons. Similarly, divergence cells might have the inverse of this relationship where they would have an inhibitory effect on the motoneurons of the medial rectus muscles, and an

excitatory effect on the motoneurons of the lateral rectus muscles through excitatory interneurons. While we do not have knowledge of the inhibitory or excitatory nature of the output of the divergence neurons found in SOA and dorsal groups, there is evidence, from antidromic activations, of direct excitatory monosynaptic connections from SOA convergence burst-tonic cells to ipsilateral medial rectus motoneurons (Zhang et al 1991). The neural targets of the dorsal area are not known.

Despite the need for lateralization with respect to the medial and lateral rectus muscles, there is no right-brain/left-brain lateralization between convergence and divergence neurons. Even more puzzling, there is currently no evidence of any kind of ipsilateral segregation at the midbrain or brainstem level. This is similar to the organization of the saccadic vertical burst neurons in rostral interstitial medial longitudinal fasciculus (riMLF), where upward and downward burst neurons appear to be clustered together on either side of the neural midline, while their torsional components are segregated. The right riMLF encodes clockwise torsion and the left encodes counterclockwise torsion (Leigh and Zee 2006).

For all conjugate systems, the premotor signals are a burst of activity, i.e. velocity pulse signals, and their last-stage burst cells connect directly to their associated motoneurons, the abducens in the horizontal case. A copy of their bursts is sent to the conjugate neural integrators, the tonic outputs of which are sent back to the motoneurons, which act as summators. This tonic component is responsible for holding the eyes in the new conjugate position at the end of the movement. As described by Robinson (1975), this pulse-step combination dramatically improves the movement dynamics, particularly for the saccadic eye movements, when compared with what would be expected from the

step alone. However, at this time, there is no evidence that vergence burst cells do the same. Within the vergence system, the burst signals, traveling from burst cells, and the tonic signals, traveling from the vergence neural integrator, appear to merge at the burst-tonic cells of the SOA before the combined signal is sent to the motoneurons. The presence of burst-tonic cells in every vergence-related area identified so far in the cerebellum, midbrain, and brainstem, suggests that vergence tonic signals might have additional functions besides just holding the new vergence angle at the end of an in-depth eye movement.

Vergence activity is also found in the trochlear motoneurons, which innervate the superior oblique muscles. While studying the relationship between vergence and excyclotorsion, the outward rotation of the eye around the principal visual ray, Mays et al (1991) found trochlear motoneuron activity to decrease with convergence for all cells recorded. The authors suggested that the excyclotorsion seen during convergence, and perhaps the lateral translation of the eye, is due to a relaxation of the superior oblique muscle. This relaxation during convergence was found to be greater than that which accompanies similar conjugate eye movements, implying the remainder is attributed to vergence activity.

Vergence Accommodation Cross-Talk and the Near Triad

When changing fixation in depth in natural environments, the demand for changes in both accommodation and vergence co-vary. Blur cues elicit accommodation, a change in lens curvature, and disparity cues elicit vergence, a change in the angle between the

two eyes. According to the Dual Interaction Model (Semmlow and Heerema 1979; Schor 1979; Zhang et al 1992), the blur controller directly stimulates the accommodation plant and sends a copy of its signal to the vergence plant, while the disparity controller directly stimulates the vergence plant and sends a copy of its signal to the accommodation plant (Fig. 11). As demonstrated by Miles et al (1987), these cross-talks are highly adaptive, being able to adjust for optically induced displacements in vergence of up to 8° in just 30 minutes.

The highly adaptable nature of this small network is not too surprising given the natural changes in the interocular distance during growth, and consequently the need to recalibrate the gains of the cross-talks fairly often throughout development. As the head grows during development, the interocular separation, the separation between the eyes, increases. As the interocular separation expands, so does the vergence angle required to fixate a target. Another way to think of this geometry would be to imagine an isosceles triangle in which the two equal sides are created by the distance between each eye and the target. The base represents the interocular separation. As the base of the triangle, the interocular separation, expands, the opposite angle, in this case, the vergence angle, also necessarily increases. Since the accommodation requirement is maintained regardless of interocular distance, this scalar change in vergence requirements inevitably affects accommodation signaling due to the crosstalk between vergence and accommodation. Therefore, a recalibration of the gains of the cross-talk pathways between vergence and accommodation becomes necessary. Similarly, the accommodative capability of the lens decreases with age, again requiring an adjustment of the cross-talk gains.

An important consequence of this cross-talk is that the vergence cells of the SOA and dorsal areas are sensitive to accommodation. This can be demonstrated by dissociating blur and disparity within the optics of the experiment (Zhang et al 1992). The optical system used in this study was of similar design; however, the blur and disparity changes in these experiments were constructed to co-vary in order to simulate natural conditions.

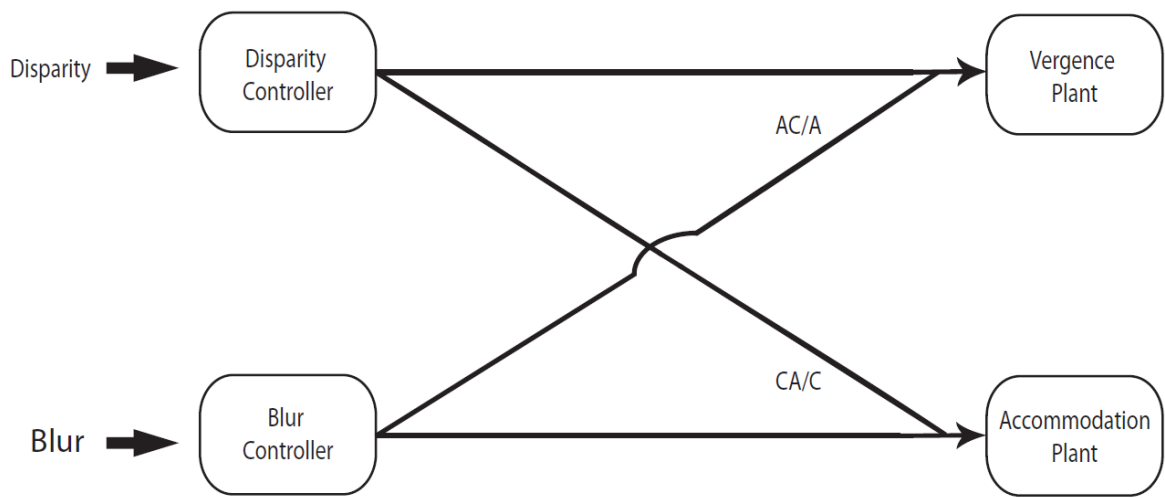


Figure 11: Schematic of the Dual Model of Interaction between vergence and accommodation. As blur and disparity are input to their respective controllers, blur drives accommodation while also contributing to vergence. Similarly, disparity drives vergence while contributing to accommodation. Accommodation convergence over accommodation (AC/A ratio) describes the portion of blur driven vergence. Convergence accommodation over convergence (CA/C) ratio describes the disparity driven accommodation.

The accommodation cells of the Edinger-Westphal nucleus (EW) are known to have lower gains and lower firing rates than their midbrain vergence cell counterparts (Gamlin et al 1994). This observation, together with the stereotaxic coordinates of the recording locations and their relative position with respect to known saccadic areas and

motoneuron locations, allow for the reasonable conclusion that all cells reported in this study are vergence-related cells. Furthermore, in most sessions an optometer was used to record the accommodation of the animal, and electrical microstimulation in our recording areas often elicited strong vergence responses usually unaccompanied by any accommodation response. When accommodation responses were present, they appeared delayed. Nevertheless, the driving signals of the vergence cell are a combination of disparity-driven and accommodation-driven components. It is therefore of paramount importance, in the study of these systems, to use real targets in depth or, as in the case of this study, to accurately calibrate the optical system to simulate strictly co-varying blur and disparity signals.

Vergence Models

The Rashbass & Westheimer (1961) model of neural vergence motor control (Fig. 12) described the vergence responses as being the result of continuous visual feedback. Their initial assumption was that vergence output would closely follow the pattern of their sinusoidal stimulus in depth simply delayed by one visual reaction time. While Rashbass and Westheimer found this to be true in some cases, their results were complicated by the highly repetitive nature of the sinusoidal stimulus, which allowed the subjects to predict and anticipate the stimulus dynamics. Consequently, subjects' ocular response patterns were shifting in advance of the changing visual stimulus; therefore the visual response did not fully imitate the path of the stimulus as would be expected under the constraints of continuous visual feedback. This model, the Rashbass Continuous Feedback Model, was developed using data acquired from human binocular eye movement recordings.

Later, researchers saw evidence of a dual control of the vergence system. For example, Semmlow, Hung, and Ciuffreda (1986) found that the type of vergence response depended on the velocity of the vergence stimulus. For slower velocities, the vergence response was a slower tracking or ocular following type of response, and for higher velocities the vergence proceeded in steps; a curious finding given that the vergence system had been previously modeled to be a continuous feedback loop (Rashbass and Westheimer, 1961; Zuber and Stark 1968; Krishnan and Stark, 1977; Krishnan and Stark, 1983). If this were the case, one would expect that the visual response would simply mimic the stimulus dynamics delayed by one visual reaction time. Westheimer & Mitchell (1956) had previously reported an initial vergence response to target steps in depth that were insufficient to reach the required vergence goal, often lacking by a full degree or more. This was followed by a slow corrective vergence response that would bring the movement the rest of the way to meet the vergence goal - further evidence for dual control of the vergence response. An additional point of counter evidence to a continuous feedback model of the vergence system was found in the

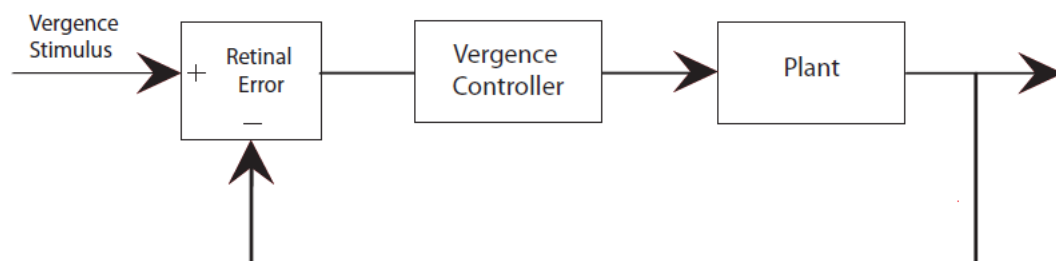


Figure 12: Rashbass continuous feedback model. Vergence demand is compared with continuous visual feedback to produce current visual error, which continues to drive the eye movement to completion.

functional restrictions on the value of the time delay element. Although experimental values of the time delay ranged from 150-200 ms, the smaller time delay value of 160 ms was needed to maintain stability of the visual loop during simulations. Time delay values ranging from 160-200 ms produced excessive oscillations and therefore instability in the modeled response. (Krishnan and Stark 1977; Krishnan and Stark 1983; Hung et al 1986)

Correlating these observations led Hung et al to reevaluate the Rashbass Continuous Feedback Model and develop the Dual Mode Model of vergence (Hung et al 1986). As the name indicates, the Dual Mode Model (Fig. 13) contains two main components. These are referred to as the slow component and the fast component. The sampler and predictor mechanisms of the fast component work together to drive the eye toward the target in discrete steps. The sampling mechanism, triggered by changes in target velocity, samples and retains information relating to target dynamics at specific sampling intervals. The prediction mechanism utilizes this information and generates an eye movement command based on an internal estimate of the future target position. An efferent copy of the vergence command is used by the fast component as an internal update of the progress of the movement. The command from the fast component is summed with the command from the slow component, which is driven continuously by the retinal error and acts similarly to the original Rashbass model. Because retinal error is the combination of the original vergence requirement and negative feedback of the current vergence command, retinal error will necessarily continue to diminish until the vergence goal is reached. The fast component drives the movement in greater steps, but only to an approximation of the vergence goal. The slow component provides an accurate reference of how the movement is progressing based on retinal information and precisely

guides the movement to completion. The fast component could be interpreted as the “coarse” system and the slow component as the “locking” system, but this was not openly stated in their model description. This model was also developed using data acquired from human oculomotor recordings.

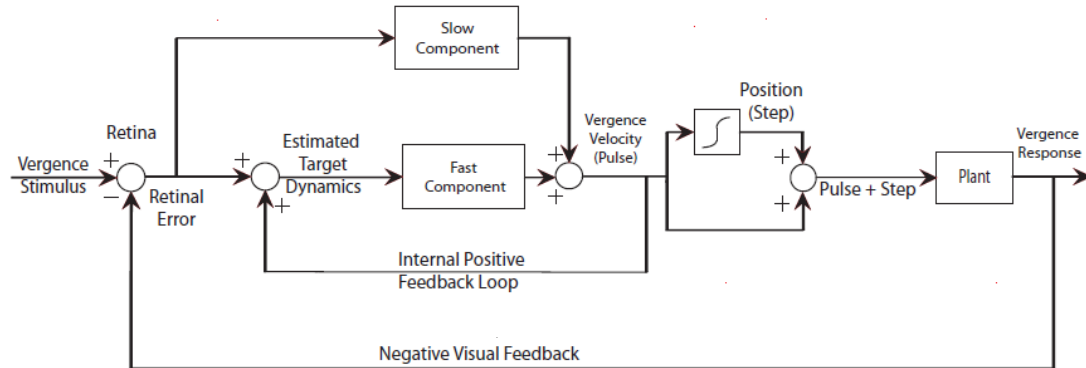


Figure 13: Dual Mode model of vergence. The Dual Mode Model of vergence is comprised of a fast component and a slow component. The slow component simply feeds the visual vergence error forward. Both a sampling mechanism and a prediction mechanism exist within the fast component. The fast component receives the retinal disparity error (Retinal Error) and an efferent copy of the vergence command (Internal Positive Feedback Loop) being sent to the plant to build an estimate of the target dynamics. This estimate is sampled at discrete intervals and used to generate open-loop commands. Since the fast component does not rely on a continuous visual update, it is a dynamically stable component that is capable of high gain responses. The slow component can rely on the visual feedback loop without stability problems, since it can have a low gain. Adapted from Hung et al 1986.

Although there is, at this time, no evidence for any kind of neural separation between the fast and slow components of Hung, or between the coarse and locking components at the premotor or motor level, a short latency, short-range vergence system has been described in both humans and monkeys (Busettini et al 1996; Busettini et al

2001; Masson et al 2001). Given this system's functional range and supporting neural circuitry, it could be the "locking" system. As was debated earlier, we do not know if the "coarse" and the "locking" commands reach the subcortical areas from separate pathways and, if not, where they are merged together. The disparity steps applied to the targets in this dissertation are large enough ($\geq 2^\circ$ convergence or divergence steps) that they most likely activate both the "coarse" and "locking" systems.

Vergence-saccadic Interactions

Though explorations of saccades and vergence eye movements are often treated separately in the scientific literature, it is true that natural eye movements occurring outside of the laboratory very rarely involve saccades or vergence exclusively. Almost all natural eye movements require both a conjugate (cyclopean) change in fixation and a change of fixation in depth (vergence). As we described earlier, the saccadic and the vergence systems are anatomically and functionally distinct, and it was reasonable to expect that the two might sum linearly, with the saccadic system driving the change in cyclopean eccentricity and the vergence system the change in depth. Another potential outcome, should there be significant nonlinear saturations in the oculomotor plant or at the level of the oculomotor muscles, was that combined responses would interfere with one another producing a decreased response when, together, they drive some parts of the plant above its linear range or overcome the contraction capabilities of the muscles. In other words, the linear sum of the two responses, conjugate and vergence, would necessitate the signaling of a movement that would be stronger, in certain aspects, than the capabilities of the ocular anatomy and physiology. Ono et al observed a clear nonlinear interaction (Ono and Nakamizo 1978; Ono et al 1978) between the two

systems, with a pronounced *acceleration* in the vergence response during the intrasaccadic periods, the opposite of what was expected during nonlinear saturations. Many researchers confirmed these initial observations, among others: Kenyon et al (1980), Enright (1992), Maxwell and King (1992), and Collewyn et al (1995). It is important to note that this effect does not necessarily invalidate Hering's law of equal innervation, as stated in some of these earlier works, as long as the saccadic-related vergence enhancement is confined inside the vergence system and delivered to the plant motoneurons by the vergence pathways. Mays and Gamlin (1995; 2000) presented preliminary evidence that some midbrain vergence cells accelerated their firing during the intrasaccadic period as required for the preservation of Hering's law of equal innervation. It seemed evident that, at the very least, within this niche of the monocular vs. binocular disagreement, the two systems remained binocular even during these types of interactions until Zhou and King reported in 1998 that the saccadic burst neurons preferentially encode the movement of one eye during the vergence enhancement; the saccadic system breaks Hering's law of equal innervation during combined vergence-saccadic eye movements. This paper re-incited the tense binocular vs. monocular disagreement in the field, which remains unabated, as can be attested to by two recent reviews (King 2011; Cullen and Van Horn 2011).

The first attempt to model this interaction as a saccade-related vergence enhancement, in keeping with Hering's law, was presented by Zee et al (1992). The foundation for the model proposed by Zee et al is the Robinson Local Feedback Model of the saccadic system (Fig. 14), which provided the framework for the saccadic portion of this model. The basic structure of the vergence portion was developed using the same

schema and adjusting the model parameters. The Robinson Local Feedback Model is based on the fact that the initiation of a saccadic eye movement occurs when the tonic inhibition of saccadic burst neurons by omnipause neurons (OPN) ceases (Robinson 1975; Zee et al 1976; Scudder 1988). An estimate of the cyclopean error (Estimated Current Cyclopean Error) drives a saccadic pulse generator, the output of which is a velocity command. A neural integrator creates a new position command using the velocity command as input. Both pulse (burst) and tonic signals are sent to the oculomotor plant, as was illustrated in the descriptions of previous models. It is important to note that since saccadic responses are faster than the visual delay, no visual information regarding the progress of the movement is available until after the movement has ended. The trajectory of the movement is determined by the initial cyclopean retinal error (Desired Saccadic Size). Once the movement is initiated, the saccadic system can no longer rely on visual information to direct the movement to the target. If the saccade fails to land the eyes on the target due to an error in the estimation of the required saccadic size or as a result of the subject purposefully generating a hypometric saccade, one or more visually-driven corrective saccades are generated. From the neural standpoint, these corrective saccades are new saccades, completely independent from the preceding saccade, and rely on a visual determination of the residual error for their programming. The Zee et al model describes the generation of vergence eye movements in a similar pattern, using an initial computation of the goal from the initial disparity information (Desired Vergence Change) and no visual feedback during the movement. For the vergence system, as will be discussed later, this is incorrect. Vergence movements occur during a much longer time course than the visual delay, allowing the

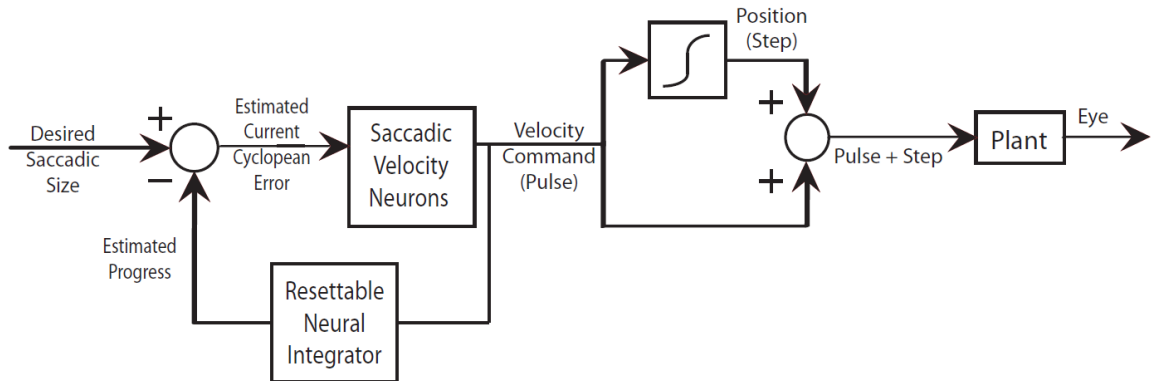


Figure 14: The Robinson Local Feedback Model of the saccadic system. Estimated Current Cyclopean Error drives a saccadic pulse generator to develop a velocity command, which is integrated to produce an eye position command. Estimated error is computed as the difference between the initial target error (Desired Saccadic Size) and an integrated efferent copy of the output of the Saccadic generator. Adapted from Robinson (1975) and Zee et al 1992.

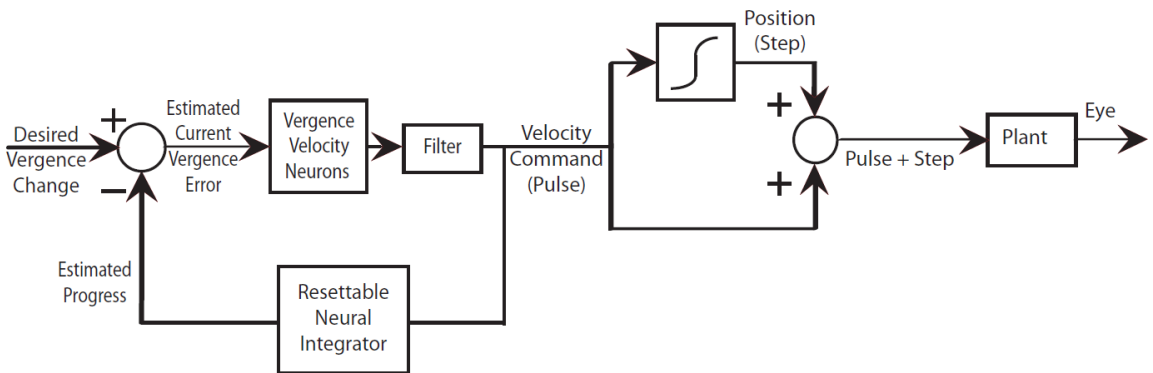


Figure 15: OPN Multiply Model. A schematic of the vergence system as depicted in the OPN Multiply Model. A fixed degree of desired vergence is used to compute the initial vergence motor error (Estimated Current Vergence Error), which in turn drives the vergence velocity neurons. The output of these neurons is then filtered to produce the vergence velocity command. As the movement progresses, the vergence motor error is updated when this velocity command is integrated by the resettable neural integrator and compared with the initial goal to obtain an estimate of the current vergence error. The velocity command is integrated by the vergence neural integrator to generate a new eye position command for the oculomotor plant. Adapted from Zee et al 1992.

vergence system to access the changes in disparity that are occurring during the course of the movement albeit with a delay due to the visual processing time.

In the vergence and saccadic portions of the OPN Multiply Model (Figs. 14 and 15), the basic means of calculating current motor error (cyclopean for the saccadic system and vergence for the vergence system) is through a comparison of the desired goal with an estimate of the progress of the movement. A resettable neural integrator computes an estimate of the instantaneous progress of the movement as an integration of an efferent copy of the velocity command sent to the oculomotor plant. In some models, this integration takes into account the dynamical properties of the plant to obtain an estimate of what the eyes are actually doing in response to the motor command being sent to the plant. This estimated progress is compared with the desired goal to compute a current estimate of the residual motor error, which will continue to drive the movement until it reaches zero. In the Zee et al models, the integrator is simulated as a leaky integration by combining burst neurons (saccadic burst neurons for the saccadic component of the model, and vergence burst neurons for the vergence portion of the model) with a low pass filtering mechanism. This scheme is certainly acceptable so long as the rate of leaking is not so fast as to alter the record of the initial goal of the movement. The name resettable refers to the fact that this integrator integrates the velocity pulse of the current movement as a measure of its progress, and therefore needs to reset to zero at the end of the movement to be ready for the next movement.

In a different saccadic model proposed by Scudder (1988), this internal tracking function is controlled by the long lead burst neurons (LLBNs), which memorize the initial desired movement size and act as a summing junction. Scudder's LLBN model is

just one of many circuits depicting saccadic local feedback and has been described here as best representing its basic principles. In this schema, the LLBNs are the resettable integrators. Before the movement they receive an excitatory burst from the superior colliculus, which is integrated inside the LLBNs and represents the movement goal. The LLBNs also receive an inhibitory efferent copy of the velocity command. As the movement progresses, this efferent signal gradually discharges the LLBNs. If the gain of this inhibitory pathway is correct, they are fully discharged and cease their firing in accordance with the completion of the eye movement, reaching the goal. There is no need for a reset in this schema since the LLBNs are fully discharged at the end of the movement. Currently there is no evidence for vergence LLBNs or any indication of where the vergence local feedback is located.

Zee et al (1992) justified their decision to model the vergence system after the saccadic system based on their previous observations of similarities between the vergence and saccadic systems (Zee and Levi 1989) and on the findings of Mays (1984), Mays et al (1986), and Judge and Cumming (1986), whose works bolstered their comparisons, namely in the similarities between the vergence burst cells and the saccadic short lead burst neurons (Mays 1986). As in their saccadic local feedback model, the fixed initial desired change in vergence is compared with an integrated copy of the actual vergence command to generate an internal estimate of the remaining vergence error, which in turn generates the current velocity command. Also, similarly to the saccadic omnipause neurons (OPN) for the saccadic system, vergence pause neurons (VPN) gate the vergence movement. Vergence pause neurons have, so far, not been found.

Of direct impact for this dissertation is this model's additional feature to simulate the intrasaccadic acceleration in vergence that is observed during combined vergence-saccadic responses. Zee et al proposed an increase in vergence velocity during saccades as a result of engaging a subpopulation of OPN-gated vergence cells. During combined saccade-vergence eye movements, OPNs stop only during the saccadic intervals (Busettini and Mays 2003) and are at or near baseline elsewhere. Thus there are two vergence signals involved in this model – the signal present during pure (saccade-free) vergence and the supplemental vergence signal, which is only present when vergence is combined with a saccade. This dichotomy is not a problem for the vergence system as long as the estimated progress of the movement includes the intrasaccadic vergence enhancement. In other words, both non-enhanced and enhanced velocity signals must be sent to the vergence resettable neural integrator for a proper upgrade of the post-enhancement vergence motor error. This feature allows for large transient increases in the gain of the vergence system without compromising the overall dynamical stability. The OPN Multiply Model was also developed using data acquired from binocular eye movement recordings in humans.

Busettini and Mays (2005a) later noted several limitations in the original OPN Multiply Model. First, it does not include a visual feedback, a requisite for vergence eye movements, the duration of which is usually longer than the delay of the visual feedback. The OPN Multiply model uses a fixed value of Desired Vergence Change, and does not account for new, incoming visual information. Busettini and Mays (2005a) also published strong evidence indicating that the dynamics of the saccadic component of the combined movement were embedded in the dynamics of the vergence enhancement. For example,

peak vergence enhancement velocity was dependent on peak saccadic velocity and, as a consequence, the vergence enhancement had a saccadic-like main sequence. None of the cell types included in the OPN multiply model would be capable of encoding this information: the uninhibited OPN-gated vergence cells would code a vergence signal and the OPNs are on-off cells that do not encode saccadic dynamics, only saccadic duration. A key feature for the models in this study was that Busetini and Mays behaviorally confirmed the presence of a local feedback loop in the vergence system. The local feedback of the OPN Multiply Model was a consequence of being an adaptation of a saccadic model, but lacked the support of actual data. The data of Busetini and Mays revealed a slowing of the post-saccadic vergence velocity due to the reduction in vergence motor error by the intrasaccadic vergence enhancement in a time frame that was incompatible with visual feedback, thus providing biological evidence of a local feedback loop encoding an estimate of the current vergence motor error.

Since their data did not support the OPN Multiply Model, Busetini and Mays (2005b) proposed two variations of a model for vergence enhancement. Both included a multiplicative saccade-vergence node within the vergence pathway and followed Hering's law of equal innervation, but differed in the location of the multiplicative node. In one version, the multiplication occurs between the vergence velocity and the saccadic burst command. In this case, the vergence motor error is not directly involved in encoding the interactive saccade-vergence command. In the other, the multiplicative interaction occurs between the vergence motor error and the saccadic burst signal. Both models incorporate a non-visual local feedback loop in addition to utilizing visual

feedback. The saccade-vergence interaction model developed by Busetini and Mays was based on data acquired through non-human primate eye movement recordings.

The most recent vergence model to be presented was a modification of the OPN Multiply Model published by Kumar et al in 2006. According to the Kumar Model, the direction and timing of the saccade have the greatest impact on the saccade vergence enhancement, whereas the Busetini and Mays model put the emphasis on the strength of the saccadic burst. The timing of the saccade with respect to the vergence movement has a direct impact on the Busetini and Mays models as well, with the enhancement driven by the vergence velocity or the current motor error at the time of the saccade, but it is not a parameter of the model. This model was also based on data acquired from human eye movement recordings. In fact, none of the existent models utilized any neural data obtained from electrophysiological recordings. This dissertation is the first study to directly analyze the behavior of midbrain vergence cells during saccade-free vergence responses and saccade-vergence combined responses in an attempt to understand the nature of the vergence enhancement.

Vergence Smooth Tracking

For conjugate oculomotor responses, there is a saccadic system specifically dedicated to achieving discrete, rapid transfers of gaze, and a smooth pursuit system specifically dedicated to smoothly tracking moving objects. This latter system is a specialization of the optokinetic visual stabilization mechanisms which help stabilize the images on the retina. The vergence system is strikingly different in that both discrete transfers of gaze in depth and smooth tracking in depth are driven by the same system

(Mays et al 1986; Judge and Cumming 1986). As is the case with vergence enhancement during saccades, a debate regarding the binocular vs. monocular nature of the smooth pursuit system arises – is the smooth pursuit system strictly a conjugate system or, alternatively, is it capable of sending asymmetric commands to the two eyes?

The key piece of evidence of a possible monocular action is seen when a moving target is perfectly aligned with one eye (Müller paradigm). There is no target motion on the aligned eye and, if the velocity of the target is sufficiently low, subjects seem able to track the target with only the eye that sees the motion, while the aligned eye does not move (King and Zhou 1995; Enright 1996). Is this evidence for monocular asymmetric smooth pursuit commands or is it simply the result of a vector sum of a pure conjugate smooth pursuit and a pure symmetric vergence tracking? Recently, Maxwell and Schor (2004) introduced a vertical vergence component (tag signal) to horizontal symmetric vergence tracking responses through adaptation. The vertical vergence “tag” was found with both horizontal symmetric and asymmetric vergence, but never in the presence of a conjugate movement, indicating that the asymmetric movements are not under monocular control.

Other behavioral data support a conjugate/vergence organization of the optokinetic and smooth tracking systems. An example, in the monkey, is illustrated in Fig. 16 (from Busetini et al 1996). This result was also replicated in humans in Busetini et al (2001). Using polarizers and a non-depolarizing screen, two large patterns were presented independently to the two eyes. Initially the two eyes saw the two patterns in register on the screen (i.e., with zero disparity). A sudden horizontal step-like shift of the pattern seen by one eye was introduced after a centering saccade, while the pattern on the

other eye remained stationary. The key element here is the response of the eye that did not see the shift. In the case of a monocularly-driven response, the eye with the stationary image would not have moved at all or, at most, in the same direction of the eye which saw the shift. On the contrary, the eye moved in the opposite direction and almost symmetrically. The oculomotor response produced by the monocular position step was a symmetric vergence with the goal of compensating for the (binocular) disparity error. There was little or no version response. In fact, the elicited response was very similar to the response to an identical disparity step introduced symmetrically to the two eyes, albeit slightly smaller and with a lower initial acceleration. This behavior is even more surprising if we consider that the cells of the main cortical area driving these responses, the middle superior temporal area (MST), are simultaneously sensitive to both the version and depth components of the movement of the scene (Takemura et al 2001). If these three-dimensional commands are to be parsed into version and vergence components, this has to occur further downstream at the premotor level.

The second part of this dissertation will explore the contribution of the vergence midbrain cells to oblique tracking in depth. If the cyclopean and the in-depth components of the oblique tracking are perfectly parsed between a conjugate smooth pursuit system (cyclopean component) and a symmetric vergence system (in-depth component), we will be able to predict the firing of the midbrain vergence cells during oblique tracking from the firing of the cell during straight ahead in-depth tracking using a simple vector decomposition.

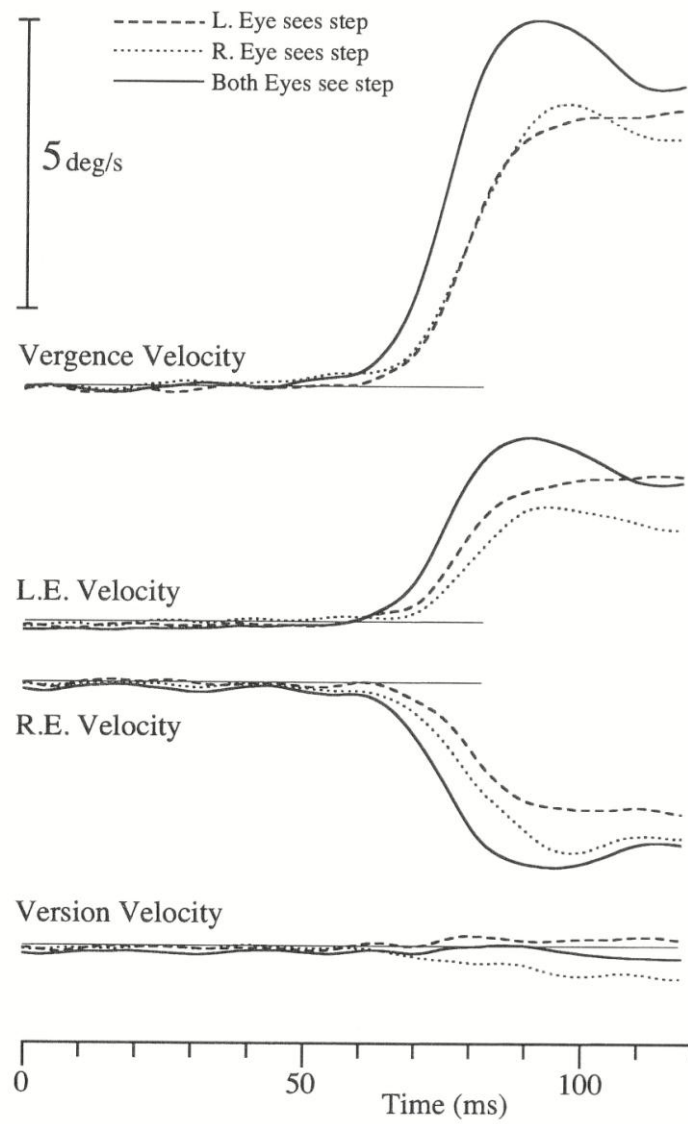


Figure 16: Monocularly induced vergence. Monocular sudden shifts of a large pattern in only one eye, while the other eye sees a stationary pattern, generate symmetric vergence responses similar to the ones generated by symmetric shifts. Adapted from Busetini et al 1996.

METHODS

Visual stimuli

The non-human primates in this study were seated in a precisely aligned optical arrangement controlled by a computer located in the equipment control anteroom, which was separated from the animal area by a closed door. The animal area was carefully darkened and only the targets were visible even after full dark adaptation. The primate

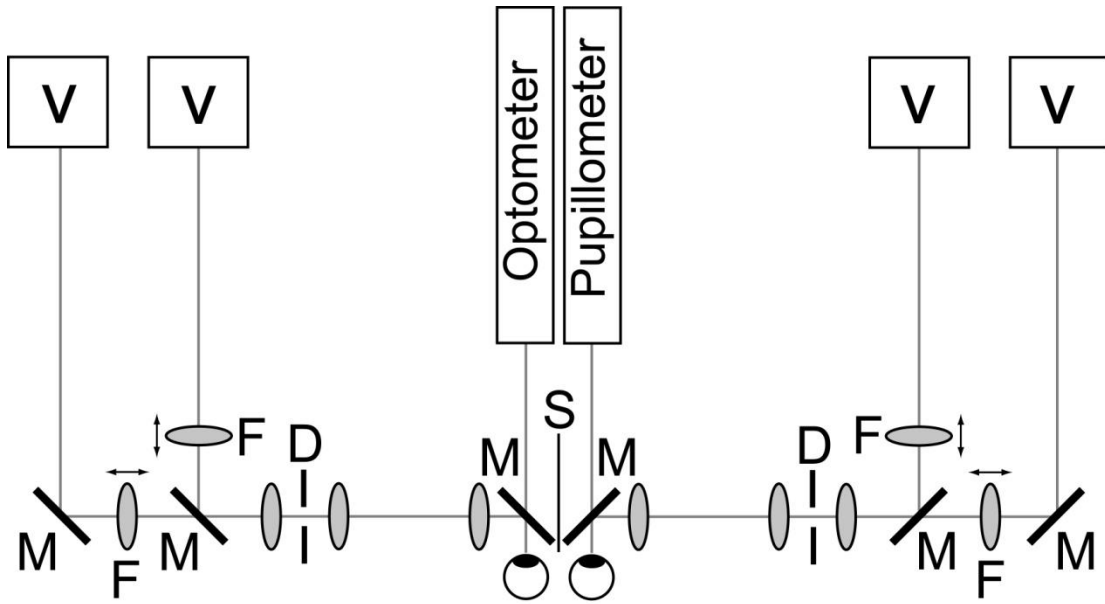


Figure 17. Optical schema of the haploscope system. **M**: mirrors; **F**: motorized lenses to manipulate blur; **V**: video monitors; **S**: black cardboard, used to guarantee the absence of any stimulus cross-talk between the two eyes; **D**: variable-aperture diaphragms, which, when reduced to their minimum aperture, act as pinholes. Additional videocameras (not shown) allow the precise alignment of the animal's eyes to the optical path of the system.

viewed white visual targets, Maltese crosses, on a black background through a video haploscope system (Walton and Mays 2003), illustrated in Fig. 17. Each eye of the animal looked directly into a 50% transmission/reflection mirror (M) that allowed both the optometer (measuring the left eye) and the pupillometer (measuring the right eye) to view the eyes at the same time. These mirrors reflected the incoming beams from the independent right-eye and left-eye optical paths into the eyes of the animal. The black separator (S) eliminated cross-talk between the two paths. Each path was further split into two additional paths, each having its own video monitor, mirrors, and motorized lenses (F). The motorized lenses controlled the blur of the target and therefore the stimulus for the accommodation system. The position of the targets on the monitors determined the conjugate and vergence stimuli. The use of two monitors for each eye, one for the “first” and one for the “second” target presented to the animal allowed for setting the motorized lenses prior to the presentation of the targets. This ensured that the speed of transition from the first to the second target was limited only by the frame rate of the monitors, 90 Hz, as required for fast discrete target changes. For smooth tracking in depth, the dynamics of the motorized lenses were fast enough that one monitor for each eye was sufficient to deliver the properly smooth changes in accommodation, disparity, and cyclopean position as the animal would have experienced viewing real objects. In this dissertation we decided to test the cells during simulated natural conditions with co-varying blur and disparity cues, and the AC/A and CA/C ratios were not determined (Zhang et al 1992).

In the first set of experiments, where the goal was to analyze the behavior of midbrain vergence cells during saccade-free vergence responses and saccade-vergence combined responses to discrete target steps, we presented the animal with three types of trials:

- Fronto-parallel target steps, to elicit conjugate saccades;
- In-depth target steps aligned with the straight-ahead direction, to elicit saccade-free vergence responses (Panels A and B in Fig. 18);
- Target steps that had both changes in depth and in cyclopean position, to elicit combined saccade-vergence responses (Panels C and D in Fig. 18);

Size and directions of the steps were randomized to avoid prediction by the animal. It is not uncommon to also have saccadic contaminations during steps in depth in the straight ahead direction. If these saccades occurred after the peak in the vergence velocity, the trial was truncated just before the saccade treated as a saccade-free response to be used for the saccade-free smooth model estimate. If the saccades occurred before the peak in vergence velocity, it was treated as a combined response. No smooth tracking trials were applied in the first set of experiments. The conjugate saccadic trials were necessary to verify that the putative burst-tonic or tonic vergence cells encountered in our searches had no modulation in their tonic firing that was sensitive to cyclopean changes in position. This qualified them as oculomotor motoneurons or interneurons (Mays and Porter 1984; Gamlin and Mays 1992). The rare cells that had a conjugate saccadic-related burst but not a tonic component were analyzed separately. In the first experiment, for conjugate saccades and convergence trials (Panels A and C in Fig. 18), the initial target

position was always straight ahead and “far” (0° or 4° vergence angle). To obtain divergence trials (Panels B and D in Fig. 18), the first target was placed at a vergence angle of 10° or 12° . Conjugate steps were also delivered while the animal was converged to prevent the animal from predicting that all trials which start with convergence will be divergence trials. For all trials in the second set of experiments, described below, the first target location was straight ahead at a vergence angle of 6° .

The second part of our study required a stimulus design that randomly interleaved:

- Fronto-parallel target steps, to elicit conjugate saccades;
- In-depth target steps aligned with the straight-ahead direction, to elicit saccade-free vergence responses (Panels A and B in Fig. 19);
- Smooth tracking trials along several oblique directions in the horizontal plane (Panel C in Fig. 19). For some cells, we also tested their sensitivity to vertical conjugate smooth tracking;

As before, the conjugate saccadic trials were used to discriminate horizontal motoneurons from tonic and burst-tonic vergence cells. The in-depth target steps aligned with the straight-ahead direction were introduced to compare the velocity sensitivity of the cell during steps and during tracking. The vertical tracking was introduced to see if the cell had any kind of trochlear-related activity (Mays et al 1991). By always placing the first target straight ahead at 6° convergence with the matching accommodation value, we avoided cueing the animal as to which type of trial would follow (step or tracking) or

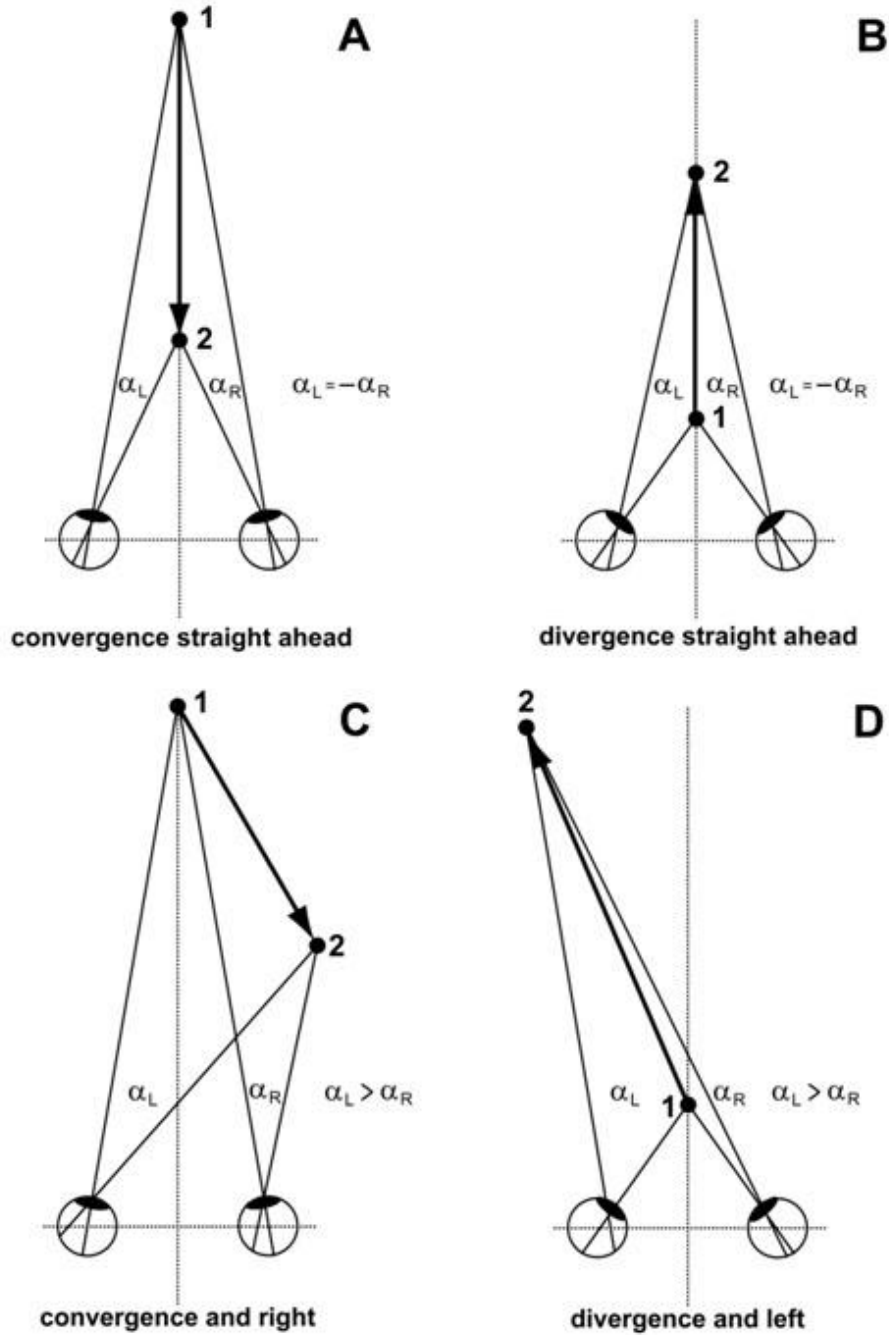


Figure 18. Examples of stimuli used in the first set of experiments. Panel A: Symmetric convergence. The left eye rotates to the right, and the right eye rotates to the left by the same amount. Panel B: Symmetric divergence. The left eye rotates to the left, and the right eye rotates to the right by the same amount. Panel C: Convergence and right. Both eyes rotate to the right, but the left eye moves more than the right eye. Panel D: Divergence and left. Both eyes rotate to the left, but the left eye rotates more than the right eye.

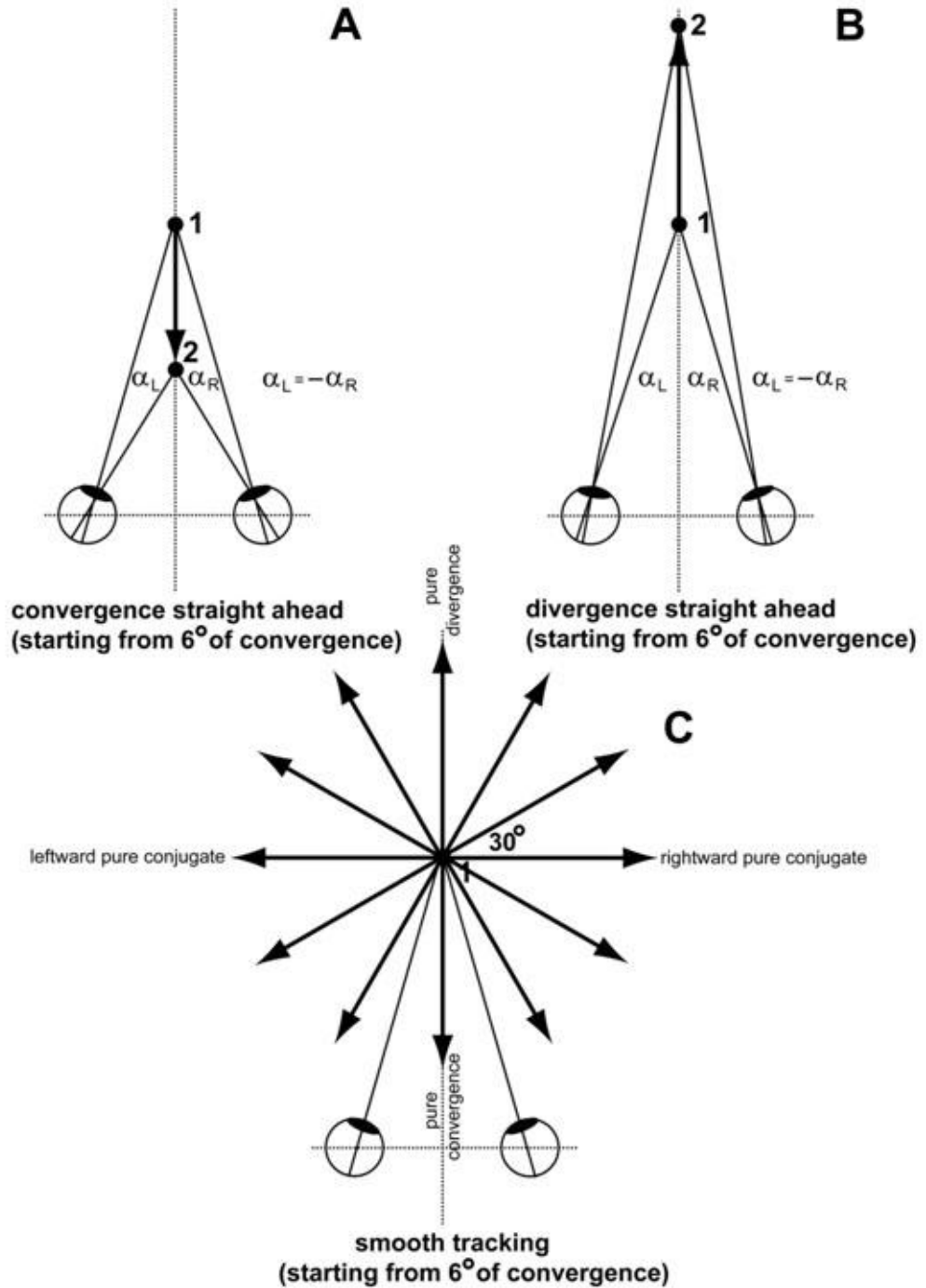


Figure 19. Examples of stimuli used in the second set of experiments. All trials started with the target straight ahead at 6° convergence. In the discrete pure convergence trials, the targets stepped near (Panel A). In the discrete divergence trials, the target stepped far. In the smooth tracking trials, the target moved at a constant angular velocity away from the initial position along one of 12 possible directions for a fixed period of time.

its direction, although it did limit the maximum amount of applicable divergence step to 6° . We could not ask the animal to diverge beyond straight ahead (0°). To maintain a balanced paradigm, the maximum size of the convergence step was also limited to 6° . Similarly, the tracking motion was limited to 6° in magnitude, along one of 12 possible directions. Since the tracking motion was limited to 6° , the duration of the ramp was determined by the speed of the ramp, which was either $10^\circ/\text{s}$, $20^\circ/\text{s}$, or $40^\circ/\text{s}$. These trials were randomly interleaved together with the step trials. To extend the initial saccade-free period of smooth tracking during conjugate smooth pursuit before the first catch-up saccade, it is common to use the “Rashbass” step-ramp paradigm, which consists of stepping back the target just before the motion onset. This is possible because the smooth pursuit is largely insensitive to steps. Stepping back the target reduces the initial positional error and therefore delays or even eliminates the need for catch-up saccades. Given that the fronto-parallel tracking trials are interleaved with oblique and in-depth trials, and vergence is sensitive to steps of disparity, we could not use the Rashbass design. Due to the limited time a cell can be recorded, not all speeds were tested with all cells.

Data Acquisition and Calibration Procedures

Presentation of the stimuli, control of the motorized lenses, evaluation of the animal behavior (by means of acceptance windows on the eye positions), reward of the animal, and data acquisition, were collectively performed by a real time Ubuntu PC, with a custom program developed in our laboratory. The eye movement and optometer traces were acquired at 1000 Hz, with 8 pole 24dB/octave 200 Hz Bessel low pass anti-aliasing

filters. A 20 kHz channel acquired the analog signal from the electrode in sync with the eye traces. These traces were band-pass filtered 10-9000 or 100-9000 Hz to eliminate interference from the magnetic field coils, aliasing effects, low frequency noise, and sub-threshold voltage fluctuations. Spikes were detected by a Bak window discriminator and the spike events were acquired as asynchronous events by the computer with a time resolution better than 0.1 ms. All paradigm menus were adjustable on-line.

Eye Movements and Accommodation Calibration. The search coil technique (Fuchs and Robinson 1966) was used to monitor the eye position of both eyes with high precision and low noise. At the beginning of each session, a calibration board with LEDs along the horizontal and vertical meridians was presented to the animal, and eye calibration data was acquired. The optometer was periodically calibrated using a wooden stick with a row of LEDs at different depths, but not at every session. The eyes of the animal were centered with respect to the optical system and the optometer by means of video cameras and monitors with markings corresponding to the center of the pupil. These markings were determined during the laboratory calibration with laser beams. Furthermore, each animal had its own chair and head post holding system to ensure the animal's head was placed in the same location during each daily session. In preliminary calibration and centering sessions, calibration data were acquired with the right eye patched, the left eye patched, and both eyes viewing, to determine the need for monocular eye calibrations. Since the monocular and binocular calibration data were found to be superimposed, indicating the animals looked at the targets with both eyes, we limited our eye calibration to binocular trials to save time and reward water. Minimal gain, offset,

and cross-talk dial adjustments of the eye phase detector (Riverbend) were required between sessions, indicating a high reproducibility of the animal alignment.

To compensate for any potential cross-talk inherent in the eye coils between the horizontal and vertical directions, horizontal (H) and vertical (V) traces were linearized according to 3rd order polynomials in both the horizontal and vertical directions, for a total of 7 calibration parameters. The optometer response inside our accommodation range was linear and a linear fit was used. The calibrated data was fit with a cubic spline of weight equal to 1×10^8 , which is the optimal filtering weight for these traces, as verified with the cross-correlation criteria described in Eubank (1988).

Recordings and Stimulations. Extracellular neural potentials were recorded using a Kopf microdrive to direct low impedance (0.1-0.3 M Ω) parylene-insulated tungsten microelectrodes into the areas of interest. To extend the range of the Kopf microdrive, which is limited to 20-25 mm when using only the Kopf microdrive, electrodes were first inserted approximately 10 millimeters by hand. The microelectrodes were purchased having been painted with parylene, with the exclusion of the micro tip at the end of the electrode. Teflon tubing added a second layer of insulation to the microelectrode while leaving only the last 10 mm of the microelectrode exposed. The Teflon-covered microelectrode was inserted into 26 gauge steel tubing to afford greater rigidity, and the two inserts were anchored on the microelectrode with cyanoacrylate glue. Although the overall thickness of the electrode was increased by the additional layers, having the last 10 mm of electrode not covered by these layers minimized the penetration damage to the area of interest while still maintaining sufficient rigidity to prevent bending of the electrode during the insertion. This multilayer electrode was then fit into a 21 gauge

hypodermic needle, which penetrated the dura and protected the microelectrode tip during the initial insertion, while acting as a guide tube. Stereotaxic coordinates and known landmark neural areas like the superior colliculus and the oculomotor nuclei were used to locate the vergence areas. At the end of each recording session, the electrodes were extracted, the recording chambers cleaned and refilled with fresh saline. The cylinder caps possessed a small screw in the center. When capping the freshly filled cylinders, the center screw remained unscrewed until after the cap was tightly fastened. This prevented the buildup of excessive pressure by air or saline in the chambers.

During the daily search for midbrain vergence cells, the animal executed a subset of randomly interleaved step and ramp convergence and divergence trials and conjugate saccades. Cells were identified as supraoculomotor vergence cells when located dorsal and lateral to the oculomotor nucleus as indicated by their stereotaxic coordinates, or the discovery of motoneurons just below them, and when their firing rate changed for vergence but was not affected by conjugate movements. We also recorded in the more superficial midbrain vergence area in front and slightly below the superior colliculus. The insertion angle of the electrode was selected to possibly cross both areas during the same penetration. In both areas we found convergence cells and divergence cells. Cells presented either only a burst of activity in correspondence with the movement (vergence burst cells), or a tonic activity related to the vergence angle, with or without a dynamic component (vergence burst-tonic or tonic cells respectively). As was stated earlier, vergence cells that exhibited some bursting for conjugate saccades but no tonic firing or when the tonic firing was unaffected by conjugate eye position were analyzed separately. Once the cell was identified as a vergence-related cell, the paradigm was switched to the

full set and the recording of the cell continued as long as there was a reliable signal from the cell or the animal stopped working.

Data Analysis. All recorded trials were first manually inspected using a visualization program that allowed the simultaneous plot of the eye traces, the optometer trace, the pupillometer trace (when present), the spike events, and the 20 kHz analog signal from the electrode. The pupillometer in these experiments was used primarily as a blink detector, and trials with blink contaminations affecting the saccadic and vergence responses were deleted. Erroneous extra spikes in the spike train that were not matched by a spike in the analog signal, for example a spike associated with electric artifacts of the reward valve, were manually deleted. Missing spikes in the spike train but clearly present in the analog record, usually missed by the window discrimination due to fluctuations in the electrode signal with the heart rate, were manually added. When a sequence of spikes revealed, from the different amplitude and/or shapes of the spikes, that more than one cell was simultaneously recorded, only the cell with the strongest signal was analyzed if its firing could be confidently isolated. Otherwise, the trial or in some cases the entire set was deleted. Once this process was completed, accepted trials were converted from the binary acquisition format to ASCII format and parsed into single-trial segments for subsequent analysis.

The eye calibration coefficients were obtained from the calibration file acquired at the beginning of the session by taking 100 ms averages of periods of steady fixation of the platform targets. These parameters were then used to recalibrate the eye traces. The optometer calibration file, obtained periodically for each animal, was used to recalibrate the optometer traces. A two-point backward differentiation of the splined and calibrated

eye position traces (HR_{POS} , HL_{POS} , VR_{POS} , VL_{POS}) was used to calculate horizontal and vertical, left-eye and right-eye velocity signals (HR_{VEL} , HL_{VEL} , VR_{VEL} , VL_{VEL}). Vergence position was defined as $HL_{POS} - HR_{POS}$. Rightward, upward, and convergence were given the sign of positive, while leftward, downward, and divergence were given the sign of negative. Similar procedures were used to determine accommodation position and velocity. Firing frequency was defined as the reciprocal of the interspike interval between the next spike and the current spike.

Once the calibration was completed and the velocity traces were added to the data, a second graphical analysis manually sorted the trials according to the different trial types. Data contaminated by blinks or other artifacts or where the animal did not follow the task, as seen by comparing target movement and animal behavior, were also deleted during this sorting process. The step trials were separated into conjugate saccade trials, smooth saccade-free vergence trials, and combined saccade-vergence trials by inspecting the conjugate horizontal and vertical velocity traces and the vergence velocity trace. Vergence trials in which the animal executed a saccade during the vergence response were classified as a combined trial, unless the saccade occurred after the peak in vergence velocity during a symmetric vergence trial. In this latter case, the trials were truncated just before the saccade and treated as smooth vergence trials. Vergence trials in which the animal did not execute a saccade during the vergence response were categorized as smooth vergence trials.

In this first set of experiments, the step-elicited smooth vergence trials were used to model vergence cell behavior as described in the experiments and results sections. For the tracking trials in the second set of experiments, straight-ahead in-depth tracking trials

were separated from the other tracking responses and were used to model the cell behavior. All other tracking directions, including the fronto-parallel rightward and leftward directions, were used to test the model of the cell. The analysis programs used were C programs developed by Dr. Busetini and run on RedHat Linux systems. Microsoft Vista/7 systems equipped with Systat and Matlab/Simulink were used during the modeling and final statistical analysis portions of this study. Unless specified otherwise, statistical significance was determined at the $P < 0.01$ level.

Animal Protocol and Veterinary Care

The procedures described in this proposal are in accordance with UAB IACUC protocol number 07720, which is associated with the NEI/NIH R01 grant titled “Neural Organization of Eye Movements in Depth”. Dr. Claudio Busetini is the principal investigator on this grant, and Mrs. Corthell was added to this protocol on March 2nd, 2009. A copy of the IACUC enrollment letter is enclosed in the dissertation as required.

As part of the Animal Resources Program (ARP), operated by the UAB Division of Animal Resources, all laboratory animals at UAB and their respective facilities are under the supervision and care of trained veterinarians and staff available 24 hours per day, including weekends and holidays. ARP is responsible for feeding and watering the animals and cleaning animal cages and holding areas. All non-human primates (NHPs) in this study participated in a behavior and enrichment program for NHPs administered by the ARP for the sake of enhancing the animals’ psychological well being. All facilities and laboratories were fully accredited by the Association for Assessment and Accreditation of Laboratory Animal Care (AAALAC) and regularly inspected by the

Institutional Animal Care and Use Committee (IACUC) and the Food and Drug Administration (FDA). In addition, periodic inspections by the UAB office of Occupational Health and Safety ensured the adherence to all safety requirements.

All surgeries were performed in an ARP or ARP-approved facility and the surgeon was assisted by an ARP senior veterinary technician, who managed the surgical preparation, intubation, and sustained anesthetization of the animal. Ketamine was used to sedate the animal while the animal was transported from the animal's housing, located in the basement of the Worrell building, to the location of the surgery, Volker Hall, and vice versa. Transportation of the animal was facilitated by the UAB Animal Transport Service. While still sedated with Ketamine, isofluorane was delivered with a face mask to deeply sedate the animal just prior to intubation. Isofluorane was also used to maintain the animal under general inhalant anesthesia after intubation. During the surgery, the animal was laid on a heating pad to help maintain body temperature, and its vital functions were monitored by the ARP staff member. No paralytic agents were used during surgery. The animal received a postoperative analgesic (Buprenex) every 12 hours for 3 days or more to minimize any pain or discomfort experienced following surgery. Since isofluorane was administered in gaseous form, the animal was able to return to its housing within half an hour of the end of surgery. Additionally, Ketamine was also administered during potentially stressful or painful non surgical procedures, such as deep cleaning around the area of the implant.

Animal Training and Surgical Procedures. This study was conducted on Rhesus Macaques (*Macaca mulatta*), two animals for the first set of experiments and two animals for the second, which is considered an acceptable number of animals for these types of

studies. Each of these animals underwent a sequence of four aseptic surgical procedures. In the first surgical procedure, two biocompatible PEEK head strips were implanted on the skull. The scalp was then sliced down the midline and folded back. The surgeon attached the head strips to the skull, using surgical grade ceramic screws. The skin was then laid over the PEEK strips and stitched back together. The animal was then given at least four weeks of rest to allow the screws to set in the bone and to allow the animal's scalp to heal. The addition of a head post was the second event in the surgical sequence. Each of the subcutaneous PEEK strips housed attachments for a head post. The attachments were exposed by making small incisions into the scalp. A head post formed from PEEK and dental acrylic was then affixed to the strips by PEEK screws. This is shown in Fig. 20, with the head post structure and the strips applied to a plastic model of a macaque skull. Attaching the head post in this manner allowed the head post to be removed and reattached during routine cleaning procedures without any damage to the scalp. Third, Teflon coated stainless steel triple coiled search coils were surgically inserted below the conjunctiva. The insertion of search coils was achieved over the course of two surgeries - one surgery for each eye. Allowing the first eye to heal fully before inserting the second search coil allowed the animal to retain sight at all times. The purpose of the final surgery was to install the recording chambers required for electrophysiological recording. A stereotaxic system was used to mark the location of the skull correspondent to the desired position of the chamber. A 15 mm diameter area of the skull was then trephined, using the mark as the center. Then, the cylinders were attached using ceramic bone screws and dental acrylic. Saline covered the exposed dura and PEEK cylinder caps sealed the cylinders. Although metal strips and



Figure 20. Illustration of the PEEK strips and of the head post. This very detailed plastic model of a macaque skull is used as a training tool for the stereotaxic technique.

steel screws could have been used for this study, the laboratory has a policy of maintaining all implants to be MRI/fMRI compatible. The stereotaxic coordinates we used were: 2 mm anterior of ear bar zero, center of cylinders 18 mm of midline, and medial/lateral angle of cylinders 25° .

Each animal was assigned to a single handler, who also scheduled and supervised the training and experimental sessions and maintained the wellbeing of the animal and the progress of the study. This arrangement provided the animal with a stable routine, facilitated smooth handling, and minimized the risks and stress for both the animal and the handler. The PI or other laboratory staff assisted the handler when needed. The handler was responsible for monitoring the animal's health, recording the amount of daily fluid intake and animal's weight, supervising the water management for that animal, caring for its head and recording chambers, and addressing whatever other issues could involve the wellbeing of that animal.

Animals were trained in stages, so as not to overwhelm them. Each animal assigned to the project was first familiarized with their handler as the handler simply entered and exited the animal area and gave the animals treats. Subsequent stages of training involved only one animal at a time. During the next phase of training, the animal was rewarded with treats for sitting on the floor after exiting its cage while being led by a pole, which was always used when handling animals. Later, the animal was trained to enter and exit the chair it would use during experiments. To familiarize the animal with the lab area, after being trained in the use of the chair, the animal was brought to the lab area in its chair and given treats. Awake, behaving animals were transferred between floors alert and in their chair covered by a linen sheet. When the animal was comfortable with entering and exiting the chair and familiar with being transferred to the lab, the head strips and the head post were implanted. The next phase of training gradually introduced the animal to the visual displays and behavioral tasks that would be used in the experiments.

During this introduction to the behavioral tasks, the eye movements were monitored with a video-oculographic system. The quality of the data generated by this system was sufficient to monitor the behavior of the animal and reliably administer the liquid reward, but not for the study proper. Once the animal demonstrated mastery of these preliminary training stages, the two eye coils were implanted. After further behavioral training, the recording chambers were implanted.

Fluid intake management. Aliquots of water and juice rewarded the animal for accurately performing the requisite behavioral tasks for which it had been adequately trained. While the animal was participating in experiments, no water or treats with high concentrations of water were given outside the session unless the handler decided that an additional amount of fluid was necessary. The animal received its daily intake of water during the time of the session, during which the animal was allowed to work and receive fluids until it showed significant disinterest by purposefully looking away from the targets or fell asleep, which were telling signs that the animal was sated with fluids. Recording sessions usually lasted only 2-3 hours, and the animal's fluid intake far exceeded the amount needed for survival. All water-managed animals were given unrestricted water during a 24 hour period every 7 days as an extra measure to ensure there was no chance of dehydration. The animal's handlers closely monitored the animal's weight, fluid intake, and general health. If the handler determined that during the course of a recording session the animal did not receive enough fluids, as might occur when an animal is learning a new task, extra water and fruit were given to the animal to compensate. Any animal not on water control, including those experiencing the 24 hour

reprieve, received unrestricted water and extra fruit. Dry treats were always permitted for all animals.

Euthanasia. When microlesions resulting from the repeated microelectrode penetrations caused an animal's performance to degenerate to the point of rendering the data recorded unusable, electrolytic lesions were made in the recording area as histological markers. Euthanasia was produced by administering pentobarbital (50 mg/Kg) intravenously before exsanguination by way of intracardiac perfusion to prepare the brain for histology. This method of euthanasia is approved by the American Veterinary Medical Association for non-human primates.

EXPERIMENTS

This project seeks to further examine the validity of Hering's law of equal innervation by attempting to determine the portion of the experimentally observed change in angle between the two eyes being encoded by the midbrain vergence cells during combined saccade-vergence responses elicited by discrete target steps and during oblique smooth tracking in depth. These are two situations where it has been suggested that Hering's law might be broken, in the first case by the saccadic system, and in the second case by the smooth pursuit system. Our working hypothesis is that the vergence system is the exclusive driver of symmetric saccade-free vergence responses to discrete target steps in depth and of symmetric smooth tracking in the straight ahead direction. All existent relevant neural data support this assumption. Saccadic burst cells do not fire during saccade-free smooth vergence. Vergence cells fire during tracking in depth along the straight ahead direction and do not fire during fronto-parallel tracking. Since the midbrain vergence pathway is the only known vergence pathway to connect directly to the motoneurons, any disconjugate component not present in its cells during these two tasks likely finds its source in monocular commands, from the saccadic system in the first case, and from the smooth pursuit system in the second case.

Saccadic omnipause neurons partially slow their firing during saccade-free vergence responses (Busettini and Mays 2003) and during saccade-free conjugate smooth pursuit (Missal and Keller 2002), but never actually stop. In both cases, the saccadic

system remains fully inhibited throughout the saccade-free response. When vergence or smooth pursuit responses are mixed with saccades, the OPNs fully stop, as they would for conjugate saccades, only during the intrasaccadic periods allowing the saccadic short-lead burst neurons to transmit their saccadic commands to the motoneurons (Busettini and Mays 2003; Missal and Keller 2002). For combined saccade-vergence responses to discrete target steps, this means that any monocular saccadic contribution is forcibly limited to the intrasaccadic periods, where we will focus our attention. Is the cell encoding the entirety of the intrasaccadic vergence profile, part of it, or just the unenhanced (smooth) component? In the smooth tracking experiment, Hering's law requires the cell to encode the vergence response irrespective of the direction of the tracking, following a simple vector decomposition into in-depth and fronto-parallel components. Therefore, our results will either provide further support for the concept of equal innervation or provide evidence that is contradictory to this principle.

In the first experiment, we examined the behavior of midbrain vergence cells during saccade-free and combined saccade-vergence responses elicited by discrete steps of a target in an attempt to define their saccade-free behavior and how these cells encode the intrasaccadic vergence enhancement, if at all. The only reports in the literature that they do encode the vergence enhancement are limited to qualitative figures in two book chapters (Mays and Gamlin 1995; Mays and Gamlin 2000). In the second experiment, the behavior of midbrain vergence cells during smooth tracking in depth along the straight ahead direction was compared to smooth tracking along oblique trajectories to better identify the contribution of the vergence system to asymmetric disconjugate tracking. A systematic study of this aspect has never before been reported.

Experiment 1

The quantification of midbrain vergence cell behavior during discrete transfers of gaze through single unit electrophysiological recordings

Rationale. Previous descriptions of midbrain vergence cells have been based on point data measures, such as peak firing rate, number of spikes, tonic firing rate, latency, etc., and exclusively on their saccade-free behavior. Additionally, previous vergence models have been focused on establishing a relationship between the visual task and the oculomotor response, and have not attempted to include actual firing behaviors in their schema. The core structures of the most contemporary models of the vergence system are derived from the OPN Multiply Model proposed by Zee et al (1992), the vergence portion of which was inspired by the structure of the saccadic system. Ours is the first study to attempt to build a dynamical model of midbrain vergence cells by comparing firing behavior and oculomotor behavior during saccade-free vergence responses. It is important to note that this study describes all supraoculomotor and dorsal midbrain vergence-related cells that we encountered in our searches, and therefore likely also includes cells that might not project to the motoneurons but could still give additional information about how the vergence system is organized. However, we did not attempt to determine their target neurons by antidromically stimulating from the oculomotor nucleus as described in Zhang et al (1992).

As we described earlier, during combined saccade vergence eye movements there is an intrasaccadic acceleration in the vergence response. The two models that portray this acceleration as an enhancement of vergence (Zee et al 1992; Busetini and Mays

2005), and therefore encoded inside the vergence system, predict that the enhancement will be seen in the midbrain burst vergence cells as an intrasaccadic velocity pulse linearly added on top of a non-enhanced component. The only difference in the two models is how the enhancement is generated. In the Zee et al (1992) model, it is the result of the disinhibition of a sub-population of vergence cells from the blocking action of the OPNs during the intrasaccadic period. Busetini and Mays (2005) proposed that this enhancement is the result of a multiplication of the internal vergence motor error estimate by the saccadic burst signal. For the tonic component of the burst-tonic and tonic vergence cells, these enhanced and non-enhanced vergence components will be encoded as integrated velocity signals. The observation that some vergence cells show an evident increase in firing rate during the intrasaccadic portion of combined saccade-vergence responses (Mays and Gamlin 1995; Mays and Gamlin 2000) supports this prediction. If the intrasaccadic vergence acceleration is mostly the result of monocular saccadic commands, the majority of the vergence cells will exclusively code the non-enhanced component. These two hypotheses are illustrated in Fig. 21 as seen from the resulting oculomotor traces. From our dynamical model of the cell, which was constructed from the saccade-free trials, we used the firing of the cell to predict the oculomotor response encoded by the cell during the combined saccade-vergence trials. If the intrasaccadic vergence enhancement is encoded by the cell, the model should accurately predict the intrasaccadic portion of the vergence movement, or at least partially. If the cell does not encode the enhancement, the cell will continue to follow the pre-saccadic smooth response. As in Fig. 21, the intrasaccadic vergence acceleration often breaks from the

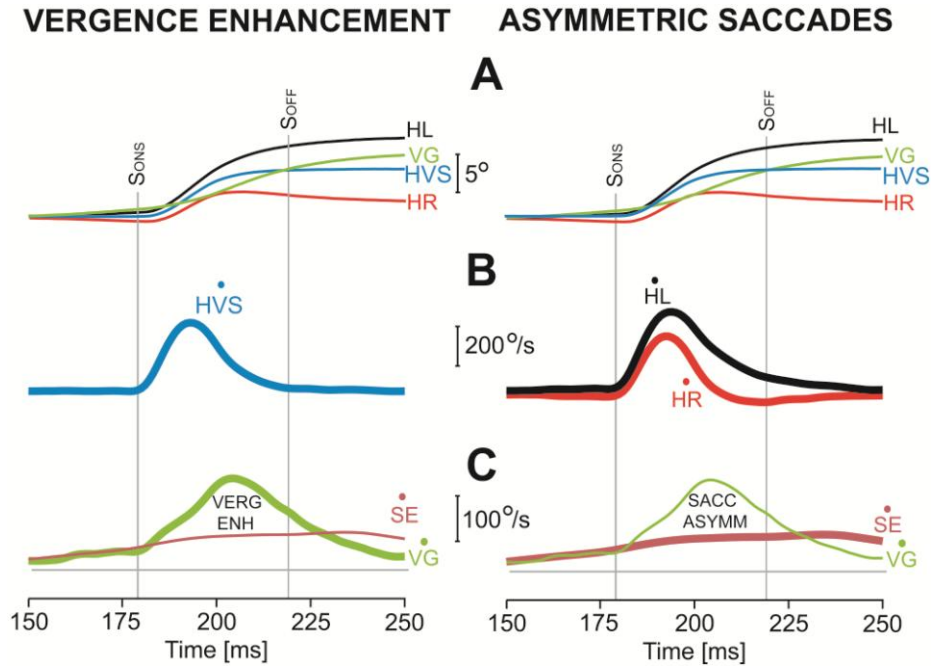


Figure 21. Oculomotor contributions encoded by the saccadic and vergence burst cells during saccade-vergence interaction. The left column shows the case of the intrasaccadic vergence acceleration being an actual vergence enhancement, the right column as the result of asymmetric (monocular) saccadic command. The panels illustrate the actual eye traces of a convergence response combined with a rightward saccade. The bold traces are what the saccadic or the vergence cells encode in each case. Of course an intermediate case between these two extremes is possible as well. S_{ONS} and S_{OFF} indicate the onset and offset of the saccade. This is also the only interval where the saccadic system is not inhibited by the OPNs (Busettini and Mays 2003). The two identical panels in row A demonstrate that it is impossible to determine the actual mechanism of saccade-vergence interaction from the oculomotor behavior alone. Row B compares the saccadic contributions in each scenario. In the case of actual vergence enhancement (left), the saccadic system remains purely conjugate, and both eyes move together. The saccadic burst cells encode horizontal version velocity (\dot{HVS}). On the right, the left eye receives a larger saccadic command (\dot{HL}) than the right eye (\dot{HR}), generating an intrasaccadic asymmetry. Row C reveals what the vergence system encodes in the two cases. On the left, during the vergence enhancement, starting at saccadic onset, there is an abrupt change in firing of the vergence cell with respect to the pre-saccadic behavior, which will generate the vergence enhancement: the cell encodes the entirety of the (enhanced) vergence response (\dot{VG}). On the right, the vergence cell will continue to follow its pre-saccadic behavior: the cell encodes only the smooth non-enhanced vergence response. The smooth trace (\dot{SE}) was estimated from a saccade-free vergence response with similar total vergence change and similar pre-saccadic profile.

pre-saccadic temporal profile quite abruptly, and it will be quite evident if the cell encodes at least part of the intrasaccadic acceleration, particularly for the burst cells.

Experimental procedures. Two rhesus macaques viewed Maltese crosses through a haploscope system (Walton and Mays 2003) that would appear first at 0° or 4° of vergence straight ahead for both conjugate and convergence trials. The conjugate saccadic trials were necessary to verify that the cell being recorded was in fact a vergence cell and not an oculomotor motoneuron. Divergence trials started at either 10° or 12° of vergence. Conjugate trials were often inserted with the animal converged at near to avoid the animal's association of a "near" start with a divergence task.

Once the animal was appropriately seated and adjusted in the experimental apparatus and proper stereotaxic coordinates of electrode penetration were set on the electrode positioner, a microdriver lowered the electrode to the appropriate depth to allow for observation and recording of midbrain vergence cells. Cellular firing patterns during the various types of trial were observed both visually and audibly through an oscilloscope and an audio output of the recording apparatus. Headphones were used to prevent the animal from hearing the sound of its own cells and getting distracted. Cells that presented bursts of activity for convergence or divergence in absence of saccades were defined as vergence burst cells. For these cells we did not put any conditions on their behavior for saccades. Saccadic burst cells do not fire for saccade-free vergence, and we wanted to objectively observe whether or not the same was true of the relationship between vergence burst cells and conjugate behavior. Cells that presented a tonic firing (with or without a burst component) that changed with the vergence angle but did not change with conjugate eye position were defined as vergence tonic or burst-tonic cells. Cells with

significant tonic changes in conjugate eye position, most often associated with strong bursts of activity for saccades in the on direction and pauses for saccades in the off direction were considered oculomotor motoneurons and the search resumed.

Data analysis. After the initial data processing (see Methods), cells were first sorted according to their neuronal firing pattern and categorized as tonic, burst, or burst-tonic. Within each of these categories, the trials for each cell were then sorted according to the qualification of the eye movement – saccade-free smooth vergence, saccade-vergence trials, or conjugate. To generate combined vergence-saccade trials the animal was intentionally presented with target steps that simultaneously changed in depth and in cyclopean position (Panels C and D in Fig. 18 of the Methods section). Some small saccades were often spontaneously generated by the animal during the course of the vergence eye movement even when a symmetric straight-ahead saccade-free vergence response was expected (Panels A and B in Fig. 18). These trials were classified as combined trials if the saccade occurred before the peak in vergence velocity. If the saccade occurred after the peak in vergence velocity, the portion of the trial occurring before the saccade was studied as a saccade-free smooth trial in order to have more data available for the determination of the smooth model.

Cell Types. Before attempting a dynamical model, we visually inspected all the cells for their firing profiles. As was somewhat expected, the categorization of midbrain vergence cells into burst, tonic, and burst-tonic cells, is an oversimplification, particularly for the burst cells. In this section we will present some examples of the most representative cell types we encountered and compare their behavior during saccade-free vergence trials and combined saccade-vergence trials. Unless specified otherwise, the

figures in this section have a similar layout, which is described below. Each figure reports two single trials: a saccade-free vergence response (traces in black, for brevity termed “smooth”) and a combined saccade-vergence trial (traces in red, for brevity termed “enhanced”). The two trials were selected to have similar disparity steps and similar pre-saccadic vergence velocity profiles. Time 0 represents the onset of the target step for the smooth trial. The enhanced trial was shifted in time to have the same vergence onset of the smooth trial. This was done to obtain the best matching of the pre-saccadic smooth vergence velocity profiles of the two trials, similarly to what was done in Busetini and Mays (2005a; 2005b) for the subtraction of the smooth component from the enhanced trials. Position traces are associated with continuous lines, while velocity traces are associated with dotted lines. Panel A shows the vergence position profiles (VG_{POS}) and the vergence velocity profiles (VG_{VEL}). S_{ON} and S_{OFF} are the onset and offset of the saccade in the enhanced trial. Panel B shows the horizontal version position (HVS_{POS}) and horizontal version velocity (HVS_{VEL}) profiles. None of the saccades reported here had significant vertical components. The scales on the y-axes in panels A and B apply to the position traces. The scale bars inside the panels apply to the velocity traces. Panel C shows the firing rate of the cell, in spikes/s.

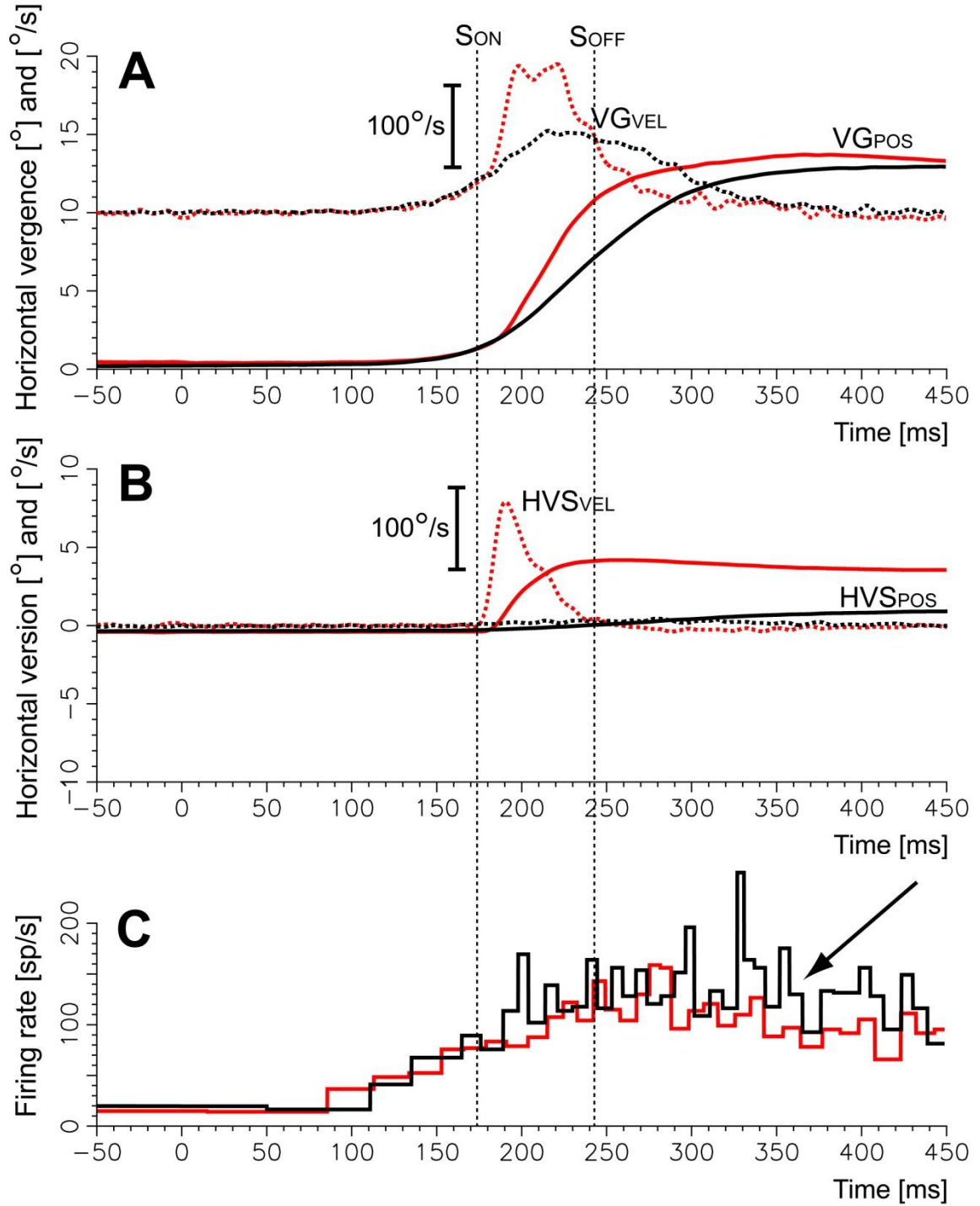


Figure 22: Primarily tonic cell with gradual buildup and no vergence enhancement. Since the enhancement reduces the vergence motor error, the cell fires less during the post-saccadic portion of the movement (arrow). Black traces: smooth trial. Red traces: enhanced trial.

Primarily tonic cell with gradual buildup and no vergence enhancement. The firing profile of this cell, illustrated in Fig. 22, is what is expected from a cell that encodes the gradual integration of the smooth-only component of the vergence velocity command. The burst component is quite weak. The enhancement reduces the vergence motor error and therefore the post-saccadic effort needed from the smooth-only component. Accordingly, the cell fires less, post-saccadically, during the enhanced trial (arrow). Note the lack of any increase in firing during the intrasaccadic period. Thus, this cell does not encode the enhancement, but it does show sensitivity to the enhancement as reduction in post-saccadic vergence motor error. Animal #1 cell d10530.

Pure tonic cell with abrupt onset and evident vergence enhancement. Several tonic and burst-tonic cells had an abrupt onset that quickly reached the firing rate present in the cell at the end of the movement, often further enhanced by a burst component. One case is illustrated in Fig. 23. As evident from the smooth traces (black), this cell has no burst component, and reaches the final tonic value just after a single spike. Although we cannot totally exclude that what we see is the effect of a burst component that, by chance, made the profile appear like a step, we consider it more likely that this cell encodes the future vergence angle, estimated from the sum of the current vergence angle – in this case zero, the animal looking at a simulated object at infinity – and the initial disparity error, i.e., the vergence goal. For the enhanced behavior, the cell has a step-like enhancement of its firing during the intrasaccadic period (arrow). Busettini and Mays (2005b) proposed, as one of the possible mechanisms for the enhancement, that the vergence system is subject to an apparent transient increase in the current vergence motor error estimate,

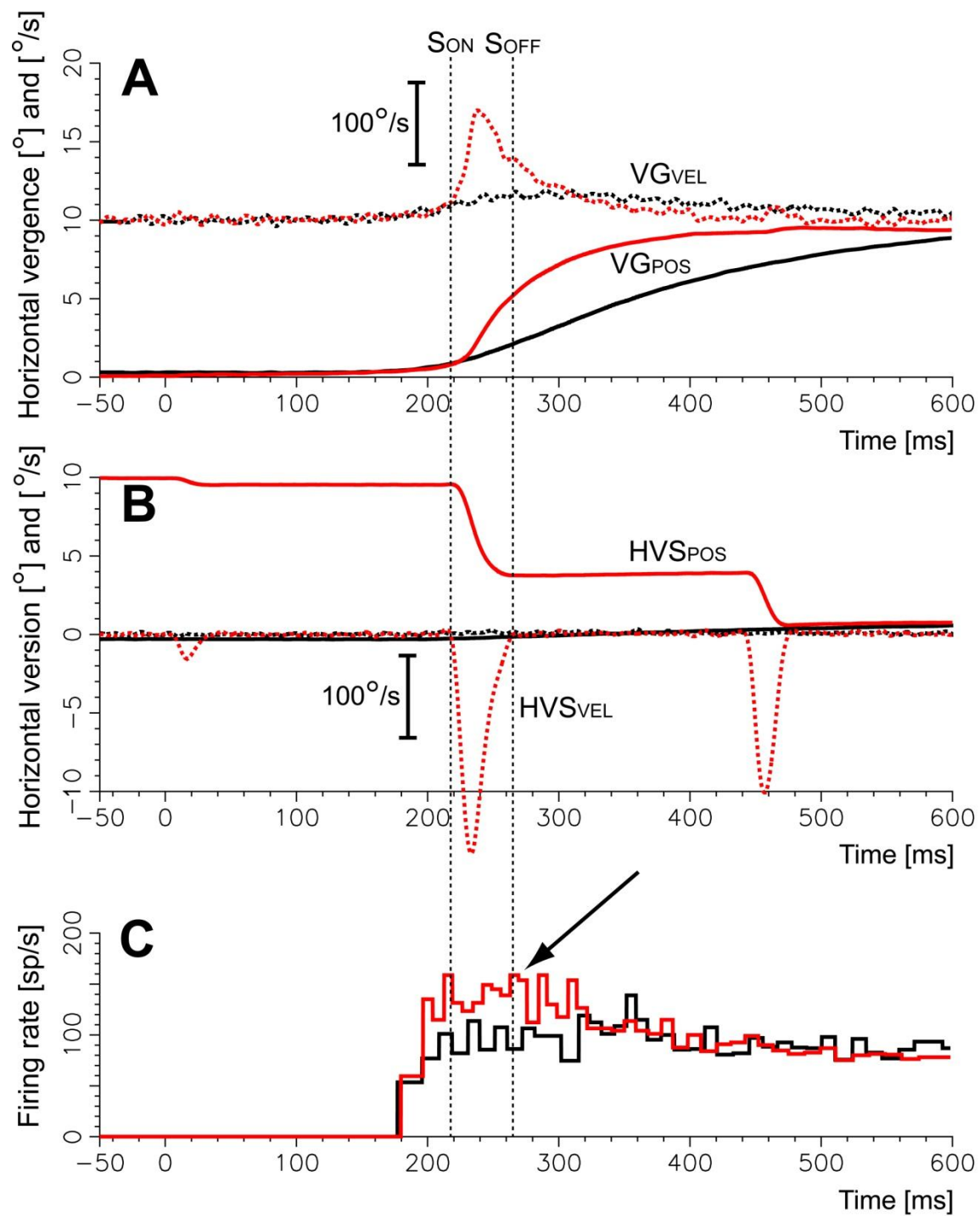


Figure 23. Pure tonic cell with abrupt onset and evident vergence enhancement. Note the step-like increase in firing (arrow) during the intrasaccadic interval. Black traces: smooth trial. Red traces: enhanced trial.

driven by a multiplicative interaction between this signal and the ongoing saccadic burst command. This makes the goal transiently appear farther away than it actually is, causing an acceleration in the vergence response. This cell would be consistent with such an idea. Note since the corrective saccade, of similar direction and amplitude, is late in the movement and the residual vergence motor error at that time is close to zero, it does not generate any enhancement, either in behavior or in cell firing. This is consistent with the observations of Busetini and Mays (2005a; 2005b): the vergence motor error at the time of the saccade plays a determinant role in the amount of the vergence enhancement. This also confirms that the increase in firing in association with the first saccade is not a superimposed saccadic-related response unrelated to the vergence enhancement. Animal #2 cell d10428.

Convergence burst cell with no vergence enhancement. Figure 24 illustrates an example of a convergence burst cell which clearly does not encode the vergence enhancement but is dramatically affected by the large intrasaccadic reduction in the post-saccadic vergence motor error caused by the enhancement (arrow). The animal cannot visually respond to the effects of the enhancement until around 100 ms after the end of the saccade. With the end of the saccade occurring 200 ms after target onset, this translates into a visually-driven correction of the vergence in response to the intrasaccadic enhancement no sooner than 300 ms from target onset. In the enhanced trial (red traces) the cell stops firing at 228 ms from target onset, and the vergence response stops soon after. This is clear evidence for an internal mechanism that keeps track of the enhancement and affects the response of the smooth-only vergence cells as well. The saccade-free trial (in black) shows that when there is no enhancement and the goal is

reached later in time, the cell continues to fire for a longer period, also suggesting that this cell is active during the “locking” phase of the vergence response. Animal #1 cell d00601.

Convergence burst cell with vergence enhancement. This cell, illustrated in Fig. 25, is very similar to the cell in Fig. 24, save for the fact that it encodes the vergence enhancement. Animal #2 cell d00604.

Encoding of the locking phase of the vergence response. One of the questions we attempted to address was whether or not there are midbrain burst vergence cells that code only the “coarse” response or, following the dual-mode model, the pre-programmed component. Similarly, we searched for cells that code only the “locking” component.

For example, the burst cell in Fig. 25 seems to continue firing after the main burst during the smooth trial, but not during the enhanced trial, even though the enhanced response also has a prolonged post-saccadic response. The cell in Fig. 26 (animal #2 cell d30439) consistently ended its firing well before the end of the vergence response. This is particularly evident for the smooth trial. Note that this cell also encodes some of the enhancement and, as expected, takes into account the enhancement contribution during the post-saccadic period. The cell in Fig. 27 had a much longer firing duration (animal #2 cell d20311), and the plot was extended to 1200 ms after target onset to verify it was not a burst-tonic cell. This cell has no evident enhancement component. Note that the cell fired during the smooth trial up to the point where the animal, having over-converged, started a slow divergence drift (arrow), further indication that it encodes the convergence response in its entirety.

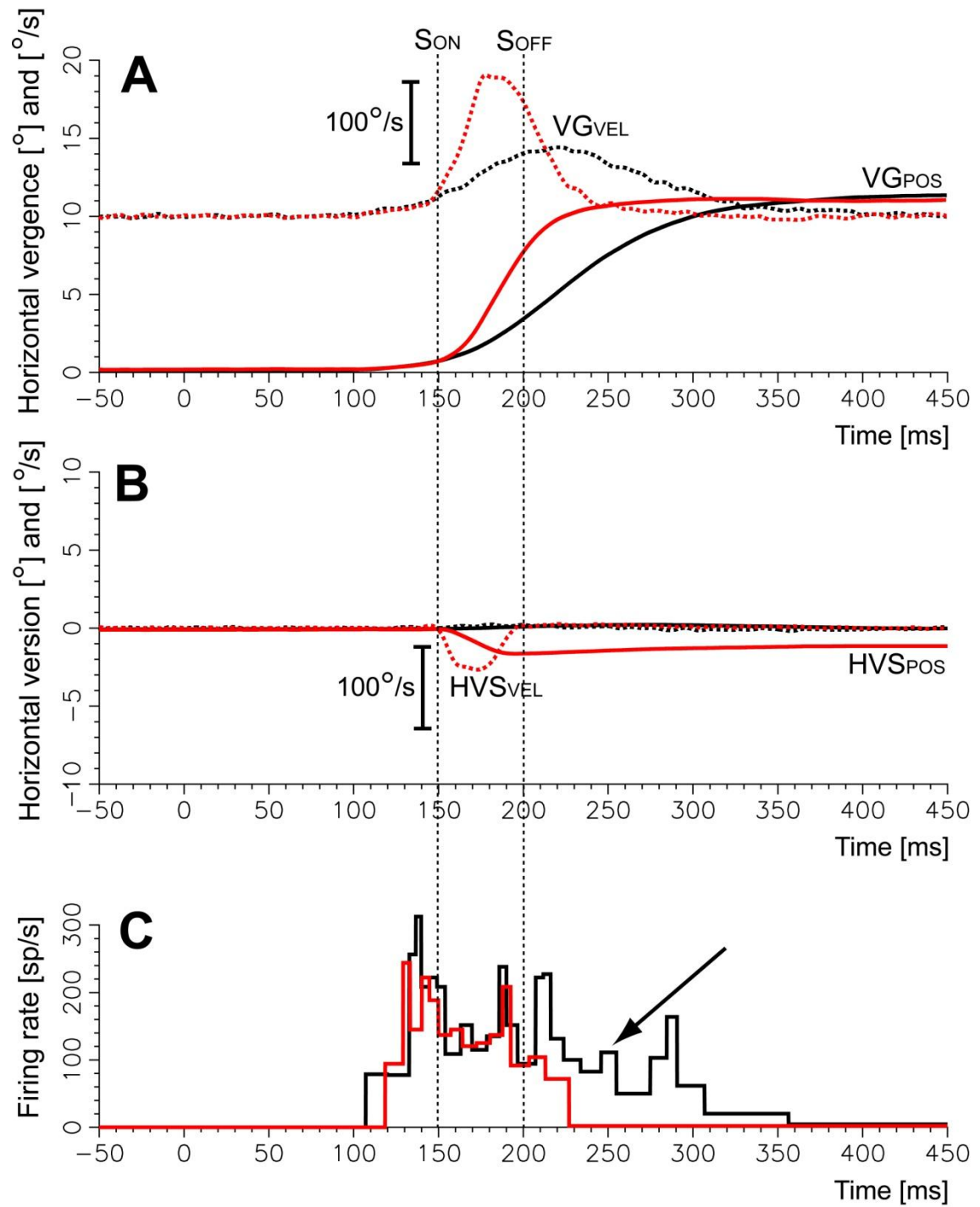


Figure 24. Convergence burst cell with no vergence enhancement. During the enhanced trial, the cell is very strongly affected by the reduction of vergence motor error caused by the intrasaccadic enhancement (arrow). Black traces: smooth trial. Red traces: enhanced trial.

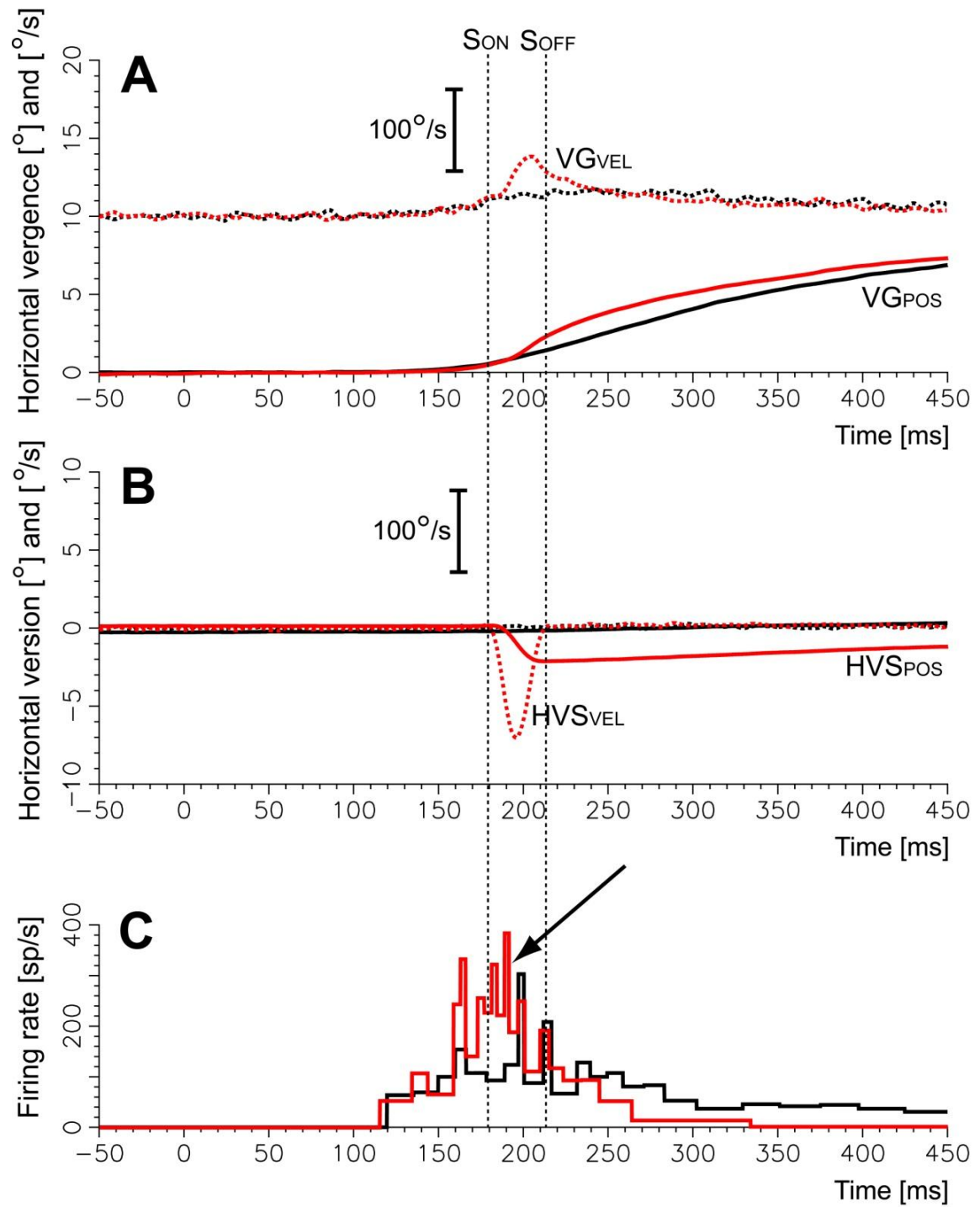


Figure 25. Convergence burst cell with vergence enhancement (arrow). Black traces: smooth trial. Red traces: enhanced trial.

We are fully aware that these observations might simply be representative of a velocity threshold of the cell, unrelated to the encoding of the locking phase. One way to try to address this issue would be to test vergence cells with the paradigms used by Busetini and Miles (1996; 1997; 2001) and others (Masson et al 1997; Cumming and Parker 1997) to elicit ultra-short latency vergence responses. The functional range of these responses suggests that they are driven exclusively by the locking mechanism. No data are available in the literature concerning the encoding of these responses in midbrain vergence cells or the existence of significant differences for these tasks between the SOA and dorsal cells.

Divergence cells. In previous studies it was reported that divergence cells are harder to find than convergence cells, and this was also the case in our study. A pair of smooth and enhanced trials from one divergence burst cell (animal #1, cell d10814) is illustrated in Fig. 28. As in the two trials in Fig. 28, the cell often presented a spike doublet or triplet early in the response. The cell had some enhancement, but clearly did not contribute to the later part of the divergence response. Fig. 29 (animal #1 cell d10827) is an example of a burst-tonic divergence cell with little indication of a divergence enhancement.

Non-standard cells. Two cells were found to differ in behavior from the other midbrain vergence cells.

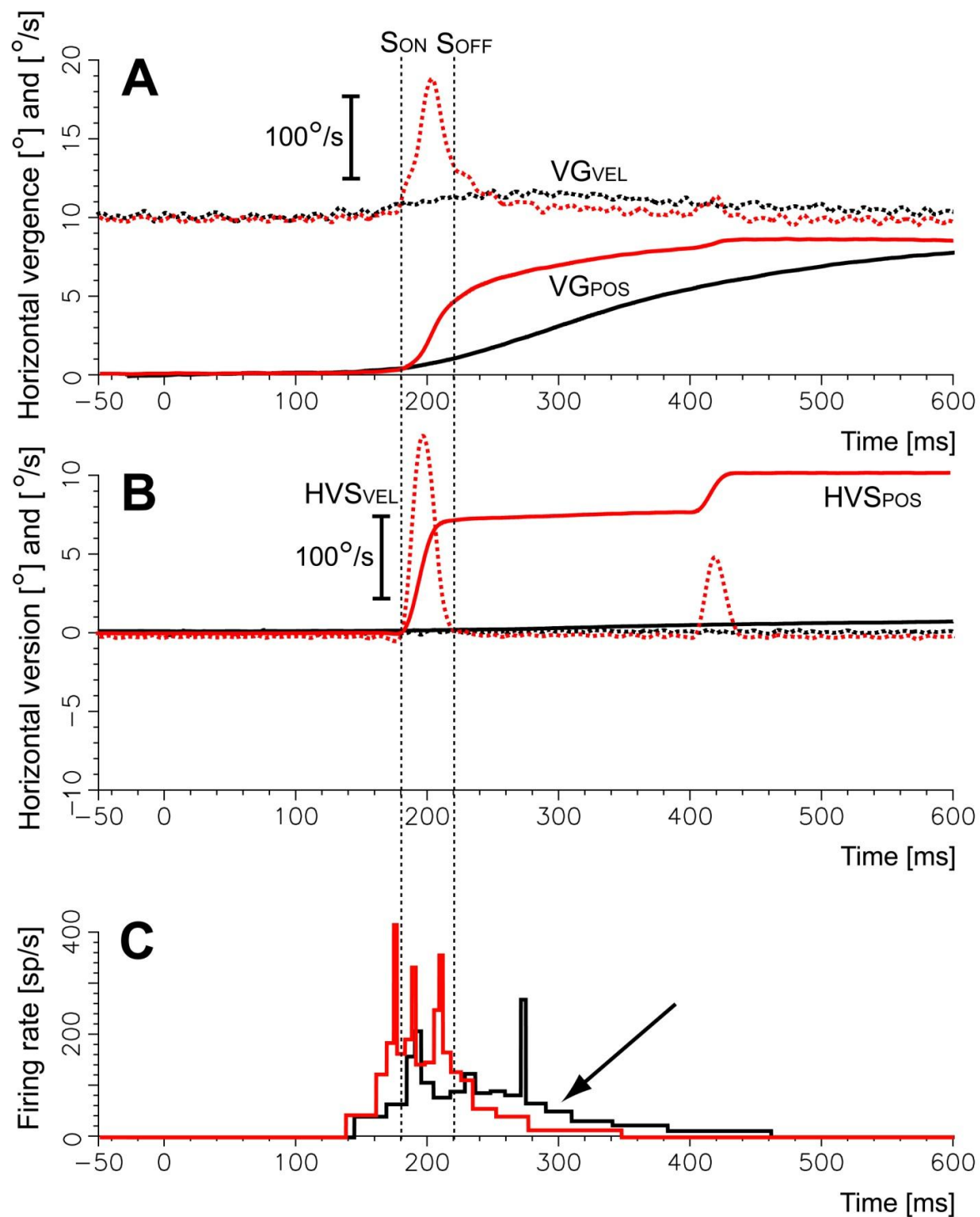


Figure 26. Example of a convergence burst cell with early cessation of firing (arrow). Black traces: smooth trial. Red traces: enhanced trial.

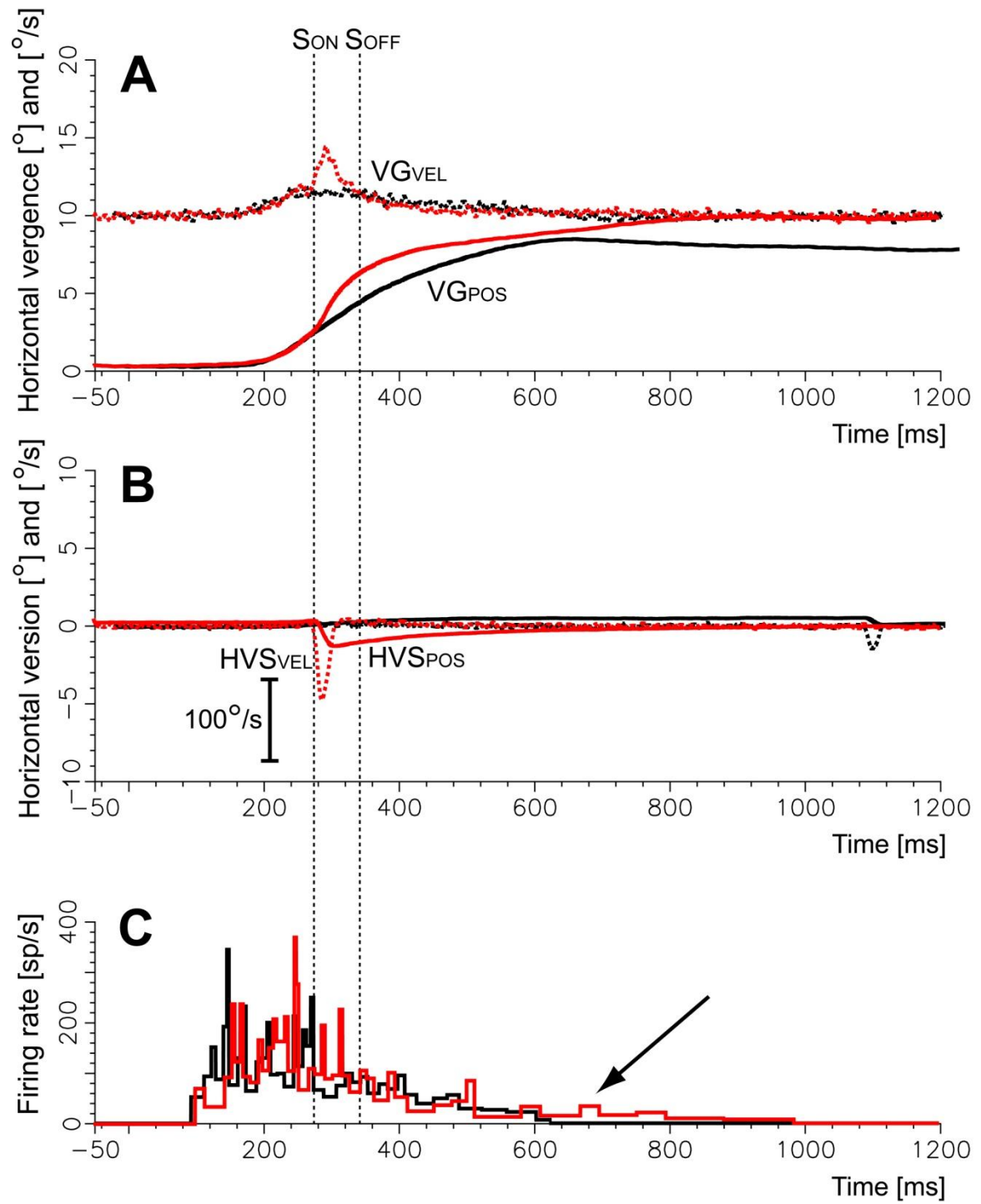


Figure 27: Example of a convergence burst cell with a firing covering the entirety of the vergence response. This cell ceases firing as the animal begins a divergence drift (arrow). Black traces: smooth trial. Red traces: enhanced trial.

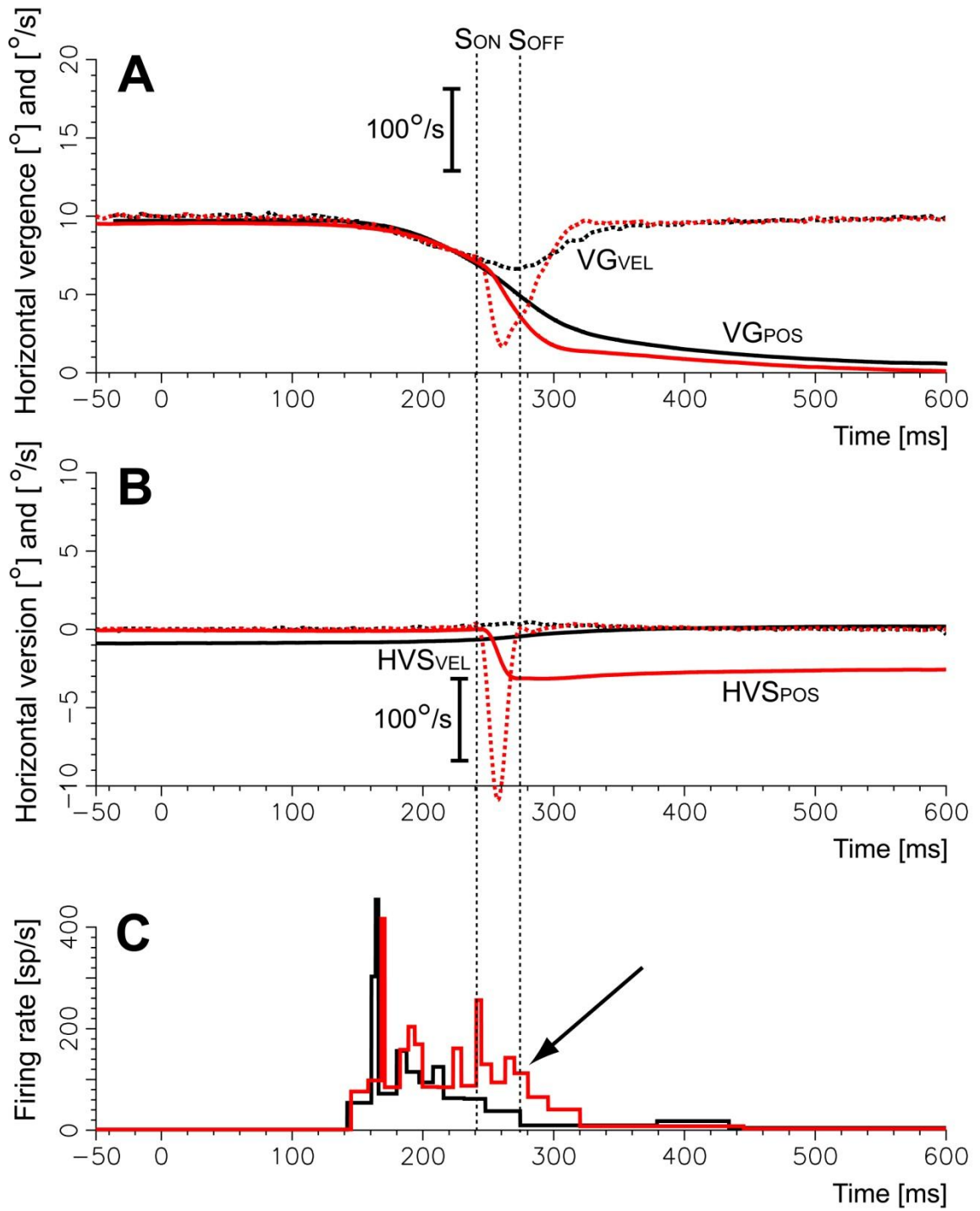


Figure 28: Example of a divergence burst cell. The non-enhanced trial reveals more plainly that this cell does not encode the later part of the vergence response (arrow). Black traces: smooth trial. Red traces: enhanced trial.

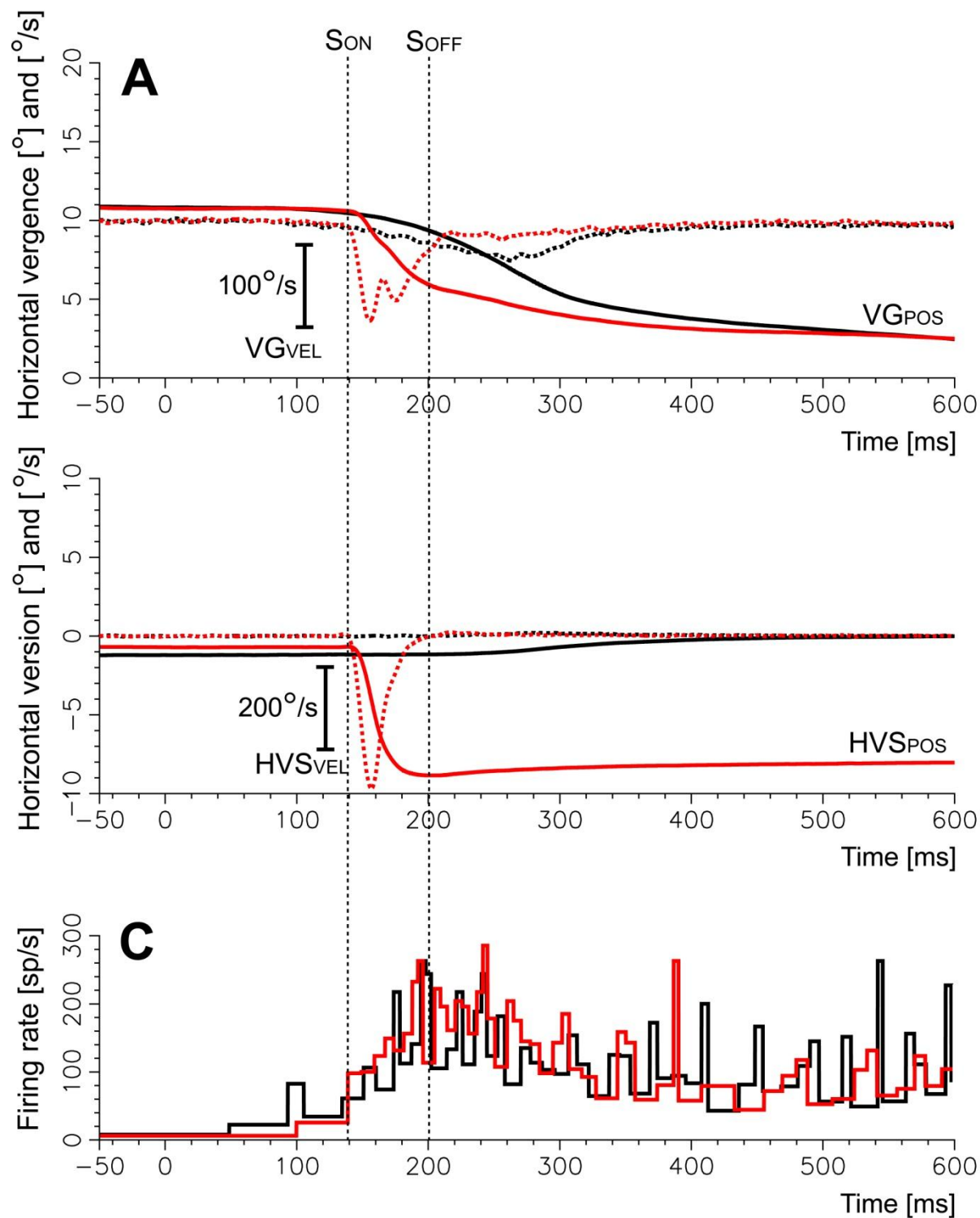


Figure 29: Example of a divergence burst-tonic cell. Black traces: smooth trial. Red traces: enhanced trial.

The first, illustrated in Fig. 30, had an extremely high enhanced response when compared with the smooth trial, but its amplitude depended on the saccadic direction. Fig. 31 depicts an enhanced convergence trial with a leftward saccade followed by a rightward saccade. Although, in this example, part of the weaker enhancement for the rightward saccade may be due to the fact that the vergence motor error is lower when the second saccade occurs, causing the cell to have a much lower pre-saccadic smooth firing, this was found to be true for primary saccades as well. Leftward and downward (not shown) saccades had the strongest enhanced responses. Weaker enhanced responses, albeit still present, were observed for rightward and upward saccades. This was also the only cell with a consistent burst for leftward and downward conjugate saccades, and often no response for rightward or upward. Examples of this conjugate firing are shown in Fig. 32. It is important to observe that this cell is not a saccadic burst neuron. This cell clearly encodes smooth vergence (Figs. 30 and 31) when the saccadic omnipause neurons are at or near baseline firing and fully inhibiting the saccadic short-lead burst neurons.

The second cell was a burst-tonic convergence cell but with a clear pause in correspondence with saccades in all directions (Fig. 33). This cell was excluded as a saccadic omnipause neuron for several reasons: 1) it was quite far, anatomically, from the omnipause area; 2) it encoded the vergence angle, with no firing for the animal diverged at infinite; 3) the onset of the pause was much earlier with respect to saccadic onset than observed in saccadic omnipause neurons (Busettini and Mays 2003; Everling et al 1998). The possible function of this type of cell is unknown.

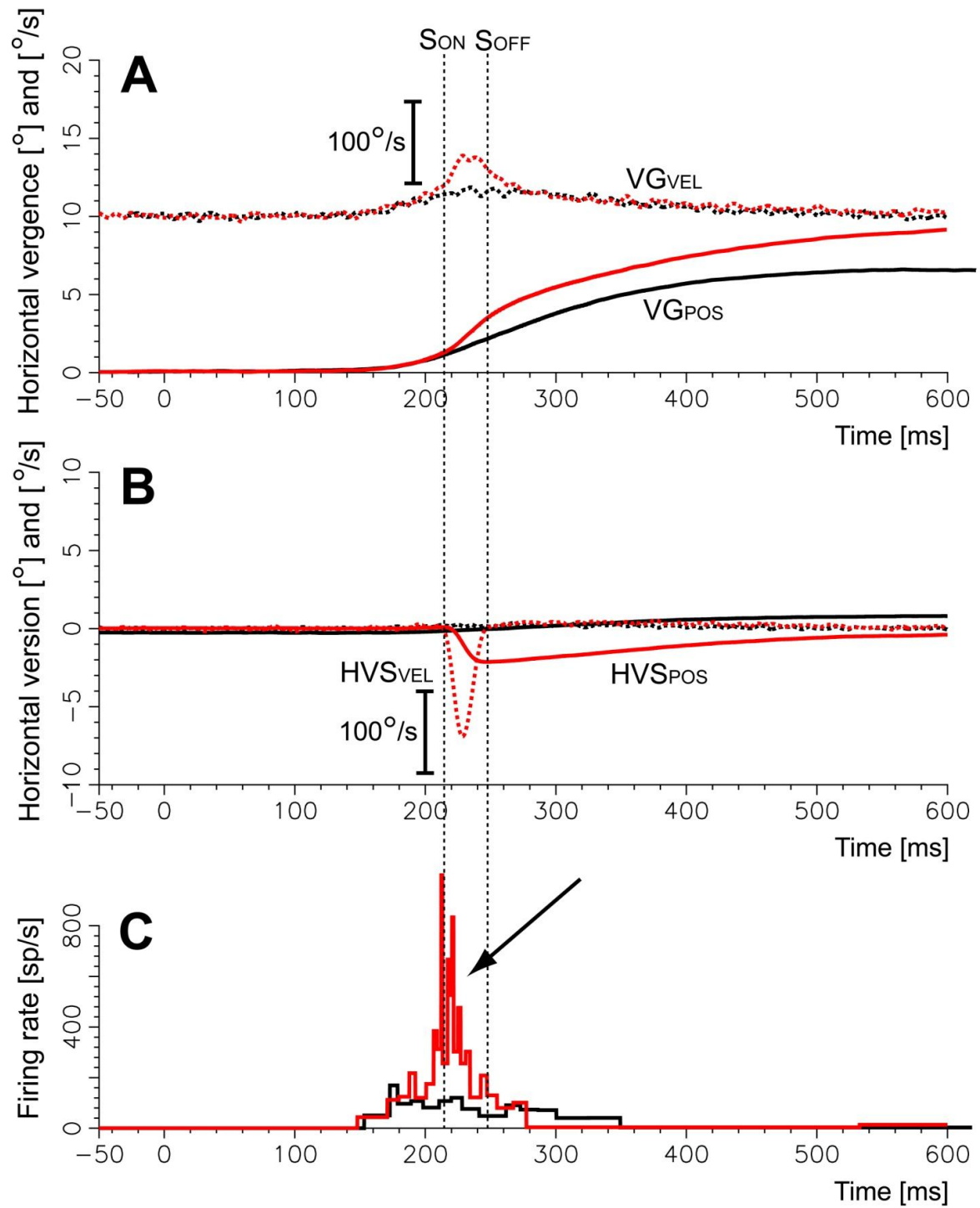


Figure 30: Convergence burst cell with directionally-dependent vergence enhancement. The enhancement is larger in the leftward direction (arrow). Black traces: smooth trial. Red traces: enhanced trial.

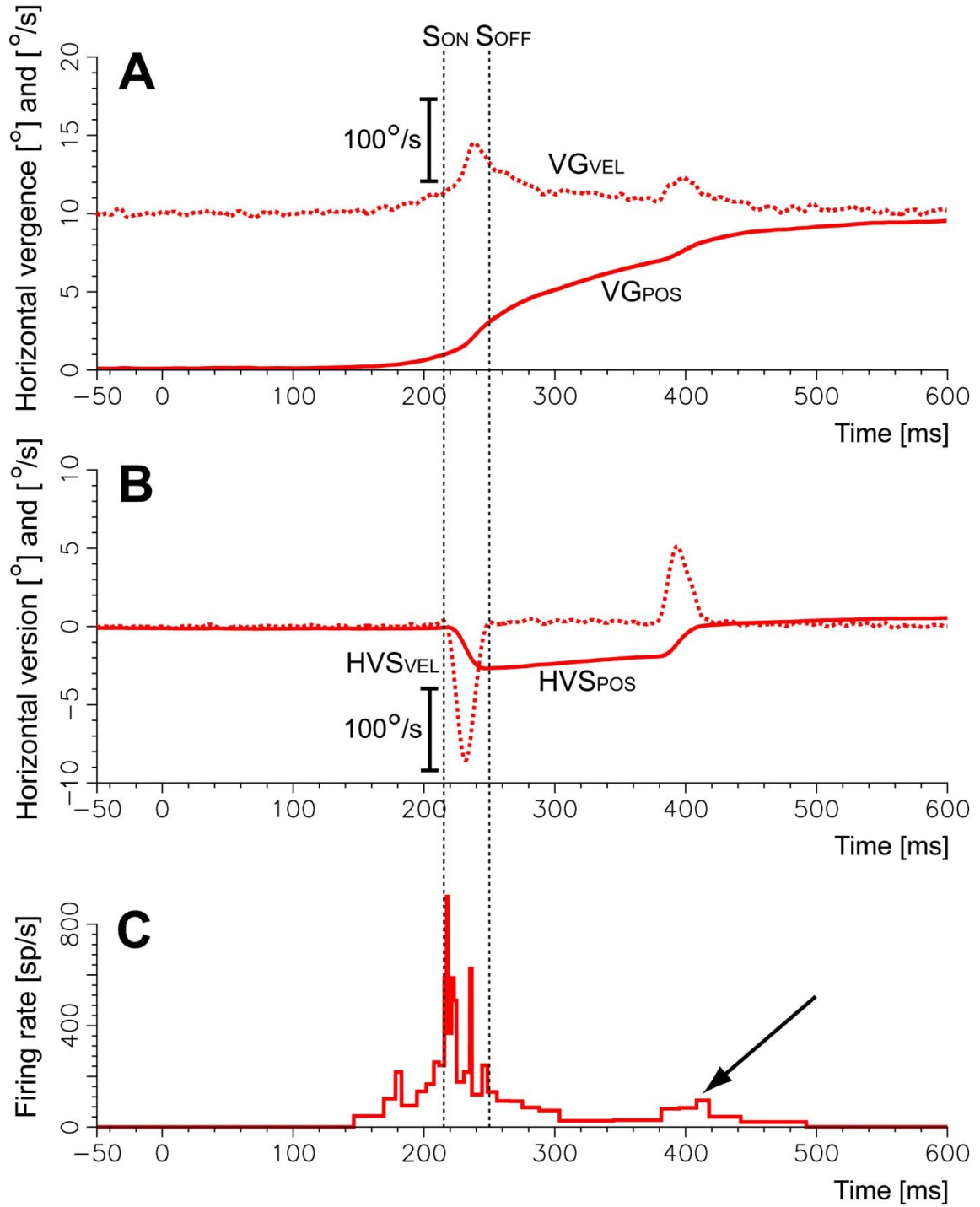


Figure 31: Same convergence burst cell found in Fig. 30: directional dependence of enhancement amplitude. The enhanced trial illustrated in the figure shows evidence that the vergence enhancement in this cell has a directional dependence in that the firing rate is much larger in the leftward direction and far more diminished in the rightward direction (arrow).

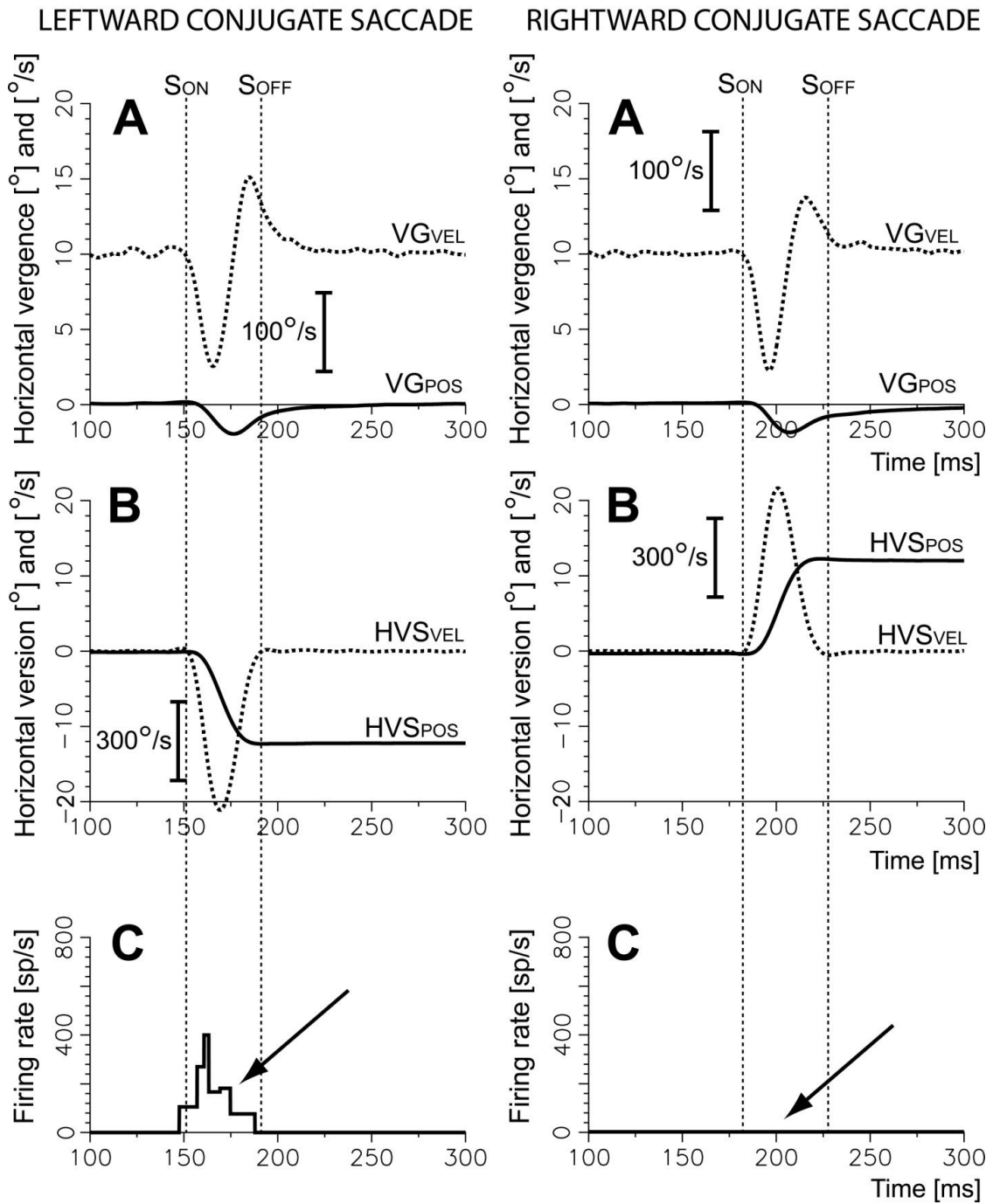


Figure 32: Same cell as Fig. 30: conjugate firing. This cell had some conjugate firing for leftward (left arrow) and downward (not shown) after upward saccades, but much less for rightward (right arrow) and upward.

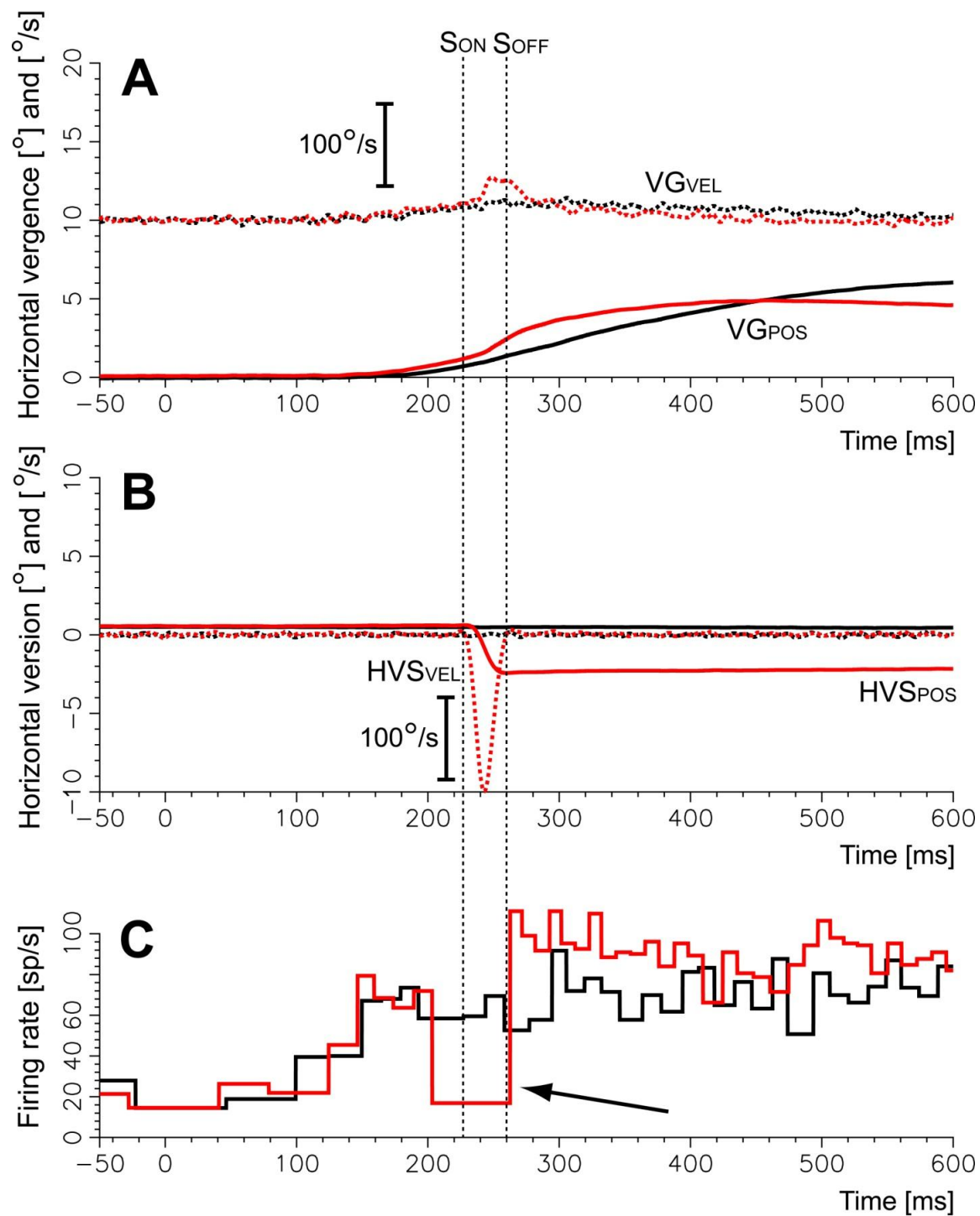


Figure 33: Convergence tonic cell with a pause for saccades. This convergence tonic cell clearly paused for saccades as is evident by the decrease in firing (arrow) in the enhanced trial. Black traces: smooth trial. Red traces: enhanced trial.

From this qualitative analysis of our cell population, it is clear that, particularly for the burst cells, midbrain vergence cells are not a uniform population. The models presented in the next section attempted to account for this variability as much as possible.

Modeling of Saccade-Free Vergence Responses to Target Steps in Depth. A dynamical model (Fig. 34) of the relationship between midbrain vergence cell firing and saccade-free smooth vergence eye movements in response to target steps was developed using the Simulink modeling package in MatLab. The model's primary component is a plant composed of a single real pole and a complex pole pair in series, similar to the plant used in the model proposed by Zee et al (1992). The plant's role here is the transformation of a properly weighted vergence cell firing frequency into its associated vergence eye movements and represents both qualities which are specific to a given cell's dynamics and animal-specific features such as visco-elastic properties of the oculomotor musculature. Complex poles, which have oscillatory qualities, have historically been used to account for this visco-elasticity. Complex poles, in addition to their oscillatory qualities, also have a damping component. By combining complex pole pairs with pure damping elements (real poles) of different time constants, complex damping systems can be modeled. More modern models of the primate oculomotor plant, such as the model proposed by Sklavos et al (2005), include a larger series of poles with fixed time constants, some of which are very long (up to ten seconds). These models were rejected for our purposes because the simpler traditional model was as effective, and our focus was on relatively short periods of dynamic movement rather than long drifts. The combination of a single complex pole pair and a single real pole was chosen after trial and error with different combinations - adding more poles did not significantly strengthen

the model, while using only the complex pair or only the real pole gave substantially worse results. The real pole was modeled as the transfer function: $\frac{1}{Tc*s+1}$, with Tc as the time constant. The complex pole was modeled as the transfer function: $\frac{w^2}{s^2 + 2*q*w*s + w^2}$, with q as the natural frequency and w as the damping constant.

One model ("position model") was used for the burst-tonic and tonic cells (Fig 34, top), and a variation on that model ("velocity model") was used for the burst cells (Fig 34, bottom). The velocity model was altered to output velocity rather than position, consistent with the proposed role of vergence burst cells as “vergence velocity-encoding” cells located upstream of the neural integrator (Mays et al 1986). Converting the vergence burst cell firing into a burst-tonic profile by integration, which would have allowed the use of the position model on all cells, was only successful for a few burst cells, and thus will not be discussed further here. No clear pattern among the cells for which this strategy worked compared to the other cells was evident, so it was not further explored.

As was previously described in the above section (Cell Types), the population of burst-tonic cells has a high within group variability. This firing pattern is also the most complex of the three characteristic firing profiles: burst, tonic, and burst-tonic. Fig. 35 showcases an example of the differences in burst relative to tonic firing in two divergence burst- tonic cells. Specifically, the cell represented by black traces in Fig. 35 has a very large initial burst compared to its tonic firing, while the cell represented by red traces has a burst that is only slightly larger than its tonic firing. Note that the vergence movements in Fig. 35 are nearly identical, despite such different properties in the firing of the two cells. For this reason, it was necessary to separate (parse) the burst and tonic components

of the cell firing, generally referred to as the pulse and the step, allowing independent gains for each.

Within the position model, the distinction between the step and the pulse was identified by the model through the use of a time threshold, t , which defined a duration threshold for the decreasing component of the pulse (Fig. 36). In this context, the pulse refers to the burst of neuronal firing at the onset of the firing in a burst-tonic cell. The step refers to the subsequent change in tonic firing required to maintain the new vergence angle. At the first recognition

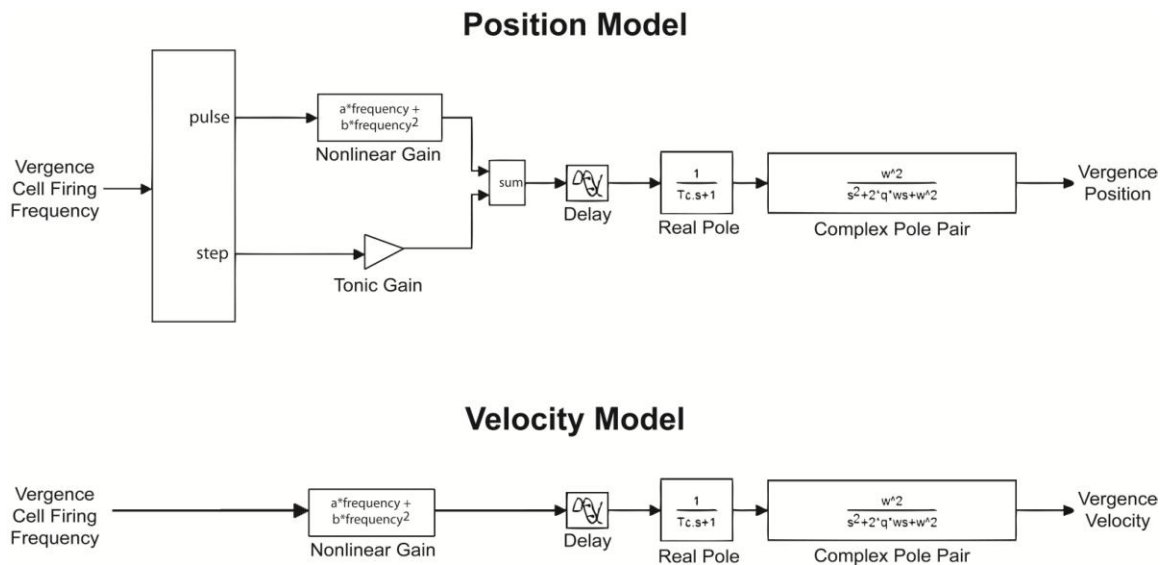


Fig 34: Position and velocity vergence models. The position model has the firing frequency of a tonic or burst-tonic vergence cell as input. The signal was then parsed into pulse and step components, each with their own gains, and summed back together. Next, the signal was passed to a real pole and a complex pole, giving the predicted vergence position. The velocity model, applied to vergence burst cells, is identical apart from the lack of parsing. Its output is predicted vergence velocity.

of any decrease in cell firing, the model began to track the duration of the decrease. When the signal was found to continuously decrease for a time interval equivalent in duration to the threshold, t , the end of this time interval was identified as the approximate end of the pulse. If the neuronal firing began to increase after the initially identified decrease, the starting point was reset and a new search started from this point until the duration of the decreasing interval of the pulse reached the specified threshold value. To avoid high frequency noise interference as the model searched for the decreasing interval of the pulse the firing frequency was low pass filtered. This filter was only for the purpose of the parsing function and was not applied to the data used for the output of the model. Once the firing frequency was found to decrease for a sufficient length of time, as defined by the threshold value, t , the end of the pulse was declared and the subsequent firing profile was classified part of the step. A complex pole pair was used to smooth the transition between the burst and tonic phases, smoothing the pulse firing to zero and the step firing from zero to the tonic firing level. For more information on this process, see Appendix B. This simple strategy was surprisingly effective and reliable and was checked during the data analysis for consistency in each cell. When it failed to function properly, the time threshold was adjusted for the whole cell, until all trials showed visually acceptable pulse-step separation.

The parsing algorithm made parameter estimation more tractable by eliminating nonlinear parameters and allowing for the use of a constant multiplier instead in estimating the tonic gain, which has been shown to have a tight relationship with tonic vergence position (Zhang et al 1992). For each trial estimated by the model, a user-specified period of stable fixation, which occurred shortly after the vergence movement,

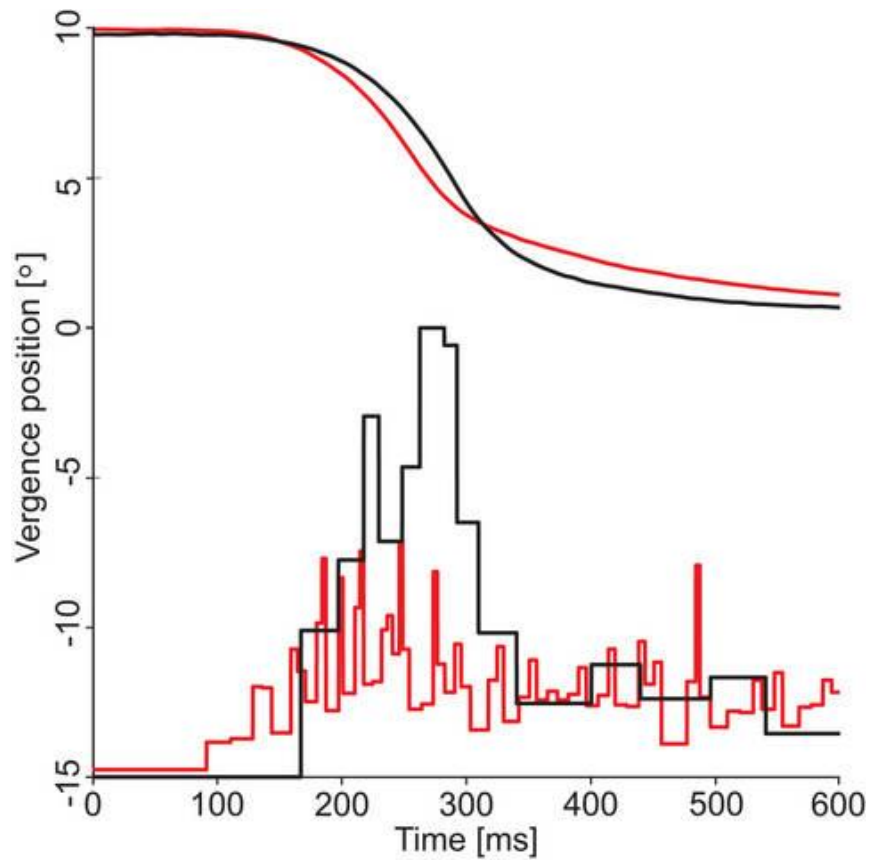


Fig. 35: Pulse-step variation. The lower traces show cell firing and the upper traces show vergence position. Black traces show a cell in which the pulse dwarfs the tonic firing. Red traces show a cell which has a pulse only slightly larger than the tonic firing. The firing frequency gains are matched with respect to their respective tonic firing rates. This figure demonstrates well how different firing patterns can be among cells of the same type during similar vergence movements.

was chosen, and the tonic gain was considered the ratio of the average firing rate and the average vergence position inside the selected interval. Because the tonic signal represents the tonic vergence angle after the end of the movement, and both the tonic firing and final vergence position are essentially static, at least in the time interval considered in the

modeling, a scalar gain fully identifies the tonic behavior of the cell. It can easily be represented by multiplication of the current signal and tonic gain.

In the case of what we describe as pure tonic cells, with no detectable burst and therefore no consistent firing decrease, the parsing sometimes failed, causing all firing frequency to be classified by the model as “pulse” and passed to the “nonlinear gain” block of Fig. 34 (for more details see Appendix B). As such, the entirety of their signal was fed into the non-linear gain and the poles worked in concert with the non linear gain estimate, without the aid of the tonic gain component, to create a prediction of both the dynamic and tonic phases of movement. Since the distinction between tonic and burst-tonic cells with small and poorly-defined pulses is often subtle, even apparently pure tonic cells were first attempted with parsing, and this parsing was successful even with very subtle bursts. The main difference between the simplified execution of the model for pure tonic cells and the more comprehensive one for cells with a burst component is that in the simplified version, the signal only travelled along one branch of the model, the branch including the “nonlinear gain”, which is composed of several estimable pulse gain parameters as opposed to the static constant multiplier of the tonic gain, making it the more effective branch for modeling the dynamic phase of the movement. For tonic cells in which there was no readily identifiable burst, the modeling algorithm treated the entire firing as a “pulse”. In these cases, it was not logical to use both the pulse and the step, and since the vergence firing frequency, in these instances, was considered to be exclusively “pulse” firing, only the non linear gain component was used to fit the data.

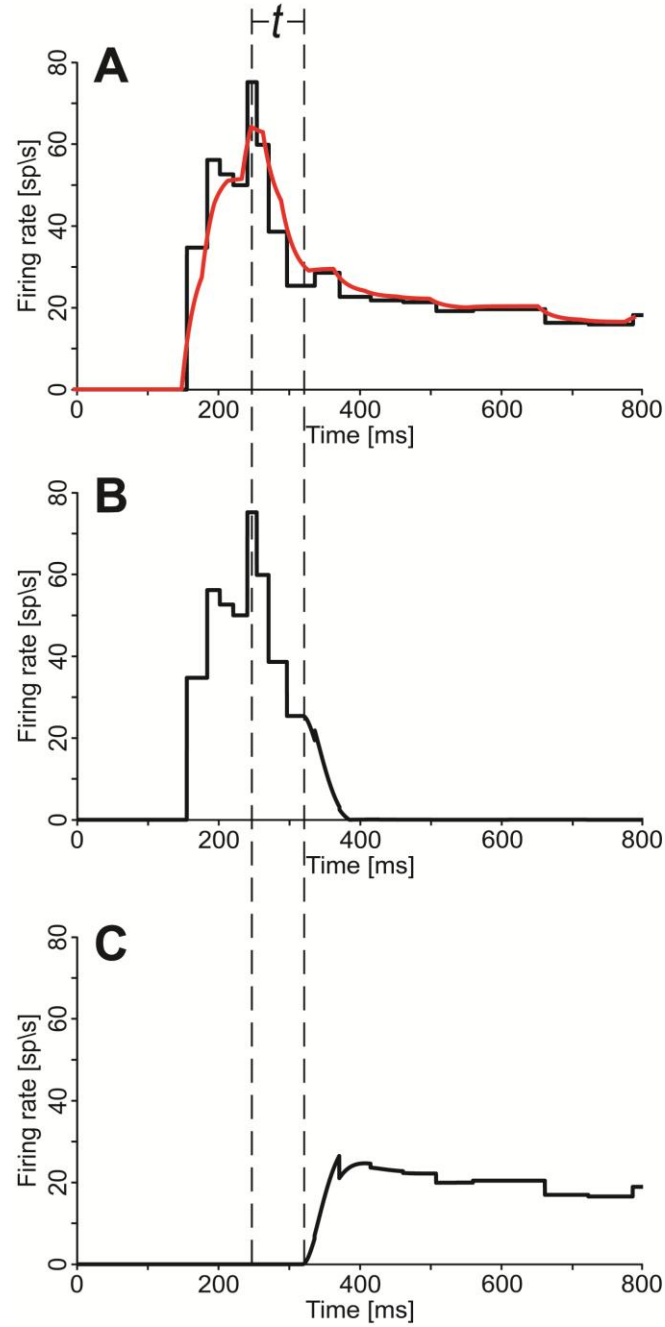


Fig. 36: Pulse-step parsing. Panel A displays burst-tonic cell firing during a saccade-free vergence eye movement, which the parsing algorithm of the position model separated into pulse (B) and step (C) components. The dotted lines represent the duration of the decreasing signal recognized by the model. The duration of this interval is equivalent to the programmed value, t , the duration threshold. At the end of this interval, the parsing of the two components began. The red trace shows the low-pass filtered version of the signal used for parsing.

Pulse gain was allowed to vary and was the result of two variables, representing a linear and quadratic component (Fig 34, "nonlinear gain"). Gain proportional to version velocity (linear and quadratic) was also added as an estimate of monocularity, but was significant in only a very small subset of cells in one animal (see Results). After the pulse and step components were multiplied by their appropriate gains, they were added back together prior to entering the poles. A small neural delay was applied when necessary to match the cell firing input to the position or velocity output.

As was previously addressed in detail in the above Data Analysis section and the Methods section, all trials were sorted and classified according to the presence and timing of saccadic activity during the vergence movement. For the portion of the study currently being discussed, only saccade-free trials, as defined in the Methods, were included. This exclusion eliminated a large percentage of trials, and only cells with at least three saccade-free smooth trials were analyzed. Although the majority of our recordings yielded data pertaining to the on direction (convergence for convergence cells and divergence for divergence cells), in the few cells where enough data was available in the off direction, modeling results were similar to the on direction, but with different parameters, similar to the results of the Zee model for vergence behavior in both directions (Zee et al 1992). Prior to using either the position model, a pre-analysis phase included selection of an area of steady fixation just prior to the cell firing associated with the vergence eye movement. The average vergence position during this time period was considered the baseline vergence position and was subtracted from the vergence position trace. Similarly, a vergence cell firing baseline was determined and subtracted. This allowed the position model to consider only the change in vergence firing as the cause of

the change in vergence position, as opposed to absolute position. This operation ignored the possibility of variations of the parameters as a function of the starting vergence angle, but this was acceptable in our data sets, since both the starting “far” vergence angle for the convergence trials and the starting “near” vergence angle for the divergence trials was the same for the entire cell data set. The output of the models, as shown in the Results section, has these baselines added back in to accurately reflect the full scope of the eye movement and firing behavior. Parameter estimation was used in Matlab to fit the gains, neural delay, and pole time constants (T_c for real, q [natural frequency] and w [damping] for the complex pair). For each animal, we found that the complex pole pair parameters often settled on similar values. This may indicate that they represent qualities related to the animal’s oculomotor plant, and unrelated to the specific cell being analyzed. For this reason, the complex pole pair parameters were left constant for each animal after average values were determined. Because the amount of data was large and a substantial number of variables were estimated with a non-linear least-squares method and the standard trust-region-reflective algorithm, this reduced set resulted in a relatively fast estimation with enough power to fit the parameters well in most cases.

R^2 analysis. MatLab functions were used to compute adjusted R^2 values as statistical estimates of the similarity of the outputs of the models with respect to the recorded vergence eye movements. The original data were re-sampled in time to match the variable time sampling rate of the model outputs using linear interpolation when necessary. Since the focus of this study was on the correlation of the neuronal firing to the vergence behavior, the selection of the intervals for these comparisons was also focused on the dynamic movement of the eye. This selection was done by visual

inspection of the vergence position trace. To ensure that an overshoot or undershoot of the model after the vergence eye movement offset would be considered in the statistic, this time was chosen to be from close to the onset of the eye movement to roughly 100 ms after the offset of the eye movement. The interval selection was done manually based on a plot of the eye movement and the firing of the cell. To prevent bias, the model's output was not displayed during this process. By limiting the estimation of the R^2 to just the very first section of the tonic part we also avoided an artificial boosting of the R^2 value.

Results. 15 cells in Animal 1 and 20 cells in Animal 2 were analyzed. Of these, we classified 15 as burst-tonic, 8 as tonic, and 12 as burst cells. Typical results of the models for these cell types are shown in Fig. 37. Our qualitative analysis indicated that the behavior of burst and burst-tonic cells has quite a large range of variability between cells, in particular the burst-tonic cells with regard to the relative pulse and step gains (Fig. 35). With the position model directly addressing the aspect of the pulse step differences through pulse-step parsing, it was expected that the position model would more closely fit the recorded data than the velocity model, which was applied only to the burst cells. This consideration was further supported by the fact that burst cells have also a much higher local variability in firing rate and, as we discussed earlier, some burst cells seem to encode only part of the response. This was often the case. Table 1 shows the adjusted R^2 values of the cells in both animals. The R^2 was both higher and less varied for burst-tonic and tonic cells than for burst cells, and was higher on average for both in Animal 1. As was mentioned previously, we tested if the insertion of a non-linear gain (a linear and a quadratic term) in non-saccadic version velocity – we are still estimating

saccade-free vergence behavior - had an impact on the quality of the model. These non-saccadic version velocities would indicate the presence of asymmetric saccadic-free vergence responses between the two eyes. It is important to note that this is a version pulse gain. A tonic version sensitivity would have qualified the cell as a oculomotor motoneuron. Student's T-test found only one instance of a significant difference in the samples of adjusted R^2 values of the model fits to the data. If the two pulse gain terms related to version velocity were omitted from the standard set of pulse gains used to fit the data, the first burst-tonic cell for Animal 1 of Table 1 was found to have a significantly worse mean adjusted R^2 value. In most cases, the model produced strikingly good results, almost completely predicting vergence eye movement (Fig. 37). In many cases of lower R^2 values for burst cells, latency was particularly damaging, as among these cells, the cell firing began slightly after the onset of the vergence. This may indicate these cells have a function other than driving vergence eye movements. For example, they might be part of the efferent copy pathway or, alternatively, they might drive only particular components of vergence eye movements which occur after the onset. If the former is true, a negative delay may have given a fit with a higher R^2 . In other words, these cells would still encode the vergence velocity in its entirety, but their latency precludes the possibility that they drive the movement. However, the quality of the fit was only impaired by allowing negative delays, as these cells typically fit only the latter part of the vergence velocity, often quite well. This indicates that these cells might still drive components of the vergence velocity command, similar to the cells which encode the entire velocity profile, but leaves the issue of their role in the vergence system, whether active or passive, unclear. One interesting hypothesis is that these cells could be

Cell Type	Animal	N	Mean	SD	Median	Range
Burst	Animal 1	20	0.880	0.167	0.943	0.610
		17	0.702	0.184	0.742	0.526
		29	0.964	0.038	0.984	0.147
		7	0.974	0.009	0.974	0.026
		93	0.908	0.059	0.923	0.330
		6	0.983	0.012	0.985	0.035
		3	0.685	0.075	0.701	0.148
		10	0.982	0.011	0.985	0.032
	Animal 2	3	0.925	0.068	0.964	0.118
		10	0.990	0.012	0.997	0.036
		25	0.959	0.048	0.971	0.233
		3	0.931	0.052	0.926	0.104
		44	0.957	0.045	0.972	0.258
		20	0.873	0.149	0.934	0.527
		6	0.959	0.025	0.966	0.070
		15	0.956	0.048	0.968	0.196
Tonic	Animal 1	8	0.962	0.032	0.975	0.081
		4	0.837	0.179	0.894	0.401
		15	0.989	0.006	0.991	0.022
		5	0.815	0.107	0.812	0.299
	Animal 2	4	0.873	0.085	0.896	0.198
		9	0.969	0.014	0.968	0.037
		4	0.965	0.024	0.971	0.055
		5	0.896	0.061	0.919	0.156
Burst	Animal 1	28	0.941	0.055	0.963	0.204
		11	0.861	0.058	0.879	0.155
		10	0.942	0.050	0.958	0.154
		18	0.729	0.131	0.759	0.502
		3	0.685	0.075	0.701	0.148
		14	0.448	0.147	0.458	0.600
	Animal 2	7	0.813	0.082	0.836	0.238
		7	0.591	0.207	0.619	0.654
		6	0.714	0.143	0.745	0.420
		4	0.790	0.081	0.786	0.166
		11	0.735	0.134	0.780	0.342
		11	0.735	0.134	0.780	0.342

Table 1 – Statistics for saccade-free model estimations using all parameters. These statistics are based on adjusted R2 values computed by comparing the vergence behavior estimated by the model and the vergence position, for burst-tonic and tonic cells, or vergence velocity, for burst cells. Each line represents a cell, and N refers to the number of trials for that cell.

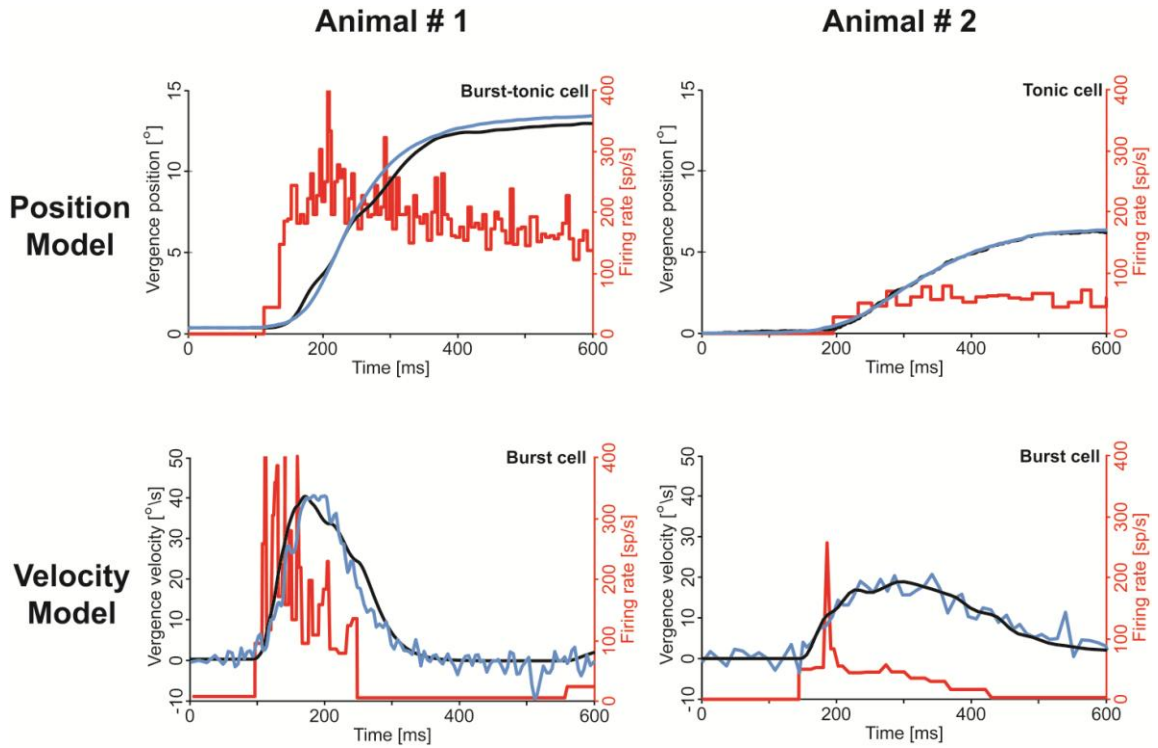


Fig. 37: Typical results of position and velocity models. The firing frequency of the cells is shown in red, with the vergence position (top) or velocity (bottom) in black. The blue trace is the predicted vergence by the position (top) or velocity (bottom) model. These colors will be used for the remaining figures.

the “locking” cells, but our stimuli are not appropriate to specifically engage only this vergence subsystem.

Vergence enhancement encoded by midbrain vergence cells. In the previous section, all trials containing saccades were eliminated in order to construct a saccade-free smooth vergence model of the cell. However, saccades which occur during vergence, and their associated vergence enhancement, are of paramount interest here, as they are a key element of the modern binocular vs. monocular debate (see Background). Are these vergence velocity increases which occur during saccades driven by the vergence system

or are they monocularly encoded in the saccadic system? If the vergence system is responsible for their generation, it is reasonable to expect that the vergence models which were quite successful in predicting the saccade-free smooth vergence responses would also apply to trials containing saccades. With that in mind, we used the smooth model of the cell, with the same parameters, to estimate the vergence response of the animal from the firing rate of the cell during combined saccade-vergence trials.

Results. Vergence enhancement was not seen in most vergence cells. Fig. 38 shows modeling results of trials from two burst-tonic cells and two burst cells with the model parameters set using only the smooth sets. In these cells, the models succeed until the onset of the saccadic movement (S_{ON}). At that point, vergence velocity drastically increased, but vergence cell firing did not, sometimes even decreasing. Typically, the model prediction became better after saccadic offset (S_{OFF}), which is consistent with the cell encoding only the non-enhanced smooth component. This component is affected by the enhancement, but only where the effect of the reduction in post-enhancement vergence motor error is concerned. Because the models correctly predicted the vergence eye movement outside of saccades, indicating the validity of the model, we see this as strong evidence that vergence enhancement is specifically not encoded within these vergence cells. Since this enhanced vergence must be coded elsewhere, presumably outside of the vergence system, this supports the monocular hypothesis. In cells with this behavior, there were some trials with saccades which occurred very close to the onset of the associated vergence movement, in which the model correctly predicted the entire vergence movement (Fig. 39). However, these trials did not include vergence enhancement. This behavior was well described both in Busettini and Mays (2005b) and

Kumar et al (2006). Large saccades, which often occur very early in the vergence response, elicit little or no enhancement. Busetini and Mays (2005b) described these results as an active suppressive mechanism at the level of the superior colliculus of the vergence enhancement for large saccades. Kumar et al (2006) modeled it as a non-linear interaction.

The cell in Fig. 40, also described in Figs 30, 31 and 32, was the only cell in our data set in which the cell firing encoded almost the entirety of the enhancement, and the smooth model closely followed the vergence enhancements.

Experiment 2

The quantification of midbrain vergence cell behavior during oblique tracking in depth through single unit electrophysiological recordings

Rationale. Conjugate oculomotor responses utilize the saccadic system specifically for rapid transfers of gaze and the smooth pursuit system specifically for smoothly tracking moving objects. The vergence system is strikingly different in that both discrete transfers of gaze in depth and smooth tracking in depth are driven by the same system (Mays et al 1986; Judge and Cumming 1986). As is the case with vergence enhancement during saccades, a debate regarding the binocular vs. monocular nature of the smooth pursuit system arises – is the smooth pursuit system strictly a conjugate system or, alternatively, is it capable of sending asymmetric commands to the two eyes?

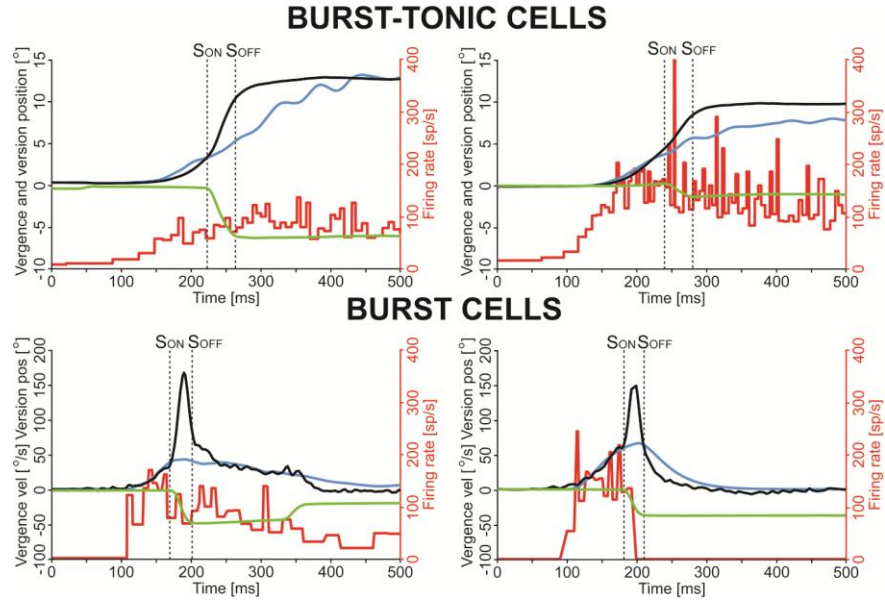


Fig 38: Vergence cells which do not encode saccadic enhancement. S_{ON} : saccadic onset. S_{OFF} : saccadic offset. Red traces: firing frequency. Black traces: vergence velocity. Blue traces: model estimation. Green traces: horizontal version.

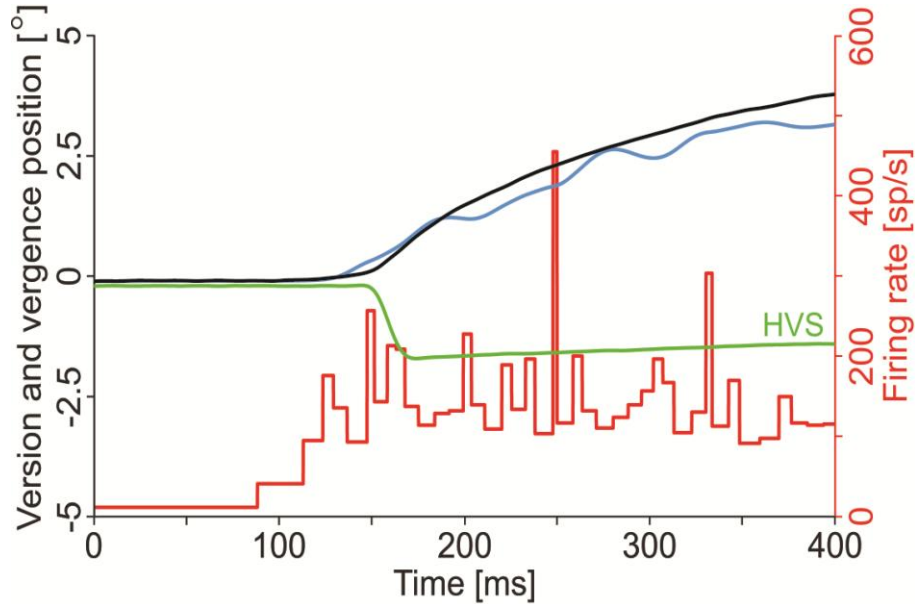
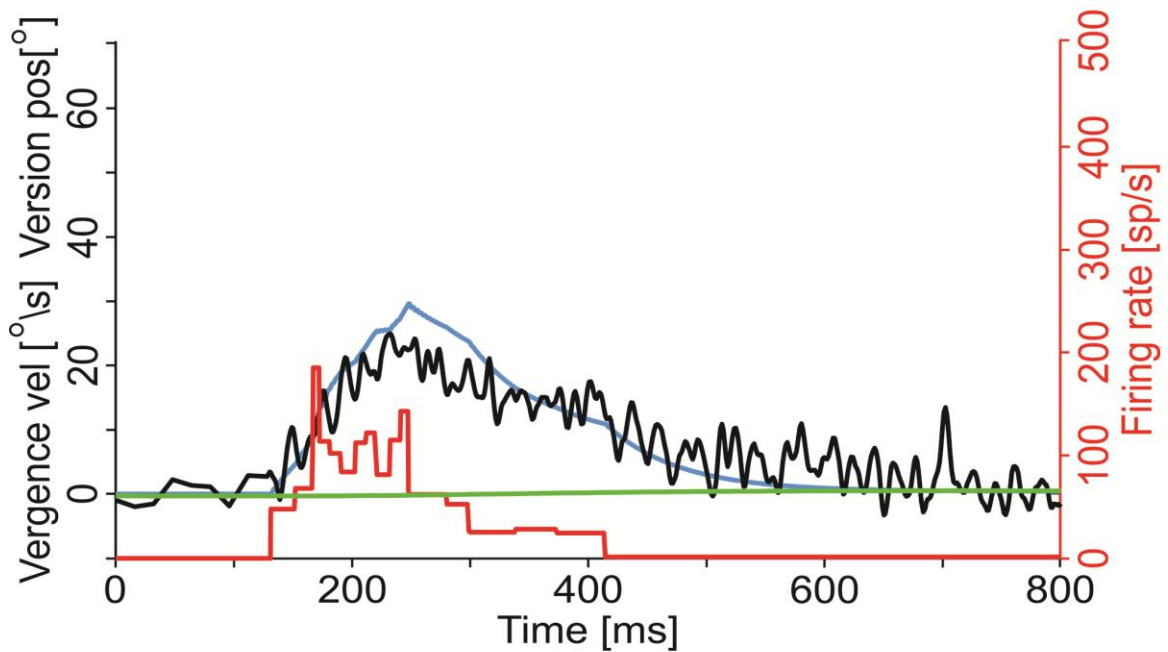


Fig. 39: Saccade at the onset of vergence. Saccades occurring early in the vergence response, usually larger saccades, often elicit little or no enhancement. Only a saccade-free like smooth response is generated. Accordingly, this cell, which does not code enhancement, perfectly encodes the entirety of the response. Note the absence of any unspecific saccadic-related response. Red traces: firing frequency. Black traces: vergence velocity. Blue traces: model estimation. Green traces: horizontal version.

SMOOTH MODEL APPLIED TO SMOOTH TRIAL



SMOOTH MODEL APPLIED TO ENHANCED TRIAL

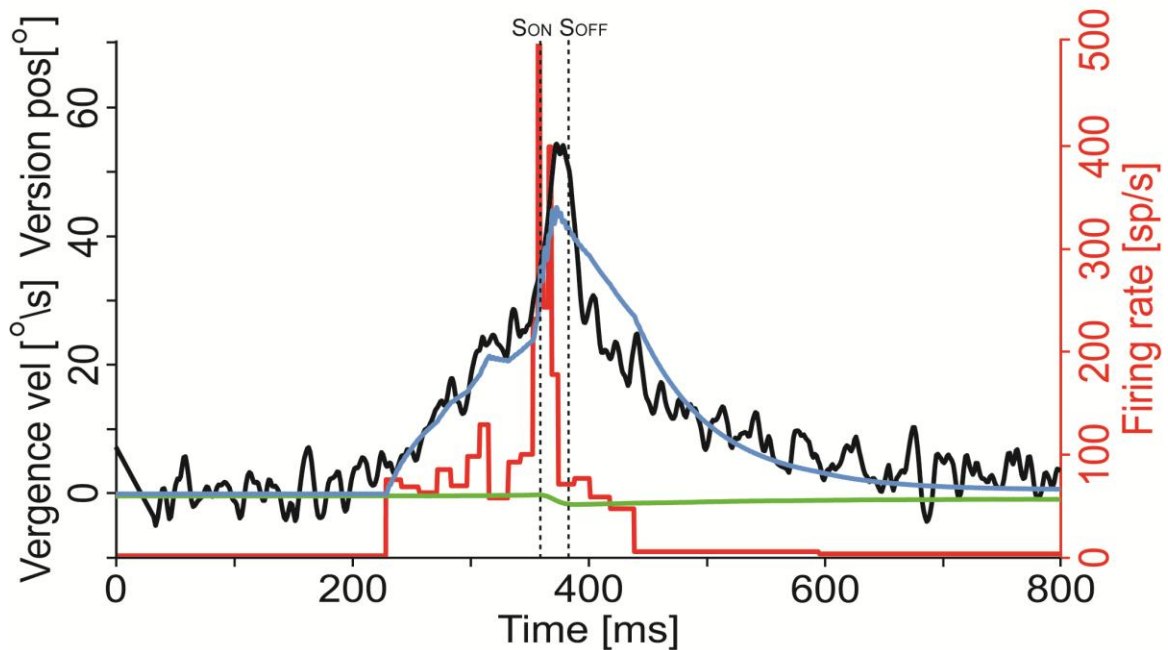


Fig 40: Example of an enhanced burst cell and the effect of this enhancement on the velocity model. Red traces: firing frequency. Black traces: vergence velocity. Blue traces: model estimation. Green traces: horizontal version.

Our specific question is if the oculomotor commands for tracking along an oblique trajectory in depth originate as monocular smooth pursuit commands or as the sum of conjugate smooth pursuit and symmetric vergence commands. There is evidence in the literature for both scenarios. Judge and Cumming (1986) reported that midbrain vergence cells are not active during conjugate tracking, but Enright (1996) reported slow velocity asymmetrical vergence responses. As was explained in more detail in the introduction, Zhou and King (1995) observed both differences between vergence and smooth pursuit dynamics and correlations of open-loop monocular retinal slip with smooth pursuit movements, and concluded that the oculomotor control of visual tracking in depth is monocularly organized. A commonly used experimental technique is the Müller paradigm, in which a subject pursues a target moving in depth which is carefully aligned with one eye. Motion is detected only in the other eye, and the subject can track with that eye leaving the eye that does not see motion stationary. This is cited as further evidence of monocular tracking. Of course, it is not possible to discern from behavior alone whether responses during the Müller paradigm are monocular tracking responses or special cases of vergence/smooth pursuit tracking, even if this is often assumed to be the case by several authors. In contrast, it has been shown through the use of polarizers that monocular step stimuli elicit symmetric ultra-short latency vergence responses (Busettini et al 1996; Busettini et al 2001). Studies of the frontal eye fields of cortex have yielded the inconclusive, relative to the monocular vs. binocular debate, discoveries of a distinct vergence area (Gamlin and Yoon 2000) and of cells that code these oblique tracking movements in three dimensions (Fukushima et al 2002); the former supporting binocular organization and the latter supporting monocular organization. The fact that several

cortical areas contain cells that encode a particular vector in space, a monocular type of encoding, counters the separation of cyclopean and vergence coding required for Hering's scheme, at least at the sensory level.

In the case of oblique tracking in depth, Hering's law of equal innervation predicts that the smooth pursuit system contributes the conjugate fronto-parallel portion of these oculomotor commands and the vergence system provides the in-depth vergence component. If the latter is true, the vergence component of oblique tracking in depth should be largely accounted for by the firing of the midbrain vergence cells during the oblique movement. If the relationship between vergence cell firing and vergence behavior during pure vergence tracking were retained during oblique tracking, this would strongly support the idea that the movement is the resulting sum of conjugate smooth pursuit commands and vergence commands. Currently, there are no data regarding the behavior of midbrain vergence cells during oblique tracking to either support or refute this occurrence. This experiment explored the contribution of the vergence midbrain cells to the oculomotor control of oblique tracking in depth. If the cyclopean and the in-depth components of the oblique tracking are perfectly parsed between a conjugate smooth pursuit system (cyclopean component) and a symmetric vergence system (in-depth component), we will be able to successfully model the relationship between vergence cell firing and vergence behavior during oblique tracking using a model found to be effective at describing straight ahead in-depth tracking.

Experimental Procedures. The methodological procedures for this experiment share a great deal of overlap with those in Experiment 1. Two rhesus macaques different from the two utilized in Experiment 1, participated in this portion of the project.

Conjugate saccadic trials were also used to verify that the cell being recorded was in fact a vergence cell as opposed to an oculomotor motoneuron. The animal experienced the same daily routine that would have been required for Experiment 1 and was appropriately seated and adjusted in the experimental apparatus, proper stereotaxic coordinates of electrode penetration were set on the electrode positioner, and a microdriver lowered the electrode to the appropriate depth to allow for observation and recording of midbrain vergence cells. Cellular firing patterns were similarly observed both visually and audibly through an oscilloscope and an audio output of the recording apparatus. The classification requirements for vergence burst cells, vergence tonic cells, and vergence burst-tonic cells from Experiment 1 were reapplied here, and again, cells with significant tonic changes in conjugate eye position, most often associated with strong bursts of activity for saccades in the on direction and pauses for saccades in the off direction were considered oculomotor motoneurons and were not further analyzed.

The central difference between this experiment and the first is that this experiment examined midbrain vergence cells during tracking behavior rather than discrete transfers of gaze between stationary targets. As a result, the key distinctions between the two experiments are not found in the basic experimental or recording procedures, but rather in the stimulus design and application of the model. The stimulus design for this experiment included randomly interleaved trials of: fronto-parallel target steps, to elicit conjugate saccades; target steps in depth aligned with the straight-ahead direction, to elicit saccade-free vergence responses (see Panels A and B in Fig. 19 of the Methods section); and smooth tracking trials along twelve different oblique directions in the horizontal plane (see Panel C in Fig. 19 of the Methods section). The sensitivity of some cells to vertical

conjugate smooth tracking was also tested to determine whether or not the cell was associated with any sort of trochlear activity (Mays et al 1991). To reduce the possibility of entrainment, the target was initially placed at 6° of vergence for all trials. The maximum applicable divergence step was therefore limited to 6° , since we could not ask the animal to diverge beyond straight ahead (0°). In order to maintain a balanced paradigm, the maximum size of the convergence step was also limited to 6° . Accordingly, the tracking motion was additionally limited to 6° . Since the tracking motion was limited to 6° , the duration of the ramp was determined by the speed of the ramp, which was either $10^\circ/\text{s}$, $20^\circ/\text{s}$, or $40^\circ/\text{s}$. The target was turned off immediately before the end of the ramp to prevent the animal from seeing the end of the movement. Due to the limited time a cell can be recorded, not all speeds were tested with all cells.

Data Analysis. As in Experiment 1, once the initial data processing (see Methods) was complete, the prepared trials were first sorted according to neuronal firing pattern being categorized as tonic, burst, or burst-tonic. Within each of these categories, trials were then sorted according to oblique direction.

Results. 61 cells were recorded in animal 3, and 20 cells were recorded in animal 4. Before oblique ramp trials could be analyzed using either the position model or the velocity model, it was necessary to ensure that both models (position and velocity), which were originally designed for trials of symmetric vergence steps in depth, were also capable of modeling symmetric vergence pursuit in response to ramp stimuli. In applying the position model to vergence pursuit movements, the parsing of pulse and step components needed to be reconsidered. While an initial burst in the firing frequency was

common during vergence tracking movements, similar to vergence movements in response to step stimuli, the later firing was more complex, not being simply tonic. There were also multiple bursts of activity in some trials, which were mirrored by oscillations in the vergence velocity. Similar oscillations are found in smooth pursuit responses during fronto-parallel tracking, which are likely associated to the local positive loop typical of tracking mechanisms. The internal negative feedback loop described earlier keeps track of the progress of the movement toward the goal. The positive feedback loop, which encodes the current velocity of the eyes, is needed to compute the velocity of the target in space as the sum of the velocity of the eyes and of the target on the retinas. When the head is stationary, as was the case in our experiments the estimated velocity of the target in space is the actual driving force of the tracking response. Positive feedback loops cause oscillatory behaviors even with very small neural delays, and this is probably the origin of our oscillations both in the cells and in the behavior. The organization of these driving signals as monocular or binocular components is also unresolved. The meaning of this multi-layered firing profile and the function of its different components are unclear, due to the general lack of knowledge about the vergence system. To ensure a proper comparison with the saccade-free vergence step results, only the first 300 ms after presentation of the stimuli was estimated by the position model. This time frame primarily consists of the open loop phase of the eye movement and is likely driven by the initial burst of activity in the cells. Since only the first 300 ms of the movement were used and the subsequent ongoing firing not considered, the parsing was not necessary and only the pulse branch of the position model was used for the burst-tonic cells. Pure tonic cells were not considered in this initial study. These issues will be addressed with more

complex models in future studies. Note that this limitation in the time interval of analysis is somewhat irrelevant for our hypothesis, since our primary concern was to study if and to what degree the vergence signal is retained for all oblique directions and this interval of firing is sufficient to give a robust indication of this relationship. Voluntary vergence tracking along the straight ahead direction and fronto-parallel smooth pursuit tracking have very similar latency, around 100 ms (Leigh and Zee 2006). This is also true for the ultra-short latency conjugate ocular following and vergence reflex stabilization mechanisms (Miles et al 1986; Busettini et al 1996). Thus, any deviation from what is expected by Hering's law of equal innervation will be present from the earliest parts of the neural responses.

Fig. 41 panels A-C show three typical model results for a convergence burst-tonic cell in animal 3 for trials similar to those of Experiment 1, with the animal responding to symmetric straight-ahead convergence steps. As resulted from the first experiment, the position model accurately predicted vergence eye movements with high precision. Using this same model, with the same parameters (T_c , q , w , and nonlinear gain variables), trials containing symmetric convergence ramps were modeled (panels D-F). The results were very similar, with precise fitting of the model's predicted vergence position to the recorded vergence position. Unlike the vergence enhancement study, in which a new trial type with different properties (high velocity) was modeled, this comparison is between very similar vergence movements, with similar vergence velocities. As such, it was anticipated that the model would fit both trial types equally well so long as the vergence cells encode both steps and ramps in the same fashion. An important observation from these symmetric tracking responses is that no vergence equivalents of the conjugate

catch-up saccades were observed, unless the animal generated an off-direction saccade with an evident cyclopean component. These trials were not included in the modeling in Fig. 41. In the case of fronto-parallel smooth pursuit, the smooth pursuit system relies on the saccade system to rapidly “catch-up” the target when excessively lagging behind. This behavior is dramatically evident in patients with damages in their tracking responses. In pathologies where the gain of the smooth pursuit is too high, they are in the opposite direction. A very interesting hypothesis is that the step-driven vergence subsystem helps the ramp-driven subsystem, and that part of the oscillations reported earlier are an expression of this synergy. Unfortunately, the dynamics of the two types of

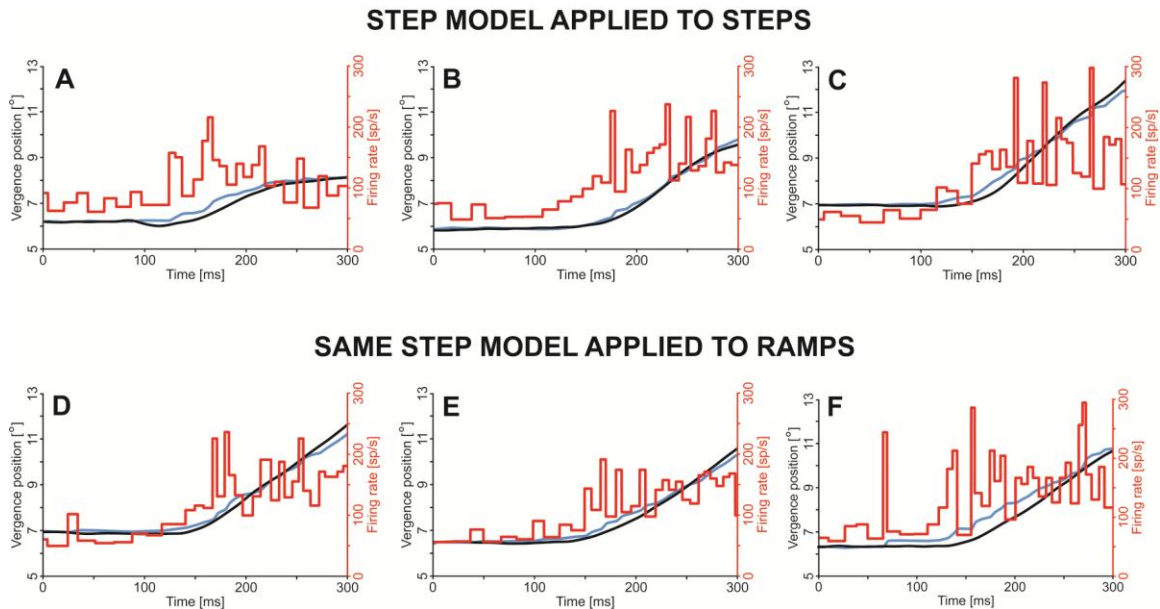


Fig 41: Symmetric convergence movements in response to steps vs. ramps. The position model parameters were set using only saccade-free vergence movements for symmetric step stimuli (A-C). When this model was applied to movements for symmetric ramp stimuli for this convergence burst-tonic neuron, it was equally effective (D-F). Red: cellular firing, black: vergence position, and blue: model estimation.

responses are likely too similar to be parsed, since neither were enhanced, unless the bursts are found to be linked to some kind of positional vergence error threshold. While the step model worked very well for the position model, applied to burst-tonic cells, the results were more complex for the velocity model, applied to burst cells. Because parsing is not relevant to the velocity model, it was applied to trials with ramp stimuli for the full duration of the movement, and parameters were set using the same time frame that was chosen during step stimuli for the first experiment (from vergence onset to 100 ms after vergence offset). The results of the analysis on a divergence burst cell in animal 3 are shown in Fig. 42, with the same format as Fig. 41. The velocity model parameters were estimated on step trials as before, with the model providing a good fit of the data (panels A-C). However, these parameters were not effective for the trials with ramp stimuli (panels D-F). The model often fit the decreasing phase of vergence velocity, the return to zero, better than the increasing phase (panels E and F). This deviation in fit is analogous to the fitting of the cells that did not include enhancement, in which the model's ability to fit the data drastically increased after saccadic offset. This could indicate that the onset of the vergence velocity for ramps is not encoded by this vergence burst cell. One possibility is that this cell could be encoding a later component of the movement. If this were the case, it could also explain the negative latency in this cell, which is much more dramatic for ramp stimuli (panels E-F) than for step stimuli (panels A-C). Interestingly, Krauzlis and Lisberger (1989) proposed that the smooth pursuit response is the result of several components, including an initial burst associated with the initial acceleration of the retinal image.

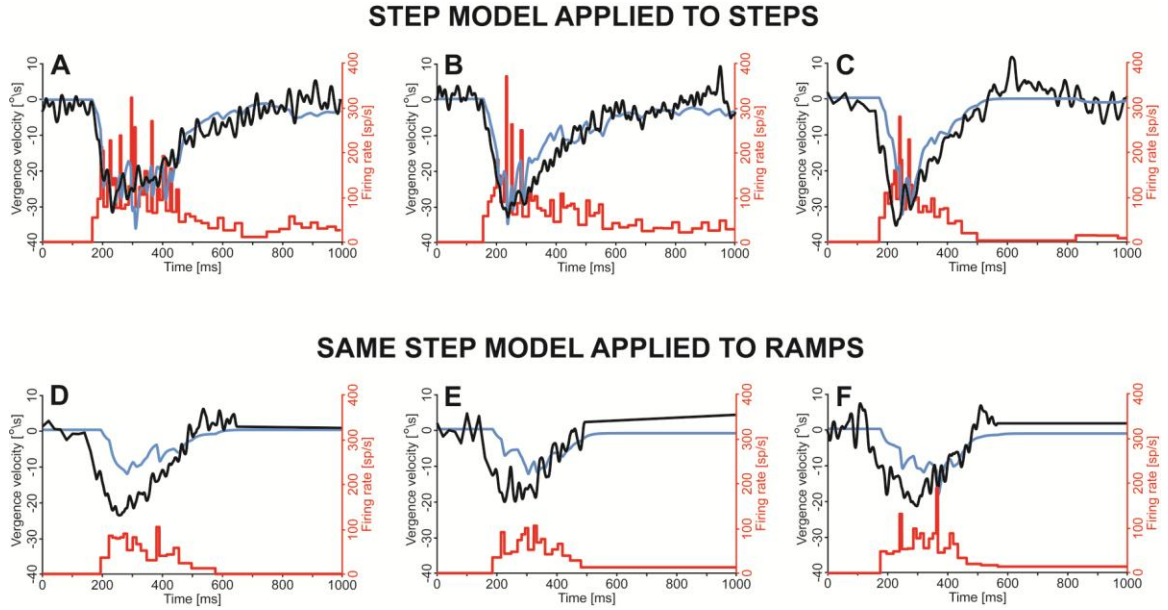


Fig. 42: Symmetric divergence movements in response to steps vs. ramps. The velocity model parameters were set using only vergence responses to symmetric steps. When this model was applied to movements for symmetric ramp stimuli for this divergence burst neuron, it was less effective, particularly in predicting the velocity of the first phase of movement (Panels E-F). Red: cellular firing, black: vergence position, and blue: model estimation.

To properly address this point, a large number of burst cells will be required, and their diversity may give way to clear categories of burst cells, some of which may encode the onset of vergence velocity for both steps and ramps in a similar manner. To this end, we have recorded vergence cells from one additional animal and will extend our analysis to those data. Although oblique tracking data were never recorded in the laboratories of Mays's or Busetini's before this study, some sinusoidal and ramp tracking trials in the straight ahead direction randomly mixed with symmetric steps trials were acquired several years ago using the same optical arrangement. We might attempt to add them to the analysis, limiting the analysis of the sinusoidal tracking to the open loop period.

The primary goal of this experiment was to determine if midbrain vergence cells encode vergence in a similar fashion for oblique pursuit movements in depth, which we tested along several trajectories. If the oblique direction must be taken into account when defining model parameters, this would imply that some external monocular mechanism is most likely involved, or, at the very least, some unknown mechanism beyond the scope of the current understanding of the vergence system. Fig. 43 shows typical results from modeling a convergence burst-tonic cell (position model) using only symmetric ramp trials at 90° - from far to near along the straight ahead direction - for parameter estimation. As we illustrated earlier, for burst-tonic cells this gave results mostly equivalent to parameter estimation based on symmetric step trials. This is the same cell shown in Fig. 41, with a good fit for symmetric convergence responses to ramp stimuli. The sufficiency of this fit was maintained for all other oblique directions, without adding any version parameters to the model. Thus, the traditional interpretation of vergence movements during saccades encoding only vergence, regardless of version movements (Mays 1984; Mays et al 1986; Judge and Cumming 1986), also extends to burst-tonic cells during oblique pursuit movements in depth.

The same question was then addressed for burst cells. As in Fig. 43, parameter estimation was first obtained using only straight ahead symmetric ramp trials. Note, for burst cells the option of using the step-derived parameters is not a viable alternative, because of our finding that burst cells behave differently for ramps and steps. In Fig. 44, a similar analysis to Fig. 43 is shown, using the burst cell from Fig. 41. Because this cell was a divergence burst cell, 90° refers to symmetric divergence. While the fit was not as good (lower R^2) as the fit for burst-tonic cells, the model fit symmetric divergence well.

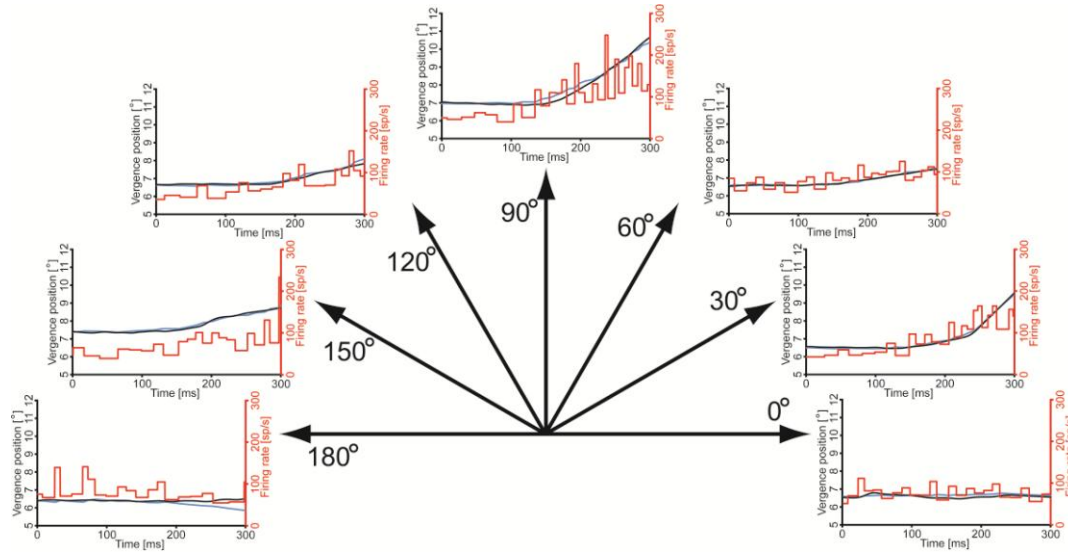


Fig. 43: Results of the position model for a convergence burst-tonic cell while executing oblique vergence movements. The parameters of the model were set using only symmetric ramps (90°), but the model was equally as effective for the oblique and fronto-parallel directions. Red: cellular firing, black: vergence position, and blue: model estimation.

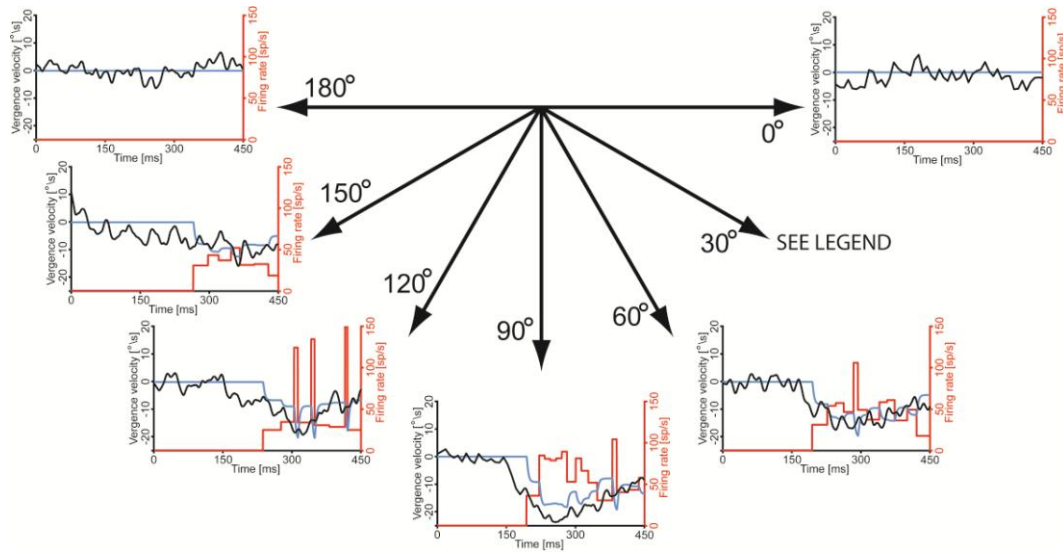


Fig. 44: Results of the velocity model for a divergence burst cell while executing oblique vergence movements. The parameters of the model were set using only symmetric ramps (90°), but the model was equally effective for the oblique and fronto-parallel directions. 30 degree movements were not recorded due to a technical error. Red: cellular firing, black: vergence position, and blue: model estimation.

As with the burst-tonic cell in Fig. 43, the fit was equally good for the oblique and fronto-parallel directions, even though the model was estimated only on the trials along the 90° direction. This is a strong indicator that, even for the varied burst cells that have complex firing profiles, the vergence during smooth pursuit is strictly encoded by the vergence system with no need for a monocular component.

CONCLUSIONS

Our study of the behavior of midbrain vergence cells during 3-D discrete transfers of gaze and during oblique tracking in depth achieved several milestones, which will be briefly illustrated here alongside the ongoing and future work that has arisen from these findings.

Coding of vergence eye movements by midbrain vergence cells during saccade-free step transfers of gaze

The main goal of this portion of the experiments was to determine a model that could reliably link the behavior of individual midbrain vergence cells to their associated vergence eye movements. This model had to be reasonably simple and return consistently accurate estimates for the largest group of cells in our recorded data set as possible. Many configurations were attempted, until we converged on a position model for the tonic and burst-tonic cells, and a velocity model for the burst cells. Both consisted of gain elements, linear or non-linear, a real pole, a pair of complex poles, and a delay. In addition, an algorithm was developed, described in Appendix B and Fig. 38, to parse the burst component from the step component in the burst-tonic cells.

As illustrated in Table 1 and Fig. 37, for all cells that yielded three or more usable trials the adjusted R^2 was often quite extraordinary, especially if one considers that the

behavior of a single cell often fully predicted the animal behavior. The burst cells were found to be more variable than the tonic and burst-tonic cells, as was also shown in the “Cell types” section, both in terms of lead/lag time of their firing and the component of the movements they encode. Additional parameters, such as a velocity threshold or a vergence motor error threshold are likely candidates to account for the observed variability. With the exclusion of these components, unaccounted for by the proposed models, the goal of finding a dynamical link between the firing of the vergence cell and the eye movement was fully successful and offers, for the first time, a quantitative dynamical analysis of these cells.

Coding of vergence eye movements by midbrain vergence cells during saccade-vergence combined trials

Both Zee et al (1992) and Busettini and Mays (2005b) predicted the existence of cells that encode only the smooth non-enhanced component of the vergence response. These cells do not code the saccade-vergence enhancement, but they are sensitive to the rapid reduction in current vergence motor error that it causes. This is clearly unmasked in the firing in the post-saccadic period. Almost all burst cells presented a decrease in their post-saccadic burst of activity after an enhancement with respect to saccade-free trials, and generally with a latency that confirmed this process to be driven by a non-visual internal feedback loop that takes into account the intrasaccadic enhancement. The majority of the cells in our data set were of this kind. Some cells, as illustrated in our Cell Types section, encoded at least part of the enhancement, but only one cell exhibited a firing that was consistent with a full encoding of the intrasaccadic response and, as noted,

this response depended on the saccadic direction. Furthermore, this cell also had a directionally dependent firing rate for conjugate saccades.

The successful application of the saccade-free smooth model to predict the vergence response during the saccade-vergence trials from the firing of the cell was the main achievement of this section of the study, offering a long-sought after objective tool to finally address the question of whether or not the intrasaccadic enhancement is encoded inside the vergence system. We are fully aware that our small data set cannot offer any conclusive statement in that regard. We can confirm the reports in Mays and Gamlin (1995; 2000) of vergence cells that encode at least some of the enhancement, but the high number of smooth-only cells might be construed as evidence for some significant monocular contributions. Nonetheless, the key finding that both smooth-only cells and enhanced cells encode the enhancement in their post-saccadic behavior confirmed a major weakness of the monocular solution: the need for a mechanism to determine the amount of total asymmetry generated by the monocular saccadic commands. This also raises the issue of the purpose in generating monocular commands. The fact that this correction is at the level of the burst cells, and therefore before the neural integration, does not support the suggestion that the correction is at the level of a single monocular neural integrator shared by both systems. Furthermore, as Mays () pointed out in a commentary on the published work of Zhou and King (1998), the monocular signals seem to be averaged out at the level of the motoneurons. Preliminary evidence (Davison et al 2004) suggests that the velocity sensitivity of the saccade-free component and not the sensitivity of the saccadic commands, which would indicate that

the enhancement is transmitted to the motoneurons by a vergence pathway, is transmitted to the motoneurons by the same pathway that delivers the smooth vergence component.

Our intention for the publication of these results is to expand the model to include the behavioral variability encountered in the burst cells, and add more data. From animals 3 and 4, used for the oblique tracking experiment, we also acquired step data along the straight ahead direction (Fig. 19 panels A and B). These data will allow the expansion of the saccade-free smooth model sets, and data contaminated with saccades that elicited evident enhancements, although not as optimal as trials with actual cyclopean changes of the target position, will be used to detect if an enhancement in the cell firing is present or not. In our cell archive we have data sets that, while not optimized for this specific goal, were acquired several years ago with the same optical system, and we plan to analyze and potentially add them to our analysis. It is important to note that the cells described in the old Mays's studies, although present in our archive, did not have the 20 kHz signal from the electrode, a feature added in 1992-1993. We consider the firing data of these sets unreliable for a dynamical modeling since they cannot be objectively verified from the electrode trace. As for all electrophysiological single unit experiments, our vergence-focused studies, as well as the saccadic-oriented studies of Cullen, van Horn, Sylvestre, Zhou, and others, it is objectively impossible to determine "how much" of a behavioral component is encoded by a cell group. We can only acquire data from a tiny fraction of the entire population. When there is behavioral variability, in our case between non-enhanced, partially enhanced, and perhaps fully enhanced cells, in the monocular data between left-eye coding cells, right-eye coding cells, and binocular cells, we are limited

to quantifying the percentage of cells found to encode a specific behavior, but not their true strength in determining the animal behavior.

Coding of vergence eye movements by midbrain vergence cells during oblique tracking in depth

We just recently completed the acquisition of the data from the second animal, and the analysis is still in progress, but our preliminary results on a subset of cells already showed some important findings.

None of the cells analyzed so far had consistent firing for fronto-parallel tracking, which excluded these cells from having monocular tracking components. This confirmed the observations by Cumming and Judge (1986) and Mays et al (1986). The application of the model determined during saccade-free steps to straight-ahead tracking was quite successful for burst-tonic cells, at least in the first 300 ms of the response, but much less for burst cells, as if they were not encoding the very first part of the response. This needs to be confirmed on the full set of cell. On the cells tested, the dynamical model based on the behavior of the cell in the straight-ahead tracking direction accurately replicated the behavior in the oblique directions. As also described in the results, the animal behavior during the later tracking (> 300 ms from target onset) was much more complex and with peak and valleys in both the vergence velocity and the cell firing. A striking difference with respect to the smooth pursuit responses was the apparent lack of catch-up saccades in the straight-ahead tracking responses, unless the animal introduced a cyclopean deviation. The higher the fronto-parallel component, the higher the number and size of

the catch-up saccades, which would indicate that they can be elicited only from a conjugate tracking. One of the planned analyses is to see if these saccades elicit any kind of vergence enhancement, in addition to helping the fronto-parallel component in its tracking task.

Our plan for the publication of these results is to include a third animal, already in training, in the study, and attempt to expand the analysis to the open loop component of sinusoidal fronto-parallel and in-depth tracking data present in some older recordings. Note that our study is the first to present a systematic analysis of the behavior of midbrain vergence cells during oblique tracking tasks. Thus, no data were available from our archives to expand the data set. We will also attempt to determine if some of the bursts in firing present during the later part of the responses might be equivalent to catch-up pulses in the vergence domain, by determining if they are associated to a threshold in current vergence error position. They would be step-like vergence responses, and therefore have dynamics similar to the tracking component, but by adding to the ongoing tracking they would help in reaching the moving target.

In summary, we believe that our work clearly demonstrates that midbrain vergence cells are much more than simple relays of a vergence motor command, and therefore, uninterestingly closely replicating the animal behavior. They are powerful tools to address many questions still open in the organization of the subcortical oculomotor pathways and the signals they encode. Our successful modeling efforts, in addition, offer a novel quantitative approach in addressing these issues which has never been attempted.

REFERENCES

- Barlow HB, Blakemore C, and Pettigrew LD.** The neural mechanism of binocular depth discrimination. *J Physiol* 193: 327-342, 1967.
- Busetтини C and Mays LE.** Pontine omnipause activity during conjugate and disconjugate eye movements in macaques. *J Neurophysiol* 90: 3838-3853, 2003.
- Busetтини C, Miles FA, and Krauzlis RJ.** Short-latency disparity vergence responses and their dependence on a prior saccadic eye movement. *J Neurophysiol* 75: 1392-1410, 1996.
- Busetтини C, Masson GS, and Miles FA.** Radial optic flow induces vergence eye movements with ultra-short latencies. *Nature* 390: 521-525, 1997.
- Busetтини C, Fitzgibbon EJ, and Miles FA.** Short-latency disparity vergence in humans. *J Neurophysiol* 85: 1129-1152, 2001.
- Busetтини C and Mays LE.** Saccade-vergence interactions in macaques. I. Test of the omnipause multiply model. *J Neurophysiol* 94: 2295-2311, 2005a.
- Busetтини C and Mays LE.** Saccade-vergence interactions in macaques. II. Vergence enhancement as the product of a local feedback vergence motor error and a weighted saccadic burst. *J Neurophysiol* 94: 2312-2330, 2005b.
- Chaturvedi V and Van Gisbergen JA.** Perturbation of combined saccade-vergence movements by microstimulation in monkey superior colliculus. *J Neurophysiol* 81: 2279-2296, 1999.
- Chaturvedi V and Van Gisbergen JA.** Stimulation in the rostral pole of monkey superior colliculus: effects on vergence eye movements. *Exp Brain Res* 132: 72-78, 2000.
- Chen AL, Ramat S, Serra A, King SA, and Leigh RJ.** The role of the medial longitudinal fasciculus in horizontal gaze: tests of current hypotheses for saccade-vergence interactions. *Exp Brain Res* 208: 335-343, 2011.
- Chen-Huang C and McCrea RA.** Viewing distance related sensory processing in the ascending tract of deiters vestibule-ocular reflex pathway. *J Vestib Res* 8: 175-184, 1998.

Cogan DG. Internuclear ophthalmoplegia, typical and atypical. *Arch Ophthalmol* 84: 583-589, 1970.

Collewijn H, Erkelens CJ, and Steinman RM. Voluntary binocular gaze-shifts in the plane of regard: dynamics of version and vergence. *Vision Res* 35: 3335-3358, 1995.

Cullen KE and Van Horn MR. The neural control of fast vs. slow vergence eye movements. *Eur J Neurosci* 33: 2147-2154, 2011.

Cumming BG and Judge SJ. Disparity-induced and blur-induced convergence eye movement and accommodation in the monkey. *J Neurophysiol* 55: 896-914, 1986.

Cumming BG and Parker AJ. Responses of primary visual cortical neurons to binocular disparity without depth perception. *Nature* 389: 280-283, 1997.

Davison RC, Busetini C, and Gamlin PDR. The behavior of medial rectus motoneuron during saccade-vergence interactions. Program No. 881.4. *Abstract Viewer/Itinerary Planner*. Washington, DC: Society for Neuroscience, 2004.

DeAngelis GC, Cumming BG, and Newsome WT. Cortical area MT and the perception of stereoscopic depth. *Nature* 394: 677-680, 1998.

DeAngelis GC and Newsome WT. Organization of disparity-selective neurons in macaque area MT. *J Neurosci* 19: 1398-1415, 1999.

Eifuku S and Wurtz RH. Response to motion in extrastriate area MSTl: disparity sensitivity. *J Neurophysiol* 82: 2462-2475, 1999.

Enright JT. The remarkable saccades of asymmetrical vergence. *Vision Res* 32: 2261-2276, 1992.

Enright JT. Slow-velocity asymmetrical convergence: a decisive failure of "Hering's law". *Vision Res* 36: 3667-3684, 1996.

Everling S, Pare' M, Dorris MC, and Munoz DP. Comparison of the discharge characteristics of brain stem omnipause neurons and superior colliculus fixation neurons in monkey: implications for control of fixation and saccade behavior. *J Neurophysiol* 79: 511-528, 1998.

Eubank RL. *Spline Smoothing and Nonparametric Regression. Statistics: Textbooks and Monographs vol. 90.* New York: Dekker, 1988.

Fuchs AF and Robinson DA. A method for measuring horizontal and vertical eye movement chronically in the monkey. *J Appl Physiol* 21: 1068-1070, 1966.

- Fukushima K, Yamanobe T, Shinmei Y, Fukushima J, Kurkin S, and Peterson BW.** Coding of smooth eye movements in three-dimensional space by frontal cortex. *Nature* 419: 157-162, 2002.
- Gamlin PD and Clarke RJ.** Single-unit activity in the nucleus reticularis tegmenti pontis related to vergence and ocular accommodation. *J Neurophysiol* 73: 2115-2119, 1995.
- Gamlin PD, Gnadt JW, and Mays LE.** Lidocaine-induced unilateral internuclear ophthalmoplegia: effects on convergence and conjugate eye movements. *J Neurophysiol* 62: 82-95, 1989.
- Gamlin PD and Mays LE.** Dynamic properties of medial rectus motoneurons during vergence eye movements. *J Neurophysiol* 67: 64-74, 1992.
- Gamlin PD and Yoon K.** An area for vergence eye movement in primate frontal cortex. *Nature* 407: 1003-1007, 2000.
- Gamlin PD, Yoon K, and Zhang H.** The role of cerebro-ponto-cerebellar pathways in the control of vergence eye movements. *Eye (Lond)* 10: 167-171, 1998.
- Gamlin PD and Zhang H.** Effect of muscimol blockade of posterior fastigial nucleus during vergence and accommodation in the primate. *Soc Neurosci Abstr* 22: 2034, 1996.
- Gamlin PD, Zhang Y, Clendaniel RA, and Mays LE.** Behavior of identified Edinger-Westphal neurons during ocular accommodation. *J Neurophysiol* 72: 2368-2382, 1994.
- Gandhi NJ and Keller EL.** Comparison of saccades perturbed by stimulation of the rostral superior colliculus, the caudal superior colliculus, and the omnipause neuron region. *J Neurophysiol* 82: 3236-3253, 1999.
- Hering E.** Die Lehre vom binocularen Sehen (English translation by B. Bridgeman and L. Stark, The Theory of Binocular Vision, New York: Plenum Press 1977). Leipzig: W. Engelmann, 1868.
- Hillis A, Flynn JT, and Hawkins BS.** The evolving concept of amblyopia: a challenge to epidemiologists. *Am J Epidemiol* 118: 192-205, 1983.
- Hubel DH and Livingstone MS.** Segregation of form, color, and stereopsis in primate area 18. *J Neurosci* 7: 3378-3415, 1987.
- Hubel DH and Wiesel TN.** Stereoscopic vision in macaque monkey. Cells sensitive to binocular depth in area 18 of the macaque monkey cortex. *Nature* 225: 41-42, 1970.
- Hung GK, Semmlow JL, and Ciuffreda KJ.** A dual-mode dynamic model of the vergence eye movement system, *IEEE Trans Biomed Eng* 33: 1021-1028, 1986.

- Inoue Y, Takemura A, Kawano K, Kitama T, and Miles FA.** Dependence of short-latency ocular following and associated activity in the medial superior temporal area (MST) on ocular vergence. *Exp Brain Res* 121: 135-144, 1997.
- Judge JS and Cumming BG.** Neurons in the monkey midbrain with activity related to vergence eye movement and accommodation. *J Neurophysiol* 55: 915-930, 1986.
- Krauzlis RJ and Lisberger SG.** A control systems model of smooth pursuit eye movements with realistic emergent properties. *Neural Computation* 1: 116-122, 1989.
- Miles FA, Kawano K, and Optican LM.** Short-latency ocular following responses of monkey. I. Dependence on temporo-spatial properties of the visual input. *J. Neurophysiol* 56: 1321-1354, 1986.
- Kawano K, Shidara M, and Yamane S.** Neural activity in dorsolateral pontine nucleus of alert monkey during ocular following responses. *J Neurophysiol* 67: 680-703, 1992.
- Kenyon RV, Ciuffreda KJ, and Stark L.** Unequal saccades during vergence. *Am J Opth Phys Opt* 57: 586-594, 1980.
- King WM and Zhou W.** Initiation of disjunctive smooth pursuit in monkeys: Evidence that Hering's law of equal innervation is not obeyed by the smooth pursuit system. *Vision Res* 35: 3389-3400, 1995.
- King WM.** Binocular coordination of eye movements – Hering's law of equal innervation or uniocular control? *Eur J Neurosci* 33: 2139-2146, 2011.
- Krishnan VV and Stark L.** A heuristic model for the human vergence eye movement system. *IEEE Trans Biomed Eng* 24: 44-49, 1977.
- Krishnan VV and Stark L.** Model of the disparity vergence system. Model of the disparity vergence system. In: *Vergence EyeMovements: Basic and Clinical Aspects*. Schor CM and Ciuffreda KJ Eds, London: Butterworths. 349-371, 1983.
- Kumar AN, Han YH, Kirsch RF, Dell'osso LF, King WM, and Leigh RJ.** Tests of models for saccade-vergence interaction using novel stimulus conditions. *Biological Cybernetics*, 95: 143-157, 2006.
- Leigh RJ and Zee DS.** Vergence eye movements. In: *The Neurology of Eye Movements*, edited by Gilman S. New York: Oxford, 2006, p. 364-365.
- Maunsell JH and Van Essen DC.** Functional properties of neurons in middle temporal visual area of the macaque monkey. II. Binocular interactions and sensitivity to binocular disparity. *J Neurophysiol* 49: 1148-1167, 1983.

Masson GS, Busetini C, and Miles FA. Vergence eye movements in response to binocular disparity without depth perception. *Nature* 389: 283-286, 1997.

Masson, GS, Busetini C, Yang DS, and Miles FA. Short-latency ocular following in humans: sensitivity to binocular disparity. *Vision Res* 41: 3371-3387, 2001.

Maxwell JS and King WM. Dynamics and efficacy of saccade-facilitated vergence eye movements in monkeys. *J Neurophysiol* 68: 1248-1260, 1992.

Maxwell JS and Schor CM. Symmetrical horizontal vergence contributes to the asymmetrical pursuit of targets in depth. *Vision Res* 44: 3015-3024, 2004.

May PJ, Porter JD, and Gamlin PD. Interconnections between the primate cerebellum and midbrain near-response regions. *J Comp Neurol* 315: 98-116, 1992.

Mays LE. Neural control of vergence eye movements: convergence and divergence neurons in the midbrain. *J Neurophysiol* 51: 1091-1108, 1984.

Mays LE. Has Hering been hooked? *Nature Med* 4: 889-890, 1998.

Mays LE and Gamlin PD. A neural mechanism subserving saccade-vergence interactions. In: *Eye Movement Research. Mechanisms, Processes and Applications*, edited by Findlay JM, Walker R, and Kentridge RW. Amsterdam: Elsevier, 1995, p. 215–223.

Mays LE and Gamlin PD. Neuronal circuits for accommodation and vergence in the primate. In: *Accommodation and Vergence Mechanisms in the Visual System*, edited by Franze'n O, Richter H, and Stark L. Basel: Birkhäuser Verlag, 2000, p. 1–9.

Mays LE and Porter JD. Neural control of vergence eye movements: activity of abducens and oculomotor neurons. *J Neurophysiol* 52: 743-761, 1984.

Mays LE, Porter JD, Gamlin PD, and Tello CA. Neural control of vergence eye movements: neurons encoding vergence velocity. *J Neurophysiol* 56: 1007-1021, 1986.

Mays LE, Zhang Y, Thorstad MH, and Gamlin PD. Trochlear unit activity during ocular convergence. *J Neurophysiol* 65: 1484-1491, 1991.

Miles FA, Judge SJ, and Optican LM. Optically induced changes in the couplings between vergence and accommodation. *J Neurophysiol* 7: 2576-2589, 1987.

Miller JM. Functional anatomy of normal human rectus muscles. *Vision Res* 29: 223-240, 1989.

Miller JM. Understanding and misunderstanding extraocular muscle pulleys. *Journal of Vision* 7: 1-15, 2007.

- Missal M and Keller EL.** Common inhibitory mechanism for saccades and smooth-pursuit eye movements. *J Neurophysiol* 88: 1880-1892, 2002.
- Moschovakis AK, Scudder CA, and Highstein SM.** The microscopic anatomy and physiology of the mammalian saccadic system. *Prog Neurobiol* 50: 133-254, 1996.
- Ono H and Nakamizo S.** Changing fixation in the transverse plane at eye level and Hering's law of equal innervation. *Vision Res* 18: 511-519, 1978.
- Ono H, Nakamizo S, and Steinbach MJ.** Nonadditivity of vergence and saccadic eye movement. *Vision Res* 18: 735-739, 1978.
- Poggio GF and Fischer B.** Binocular interaction and depth sensitivity in striate and prestriate cortex of behaving rhesus monkey. *J Neurophysiol* 40: 1392-1405, 1977.
- Poggio GF, Motter BC, Squatrito S, and Trotter Y.** Responses of neurons in visual cortex (V1 and V2) of the alert macaque to dynamic random-dot stereograms. *Vision Res* 25: 397-406, 1985.
- Poggio GF, Gonzales F, and Krause F.** Stereoscopic mechanisms in monkey visual cortex: binocular correlation and disparity selectivity. *J Neurosci* 8: 4531-4550, 1988.
- Poggio GF and Talbot WH.** Mechanisms of static and dynamic stereopsis in foveal cortex of the rhesus monkey. *J Physiol* 315: 469-492, 1981.
- Preslan MW and Novak MS.** Baltimore vision screening project. *Ophthalmology* 103: 105-109, 1996.
- Rashbass C and Westheimer G.** Disjunctive eye movements. *J Physiol* 159: 339-360, 1961.
- Robinson DA.** Oculomotor control signals. In: *Basic Mechanisms of Ocular Motility and Their Clinical Implications*, edited by G. Lennerstrand, and P. Bach-Y-Rita. Oxford: Pergamon Press, p. 337-374, 1975.
- Roy JP, Komatsu H, and Wurtz RH.** Disparity sensitivity of neurons in monkey extrastriate area MST. *J Neurosci* 12: 2478-2492, 1992.
- Sander T, Sprenger A, Neumann G, Machner B, Gottschalk S, Rambold H, and Helmchen C.** Vergence deficits in patients with cerebellar lesions. *Brain* 132: 103-115, 2009.
- Schor CM.** The relationship between fusional vergence eye movements and fixation disparity. *Vision Res* 19: 1359-1367, 1979.

- Schiller PH and Stryker M.** Single-unit recording and stimulation in superior colliculus of the alert rhesus monkey. *J Neurophysiol* 35: 915–924, 1972.
- Schwarz U, Busetini C, and Miles FA.** Ocular responses to linear motion are inversely proportional to viewing distance. *Science* 245: 1394–1396, 1989.
- Scudder CA.** A new local feedback model of the saccadic burst generator. *J Neurophysiol* 59: 1455–1475, 1988.
- Scudder CA, Moschovakis AK, Karabelas AB, and Highstein SM.** Anatomy and physiology of saccadic long-lead burst neurons recorded in the alert squirrel monkey. I. Descending projections from the mesencephalon. *J Neurophysiol* 76: 332–352, 1996.
- Scudder CA, Moschovakis AK, Karabelas AB, and Highstein SM.** Anatomy and physiology of saccadic long-lead burst neurons recorded in the alert squirrel monkey. II. Pontine neurons. *J Neurophysiol* 76: 353–370, 1996.
- Semmlow JJ and Heerema D.** The synkinetic interaction of convergence accommodation and accommodative convergence. *Vision Res* 19: 1237–1242, 1979.
- Semmlow J, Hung G, and Ciuffreda KJ.** Quantitative assessment of disparity vergence components. *Invest Ophthalmol Vision Sci* 27: 558–564, 1986.
- Sherrington CS.** Experimental note on two movements of the eye. *J Physiol* 17: 27–29, 1894.
- Shidara M and Kawano K.** Role of purkinje cells in the ventral paraflocculus in short-latency ocular following responses. *Exp Brain Res* 93: 185–195, 1993.
- Sklavos S, Porrill J, Kaneko CR, and Dean P.** Evidence for wide range of time scales in oculomotor plant dynamics: implications for models of eye-movement control. *Vision Res* 45: 1525–1542, 2005.
- Steinman SB, Steinman B, and Garzia RP.** *Foundations of Binocular Vision*. New York: Mc Graw-Hill Professional, 2000.
- Sylvestre PA and Cullen KE.** Dynamics of abducens nucleus neuron discharges during disjunctive saccades. *J Neurophysiol* 88: 3452–3468, 2002.
- Sylvestre PA, Choi JTL, and Cullen KE.** Discharge dynamics of oculomotor neural integrator neurons during conjugate and disjunctive saccades and fixation. *J Neurophysiol* 90: 739–754, 2003.
- Takemura A, Inoue Y, Kawano K, Quaia C, and Miles FA.** Single-unit activity in cortical area MST associated with disparity-vergence eye movements: evidence for population coding. *J Neurophysiol* 85: 2245–2266, 2001.

- Takemura A, Murata Y, Kawano K, and Miles FA.** Deficits in short-latency tracking eye movements after chemical lesions monkey cortical areas MT and MST. *J Neurosci* 27: 529-541, 2007.
- Van Gisbergen JA, Van Opstal AJ, and Tax AA.** Collicular ensemble coding of saccades based on vector summation. *Neuroscience* 21: 541–555, 1987.
- Van Opstal AJ, Hepp K, Hess BJ, Straumann D, and Henn V.** Two- rather than three-dimensional representation of saccades in monkey superior colliculus. *Science* 252: 1313-1315, 1991.
- Van Horn MR and Cullen KE.** Dynamic characterization of agonist and antagonist oculomotoneurons during conjugate and disconjugate eye movements. *J Neurophysiol* 102: 28-40, 2008.
- Van Horn MR and Cullen KE.** Dynamic coding of vertical facilitated vergence by premotor saccadic burst neurons. *J Neurophysiol* 100: 1967-1982, 2008.
- Van Horn MR, Sylvestre PA, and Cullen KE.** The brain stem saccadic burst generator encodes gaze in three-dimensional space. *J Neurophysiol* 99: 2602-2616, 2008.
- Waitzman DM, Van Horn MR, and Cullen KE.** Neuronal evidence for individual eye control in the primate cMRF. *Prog Brain Res* 171: 143-150, 2008.
- Walton MM and Mays LE.** Discharge of saccade-related superior colliculus neurons during saccades accompanied by vergence. *J Neurophysiol* 90: 1124-1139, 2003.
- Wasicky R, Ziya-Ghazvini F, Blumer R, Lukas JR, and Mayr R.** Muscle fiber types of human extraocular muscles: a histochemical and immunohistochemical study. *Invest Ophthalmol Vis Sci* 41: 980-990, 2000.
- Westheimer G and Mitchell AM.** Eye movement responses to convergence stimuli. *Arch Ophthalmol* 55: 848-856, 1956.
- Zee DS and Levi L.** Neurological aspects of vergence eye movements. *Rev Neural (Paris)* 145: 613-620, 1989.
- Zee DS, Optican LM, Cook JD, Robinson DA, and Engel WK.** Slow saccades in spinocerebellar degeneration. *Arch Neurol* 33: 243-251, 1976.
- Zee DS, FitzGibbon EJ, and Optican LM.** Saccade-vergence interactions in humans. *J Neurophysiol* 68: 1624-1641, 1992.
- Zhang H and Gamlin PD.** Neurons in the posterior interposed nucleus of the cerebellum related to vergence and accommodation. I. Steady-state characteristics. *J Neurophysiol* 79: 1255–1269, 1998.

Zhang Y, Gamlin PD, and Mays LE. Antidromic identification of midbrain near response cells projecting to the oculomotor nucleus. *J Neurophysiol* 84: 525-528, 1991.

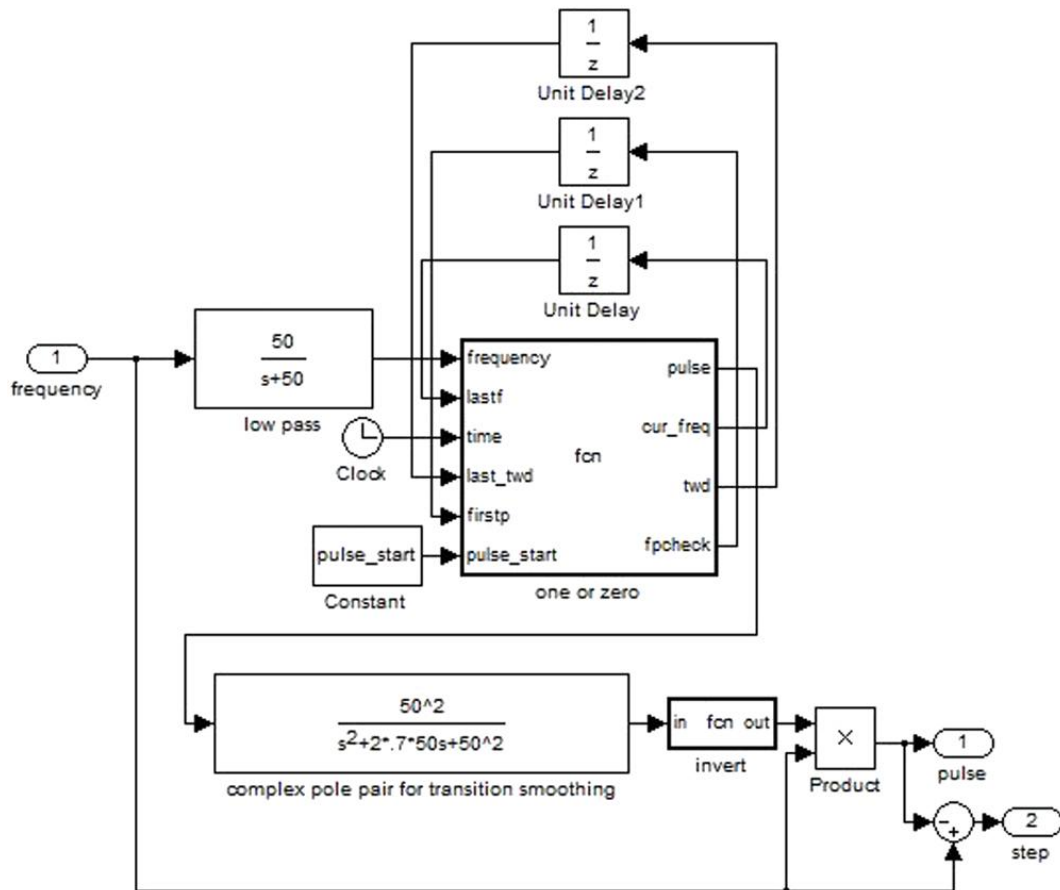
Zhang Y, Mays LE, and Gamlin PDR. Characteristics of near response cells projecting to the oculomotor nucleus. *J Neurophysiol* 67: 944-960, 1992.

Zhou W and King WM. Premotor commands encode monocular eye movements. *Nature* 393: 692-695, 1998.

Zuber BL and Stark L. Dynamical characteristics of the fusional vergence eye movement system. *IEEE Trans Syst Sci Cybern* 4: 72-79, 1971.

APPENDIX A

PARSING MATLAB SIMULINK MODEL



With burst-tonic vergence cell firing frequency as its input, the parsing model outputs pulse and step components separately. In this context, these two components are defined by their visual profiles, with the "pulse" being the initial burst of firing and the "step" being the subsequent tonic firing. The "low pass" block is a low pass filter coded as a transfer function, designed to smooth the signal input to the "one or zero" function

block, attenuating high frequency changes in the firing rate. This is necessary, as the purpose of the “one or zero” function is to monitor the vergence cell firing frequency for a continuously decreasing phase over a time interval of a duration equal to the user defined constant “pulse_start.” High frequency firing changes would prevent this time threshold from ever being reached.

The value “pulse_start” defines the temporal distinction between the pulse and the step by specifying a duration threshold for the decreasing interval of the pulse. When “one or zero” examines the filtered signal, the first comparison between current and previous firing frequency values to reveal a decrease in signal initializes a counting variable, “time_going_down”. At every detected decrease in value, the SimuLink ‘clock’ is accessed and the time at which the signal began to decrease, “twd,” is subtracted from the current time. This difference continues to increase in value until it becomes larger than the “pulse_start” threshold, as signified by the value of “time_going_down” being greater than “pulse_start”.

When the “pulse_start” threshold has been reached, the binary value “pulse” of the “one or zero” function is then permanently switched from “0” to “1”. This switching is very sharp, so a complex pole pair was used to smooth the transition through the action of its damper, slowing the shift from 0 to 1. Values (Tc, q, and w) were left constant and selected to give pulse outputs similar in shape to burst cells and step outputs similar in shape to tonic cells. Due to the “invert” function, $\text{output} = 1 - \text{input}$ (coming from the complex pole pair), a “0” output from the complex pole pair will result in an output of “1” from the “invert” function. As the next action of the model is to multiply this value by the current signal, this will result in all of the original firing frequency being output as

a "pulse". An output of “1” by the complex pole pair will result in the current signal being multiplied by “0”, thus “0” is the value for the pulse, “0” is subtracted from the step, and the entire signal is routed to the "step" output. In this manner, when the binary value of “pulse” of the “one or zero” function, is converted from “0” to “1” by the reaching of “pulse_start”, the “pulse” ends and the “tonic” signal begins.

The “pulse_start” value is an estimate of the duration of the decreasing interval of the pulse. While it is true that this interval estimate could prove to be either shorter or longer than the actual decreasing interval, this approximation was sufficient to allow the model to make robust estimates, due to the actions of the complex pole pair smoothing the transition between the "pulse" and the "step". While it is more likely that some of the pulse firing was included in the step as a result of underestimating the “pulse_start” value, in the event that the “pulse_start” value was overestimated, the pulse and step were never parsed and the entirety of the vergence cell firing for that trial was, for the model’s purposes, considered the pulse. The word ‘pulse’ in this scenario is a slight misnomer in that the only difference between the “pulse” and “step” firing, from the model’s perspective, is that the vergence cell firing frequency being labeled as “pulse” by the model is fit with the multiple gain parameters found in the “nonlinear gain” function of Fig. 36, while the "step" has a single static gain.

The code for the function "one or zero," which uses the "clock" block and unit delays to function with both variable and constant steps of the model solver:

```
function [pulse, cur_freq, twd, fpcheck]= fcn(frequency, lastf, time, last_twd, firstp, pulse_start)
```

```

% "twd" is the time (from clock) that the frequency began to decrease, 9 if no decrease
yet

% "firstp" is 0 if on the first peak

% "last" is last frequency and boolean if past first pulse

cur_freq = frequency;

if (time < pulse_start)

    last_twd = 9;

end

if (frequency < lastf) && (last_twd == 9)

    twd = time;

else if (frequency < lastf)

    twd = last_twd;

else

    twd = 9;

end

end

% The amount of time frequency is decreasing - 9 if not decreasing

if (twd == 9)

    time_going_down = 0;

else

    time_going_down = time - twd;

end

if (time_going_down > pulse_start) || (firstp > 0)

    fpcheck = 1; %positive component of pulse has ended

    pulse = 1;

```

```
else  
    fpcheck = 0;  
    pulse = 0;  
end
```

APPENDIX B

IACUC Approval Form



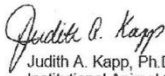
THE UNIVERSITY OF ALABAMA AT BIRMINGHAM

Institutional Animal Care and Use Committee (IACUC)

Notice of Approval for Protocol Modification

DATE: March 2, 2009

TO: Claudio Busetini, Ph.D.
WORB 402 4390
FAX: 934-5725

FROM: 
Judith A. Kapp, Ph.D., Chair
Institutional Animal Care and Use Committee

SUBJECT: Title: Neural Organization of Eye Movements in Depth
Sponsor: NIH
Animal Project Number: 081207720

On March 2, 2009, the University of Alabama at Birmingham Institutional Animal Care and Use Committee (IACUC) reviewed the animal use proposed in the above referenced application. It approved the modification as described: Additional Personnel to protocol: Leah C. Cooper. The sponsor for this project may require notification of modification(s) approved by the IACUC but not included in the original grant proposal/experimental plan; please inform the sponsor if necessary. The following species and numbers of animals reflect this modification.

Species	Use Category	Number in Category
Primates	B	Zero - Procedural modification only

Animal use is scheduled for review one year from December 2008. Approval from the IACUC must be obtained before implementing any changes or modifications in the approved animal use.

Please keep this record for your files.

Refer to Animal Protocol Number (APN) 081207720 when ordering animals or in any correspondence with the IACUC or Animal Resources Program (ARP) offices regarding this study. If you have concerns or questions regarding this notice, please call the IACUC office at 934-7692.

Institutional Animal Care and Use Committee
B10 Volker Hall
1670 University Boulevard
205.934.7692
FAX 205.934.1188

Mailing Address:
VH B10
1530 3RD AVE S
BIRMINGHAM AL 35294-0019



THE UNIVERSITY OF ALABAMA AT BIRMINGHAM

Institutional Animal Care and Use Committee (IACUC)

NOTICE OF RENEWAL

DATE: December 22, 2010

TO: CLAUDIO BUSETTINI, Ph.D.
WORB-654 4390
FAX: (205) 934-5725

FROM: 
Judith A. Kapp, Ph.D., Chair
Institutional Animal Care and Use Committee (IACUC)

SUBJECT: Title: Neural Organization of Eye Movements in Depth
Sponsor: NIH
Animal Project Number: 110107720

As of January 21, 2011, the animal use proposed in the above referenced application is renewed. The University of Alabama at Birmingham Institutional Animal Care and Use Committee (IACUC) approves the use of the following species and numbers of animals:

Species	Use Category	Number in Category
Primates	B	2

Animal use must be renewed by December 2, 2011. Approval from the IACUC must be obtained before implementing any changes or modifications in the approved animal use.

Please keep this record for your files, and forward the attached letter to the appropriate granting agency.

Refer to Animal Protocol Number (APN) 110107720 when ordering animals or in any correspondence with the IACUC or Animal Resources Program (ARP) offices regarding this study. If you have concerns or questions regarding this notice, please call the IACUC office at (205) 934-7692.

Institutional Animal Care and Use Committee
CH19 Suite 403
933 19th Street South
205.934.7692
FAX 205.934.1188

Mailing Address:
CH19 Suite 403
1530 3RD AVE S
BIRMINGHAM AL 35294-0019